AVR TUNING FOR BETTER ON-LINE GENERATOR PERFORMANCE

A Thesis

Submitted to the Faculty of Graduate Studies

in Partial Fulfilment of the Requirements

for the Degree of

Master of Science

in the Department of Electrical Engineering

University of Saskatchewan

by

Ronald R. Lalonde

Saskatoon, Saskatchewan

February, 1976

The author claims copyright. Use shall not be made of the material contained herein without proper acknowledgment, as indicated on the following page.

The author has agreed that the Library, University of Saskatchewan, may make this thesis freely available for inspection. Moreover, the author has agreed that permission for extensive copying of this thesis for scholarly purposes may be granted by the professor or professors who supervised the thesis recorded herein, or, in their absence, by the Head of the Department or the Dean of the College in which the thesis work was done. It is understood that due recognition will be given to the author of this thesis and to the University of Saskatchewan in any use of material in this thesis. Copying or publication or any use of the thesis for financial gain without approval by the University of Saskatchewan and the author's written permission is prohibited.

Requests for permission to copy or make use of material in this thesis in whole or in part should be addressed to:

Head of the Department of Electrical Engineering
University of Saskatchewan
Saskatoon, Canada

ACKNOWLEDGMENTS

The author wishes to express his sincere gratitude to Professor K.E. Bollinger for his enthusiastic assistance and for his friendship during the course of this project. The author also wishes to thank his wife who not only helped a great deal during the preparation of the thesis but who provided the essential moral support.

The data required for the study was provided by Calgary Power Ltd.

The project was financed by the National Research Council and the University of Saskatchewan.

UNIVERSITY OF SASKATCHEWAN

Electrical Engineering Abstract No 76A175

AVR TUNING FOR BETTER ON-LINE GENERATOR PERFORMANCE

Student: Ronald R. Lalonde Supervisor: K.E. Bollinger

M.Sc. Thesis presented to the College of Graduate Studies
February 1976

ABSTRACT

Tradition dictates that automatic voltage regulators be tuned with the synchronous generator open-circuited. In this thesis it is shown that considerable improvement in the dynamic voltage response of a loaded generator can be achieved by tuning the AVR for on-line conditions. This is done using a reduced order model of the loaded generator arrived at by calculating the generator frequency response using a transient stability program. In a specific application it is shown that considerable improvement in the dynamic voltage response of Calgary Power's Sundance #3 plant can be achieved with no hardware modifications. Further improvement is possible with the addition of cascade complex compensators. The effects of load variations are investigated and in all cases it is shown that the generator remains stable when open-circuited. Because the SD 3 static AVR has a special feature of internal current feedback, a system with a more standard static AVR is also retuned for on-line conditions. An important result of the study was that in all cases where terminal voltage response was improved, additional damping was also provided to electric power transients.

TABLE OF CONTENTS

	Page
COPYRIGHT	ii
ACKNOWLEDGMENTS	iii
ABSTRACT	iv
TABLE OF CONTENTS	v
LIST OF FIGURES AND TABLES	vii
1. INTRODUCTION	1
2. TECHNIQUES OF GENERATOR MODELLING FOR VOLTAGE CONTROL STUDIES	5
2.1 Introduction	5
2.2 Two Approaches to Generator Modelling	6
2.3 Traditional Generator Models for Voltage Control Studies	8
2.4 Modelling the Sundance 3 Generator Using a Transient Stability Program	12
2.4.1 Outline of Procedure	12
2.4.2 Application to Sundance 3 Generator	15
2.4.3 Evaluation of the Machine Model	24
3. TUNING THE SUNDANCE 3 AVR USING EXISTING HARDWARE	28
3.1 Introduction	28
3.2 The AVR and Exciter Models	29
3.3 Tuning the AVR for Open Circuit Conditions	33
3.3.1 Introduction	33
3.3.2 The open circuit system model	35
3.3.3 Tuning the lead lag compensator	35
3.3.4 Adjusting the current feedback	45
3.3.5 Time domain performance	45
3.4 Tuning the AVR for On-Line Conditions	48
3.4.1 Introduction	48
3.4.2 The on-line system model	48
3.4.3 Tuning the lead lag compensator	49
3.4.4 Effect of current feedback	56
3.4.5 System time domain performance	58
3.4.6 Effect on power oscillations	62

4. TUNING THE SUNDANCE 3 AVR USING COMPLEX COMPENSATORS 66
4.1 Introduction 66
4.2 General Description 67
4.3 The Type 1 Complex Compensator 71
4.3.1 Description 71
4.3.2 Tuning the system 72
4.3.3 System performance 77
4.4 The Type 2 Complex Compensator 80
4.5 Effects on Power Oscillations 82

5. EFFECTS OF LOAD VARIATIONS 90
5.1 Introduction 90
5.2 Model of the Sundance Generator at Reduced Load 91
5.2.1 Use of reduced admittance matrix for load flow analysis 91
5.2.2 Identification results 92
5.3 Performance of Compensated System at Reduced Load 99
5.3.1 Analysis in the S Plane 99
5.3.2 Simulation results 101

6. TUNING A STATIC EXCITATION SYSTEM THAT HAS NO CURRENT FEEDBACK 105
6.1 Introduction 105
6.2 "Standard" Static Excitation System Model 106
6.3 Generator Model Re-evaluation 108
6.4 Addition of Real Root Compensation 110
6.5 Addition of Complex Root Compensation 117
6.5.1 Type 1 Complex Compensator 117
6.5.2 Type 2 Complex Compensator 123

7. CONCLUSIONS 128

8. REFERENCES 131

9. APPENDICES 136
9.1 Appendix I 136
9.2 Appendix II 138
9.3 Appendix III 140

LIST OF FIGURES

FIGURE		Page
2.1	Heffron-Phillips generator model.	11
2.2	Flow chart of procedure to obtain on-line machine transfer function.	13
2.3	Block diagram of generator control system.	20
2.4	Frequency response of Sundance 3 generator leading to the transfer function V_t / E_f.	21
2.5	Frequency response of Sundance 3 generator leading to the transfer function I_f / E_f.	22
2.6	Sundance 3 full load generator transfer functions.	23
2.7	Sundance 3- V_t /E_f transfer function fit.	25
2.8	Sundance 3- I_f /E_f transfer function fit.	25
2.9	Comparison of full load step response from the reduced order model and from USTRAN simulations.	27
3.1	Sundance 3 voltage control system.	30
3.2	Sundance 3 voltage control system model.	31
3.3	Range of adjustment of lead and lag compensators at Sundance.	34
3.4	Sundance 3 generator open circuit model.	36
3.5	Analog circuit of Sundance 3 excitation system.	37
3.6	Root locus of open circuit system with no series compensation.	39
3.7	Open circuit dominant eigenvalue trajectories for variation of lead-lag compensation.	42
3.8	Root locus of open circuit system with lag compensation.	44
3.9	Effect of current feedback on dominant open circuit system root.	46

3.10	Voltage step response of open circuit system with "open circuit settings".	47
3.11	Analog circuit of V_t / E_f .	50
3.12	Analog circuit of I_f / E_f .	50
3.13	Root locus of on-line system with open circuit settings.	51
3.14	On-line system closed loop poles and zeros.	53
3.15	On-line system eigenvalue trajectories for variation of lead lag compensation.	55
3.16	Effect of current feedback on dominant on-line system eigenvalue.	57
3.17	Full load voltage step response with on-line lead lag compensator setting.	59
3.18	Full load voltage response after a line outage with on-line lead lag settings.	61
3.19	Open circuit step response with on-line lead lag settings.	63
3.20	Full load real power oscillations after a line outage with on-line lead lag settings.	64
4.1	Bridged-T network implementation of complex compensator.	68
4.2	Analog circuit of complex compensator.	68
4.3	Root locus showing effect of complex compensator on Sundance dominant roots.	70
4.4	Effect of Type 1 complex and lead lag compensators on dominant eigenvalue.	75
4.5	Full load terminal voltage step response with Type 1 complex compensator.	78
4.6	Full load voltage response after line outage - with Type 1 complex compensator.	79
4.7	Open circuit voltage step response with Type 1 complex compensator.	81
4.8	Full load voltage step response with Type 2 complex compensator.	83

4.9	Full load terminal voltage response after line outage. Comparison of 4 cases.	84
4.10	Open circuit voltage step response. Comparison of 4 cases.	85
4.11	Power oscillations after line outage. Comparison of 4 cases.	87
5.1	Bode plot of V_t / E_f obtained from USTF.	94
5.2	Bode plot of I_f / E_f obtained from USTF.	94
5.3	Bode plot of fitted transfer function for V_t / E_f .	95
5.4	Bode plot of fitted transfer function for I_f /E_f .	95
5.5	Comparison of 60% load generator model responses.	97
5.6	Main open loop poles and zeros at full load and 60% load.	98
5.7	Effect of load reduction on root locus of compensated system.	100
5.8	Step response at 60% load.	103
6.1	IEEE Type 1 S static excitation system model.	107
6.2	Root locus of Sundance system with "standard" AVR and on-line machine model.	109
6.3	Voltage step response of Sundance system with "standard" AVR and machine at full load.	111
6.4	Principal branch of the system root locus with and without lead compensation.	113
6.5	Time responses of voltage control system with "standard ststic" AVR.	115
6.6	Real power oscillations with lead compensation.	116
6.7	"Standard" static AVR with series compensators.	118
6.8	Trial locations of Type 1 complex compensator poles.	118
6.9	Asymptotic bode plot of Type 1 complex compensator with poles at $-20 \pm j\ 12$.	120

6.10 Effects of Type 1 complex compensator for the best 2 settings. 122

6.11 USTRAN simulation with setting B of Type 1 complex compensator. 124

6.12 Full load voltage response of system with "standard" AVR and Type 2 complex compensator. 126

LIST OF TABLES

TABLE

3.1 Values of constants and variables of the Sundance 3 excitation system model. 32

4.1 Eigenvalues for the best setting of the Type 1 complex compensator. 76

4.2 Settling time of terminal voltage with machine at full load. 88

1. INTRODUCTION

Both short and long term forecasts of our future needs indicate that the worldwide demand for electrical power will continue to increase. This is likely to happen even if our society realizes that it cannot forever continue increasing its consumption of energy and raw materials. Energy can be extracted from still available fossil fuels more efficiently and economically in large plants. This is the case also, in the forseeable future at least, for nuclear energy. The electrical power produced is being distributed by transmission systems that are ever-increasing in size and complexity. As systems grow and become more interlaced, new problems are arising and old ones are becoming aggravated. This fact, allied with the increasingly high demand for reliability and quality of service by a society that is more than ever dependant on electrical power, is placing a great responsibility on the shoulders of power system engineers.

In recent years, many new developments have made the task at hand somewhat easier to grasp. The digital computer has permitted the analysis of large and complex systems with the use of special numerical techniques. In the field of control, classical and modern

control theory are being applied to the solution of power system problems. Optimal control theory has been applied to many cases [1],[2] but until now the implementation of controllers arrived at has been difficult.

The area of voltage control has been especially active in the past years. Static excitation systems were introduced relatively recently and now these are almost exclusively being installed by utilities. With the growth of power systems and the increase in quantities of transmitted energy, problems such as local and inter-area power oscillations have been remedied by the addition of feedback compensators known as power system stabilizers. There has been a tremendous amount of work done in this area, as evidenced by the large number of recent publications [3],[4],[5].

The project reported in this thesis originated from work done in the area of tuning power system stabilizers. In this previous work, a method was devised to arrive at a reduced order model of a synchronous generator that is operating at full load [6]. With this method the transfer function relating any two generator variables can be calculated. The transfer functions relating generator terminal voltage to field voltage that were found were quite different from generator models normally used in voltage control studies. It occurred that these models could be very useful in the tuning of voltage regulators.

Traditionally, AVR's have been tuned with the machine open-circuited. The tuning procedure normally involves preliminary studies where models of the excitation system and open-circuit machine are used. These settings are then fine-tuned at the plant during commissioning, again with the generator open-circuited. The aim is usually to arrive at a time response that is characterized by a fast rise with one single overshoot and no further oscillations. A system with such a response is characterized in the S plane by a single pair of complex roots which have a damping factor of .707. At the plant, it is then usually verified that the machine is not unstable when operated under load. If excessive oscillations persist with the machine loaded, then the AVR is not usually readjusted, but additional feedback in the form of a power system stabilizer is added.

The study presented here uses a reduced order on-line model of a generator in an attempt to tune the AVR to provide the best possible performance when the generator is fully loaded. For each case, it is then verified that the system is still stable under open circuit conditions. In order to make use of classical control techniques, a single input - single output model of the generator is used. The power system is actually a complex multiple-input multiple-output system. This

is taken into account by testing all settings arrived at by simulating the Alberta power system with a transient stability program where the main machines and controllers are modelled in detail. The bulk of this study is concerned with one particular installation, the Sundance 3 unit of the Calgary Power system. Because the static excitation system used at Sundance 3 has a special feature of internal field current feedback, the final portion of the study is an attempt to reassess tuning procedure for a plant where a more standard static excitation system is used.

In chapter 2, two different approaches to generator modelling are discussed. The method used here to arrive at an on-line generator model, where a simulated noise signal is applied to the transient stability program, is described in the same chapter. The on-line model of the Sundance generator is used in chapter 3 to retune the Sundance AVR for on-line conditions. In chapter 4, cascade complex compensators are added to the system in an attempt to further improve performance. The effects of load variations on system performance are investigated in chapter 5. Chapter 6 presents a similar AVR tuning study where the Sundance on-line machine model is used once again, but where the excitation system is replaced by a more standard static AVR where no internal current feedback is included.

2. TECHNIQUES OF GENERATOR MODELLING FOR VOLTAGE CONTROL STUDIES

2.1 Introduction

Dynamic stability studies of the voltage control system of synchronous generators require mathematical models of the voltage regulator, the exciter, and the machine. To permit the use of linear control system theory, these models should be linear and expressed in the form of transfer functions. The models that can be used for the generator are the subject of this chapter.

The first section describes in general terms two possible approaches that can be used to obtain a model for a physical system. This can be done by deriving the transfer function from the system equations, or by a graphical method by which a transfer function is fitted to the frequency response of the system. The following section describes the generator models normally used in voltage control studies.

An identification procedure by which transfer functions can be obtained directly from a transient stability program is then described. This process is used to obtain the generator model of the Sundance 3 plant. This model is used in subsequent chapters to tune the plant AVR

and to design special system compensators.

2.2 Two Approaches to Generator Modelling

System models can be obtained either analytically, from the system equations, or from the frequency response of the system.

In the case of synchronous generators, the analytical technique begins with the equations that define the voltages across the various coils of the machine. These are differential equations with time varying coefficients. A linear transformation developed by Park [7] is used to eliminate this time variance. It has the effect of transforming the stationary stator windings of the machine to rotating d_{qo} windings. The transformed equations can then be per unitized, linearized about an operating point, [8] and simplified if necessary by eliminating negligible terms. The transfer functions required for voltage control studies can then be derived algebraically from these equations by successive elimination of all but the two desired variables. This process can be very long and the result very complex.

The second method of obtaining a generator model is to do so by first obtaining the frequency response of the machine. A transfer function can then be fitted graphically.

There are two possible methods of arriving at the frequency response of a machine. It can be measured

at the plant [9] with the machine operating at the required conditions or it can be measured on the simulated system [6] using numerical methods.

Measurement at the plant is preferable from the point of view of model accuracy. The best known and widely used procedure in this case is to disturb the system with a sinusoidal signal. When transients have died out, the signals at the required input and output points are recorded. From these, the system gain and phase shift at that particular frequency are obtained. If this test is repeated at a number of different frequencies within the range of interest, the complete frequency response of the machine is obtained.

The frequency response of a generator has also been measured successfully with the use of a noise signal. [9] This noise signal can be adjusted to contain all the frequencies over the range of interest. In this case, only one measurement is required. The input and output signals of the plant being identified are then digitized and analyzed either on a commercial Fourier Analyser or with any Fast Fourier Transform algorithm. The result is the machine frequency response.

Measurements at the plant can be difficult and are sometimes impossible. This is the case when a plant is still in the design or construction stage. In this case the frequency response of the generator, or other

system components, can be measured on the simulated system. The power system is simulated with a transient stability program. Either of the two identification procedures described above (discrete frequency or noise signals) can be used. It is much more economical however to use a noise signal. As in the case of physical tests, the simulated system is disturbed by a noise signal. The frequency response is obtained by a Fourier analysis of the input and output signals measured after transients have died out. This identification method has been tested and shown to produce results that agree closely with the frequency response obtained by measurement at the plant itself. (10)

The generator models required for the studies described in this report were obtained using the method described above where noise signals were applied to the simulated power system. This technique is discussed in more detail in section 2.4. Before going on to that, the generator models that are now commonly used in voltage control studies will be described.

2.3 Traditional Generator Models for Voltage Control Studies

Traditionally, great importance has been attached to the behavior of the voltage control system under open circuit conditions. In fact, the standard procedure for setting AVR'S at commissioning time is to do so with the machine open circuited. It is usually assumed that this

will also provide a good setting for loaded conditions. It is thus simply verified that the system is not unstable with the machine on line. Appendix I contains part of a manufacturer's instructions for the commissioning of a rotating excitation system. This is included to provide some insight into present commissioning procedures.

The well known open circuit model of a generator is:

$$\frac{\Delta V_t}{\Delta E_f} = \frac{K}{1 + T_{do}' S} \qquad (2.1)$$

ΔV_t = Incremental change in terminal voltage

Where ΔE_f = Incremental change in field voltage

K = Small-signal gain

T_{do}' = Open-circuit field time constant

The small-signal gain of the machine, K, is determined from the slope of the open circuit characteristic of the machine at a particular operating point.

The model commonly used for AVR studies for loaded conditions is given by [11]

$$\frac{\Delta V_t}{\Delta E_f} = \frac{K_L}{1 + T_d' S} \qquad (2.2)$$

Where

T_d' = Field time constant

$$= \left[\frac{X_d' + X_e}{X_d + X_e}\right] T_{do}'$$

and K_L = Gain at the given operating conditions.

X_d = Generator synchronous reactance.

$X_{d'}$ = Generator transient reactance.

X_e = External Reactance.

In this model, the effect of changes of load angle on the terminal voltage is neglected. This can be seen clearly if the above model is shown as part of the "Heffron-Phillips model" [12] of a synchronous machine supplying power to an infinite bus (figure 2.1).

The constants in this model are given in Appendix II.

The constant K_4 defines the amount of demagnetizing effect produced by a change in rotor angle. The constant K_5 relates the change in terminal voltage to the change in rotor angle. If these two effects are neglected, the resulting transfer function relating terminal voltage to field voltage is

$$\frac{\Delta E_t}{\Delta E_f} = \frac{K_3 \; K_6}{1+S \; K_3 \; T_{do'}} \qquad (2.3)$$

For the case of zero external resistance the constants are:

$$K_3 = \frac{X_{d'} + X_e}{X_d + X_e}$$

$$K_6 = \frac{X_e}{X_e + X_{d'}} \quad \frac{E_{qo}}{E_{to}}$$

where E_{qo} = Base quadrature axis armature voltage

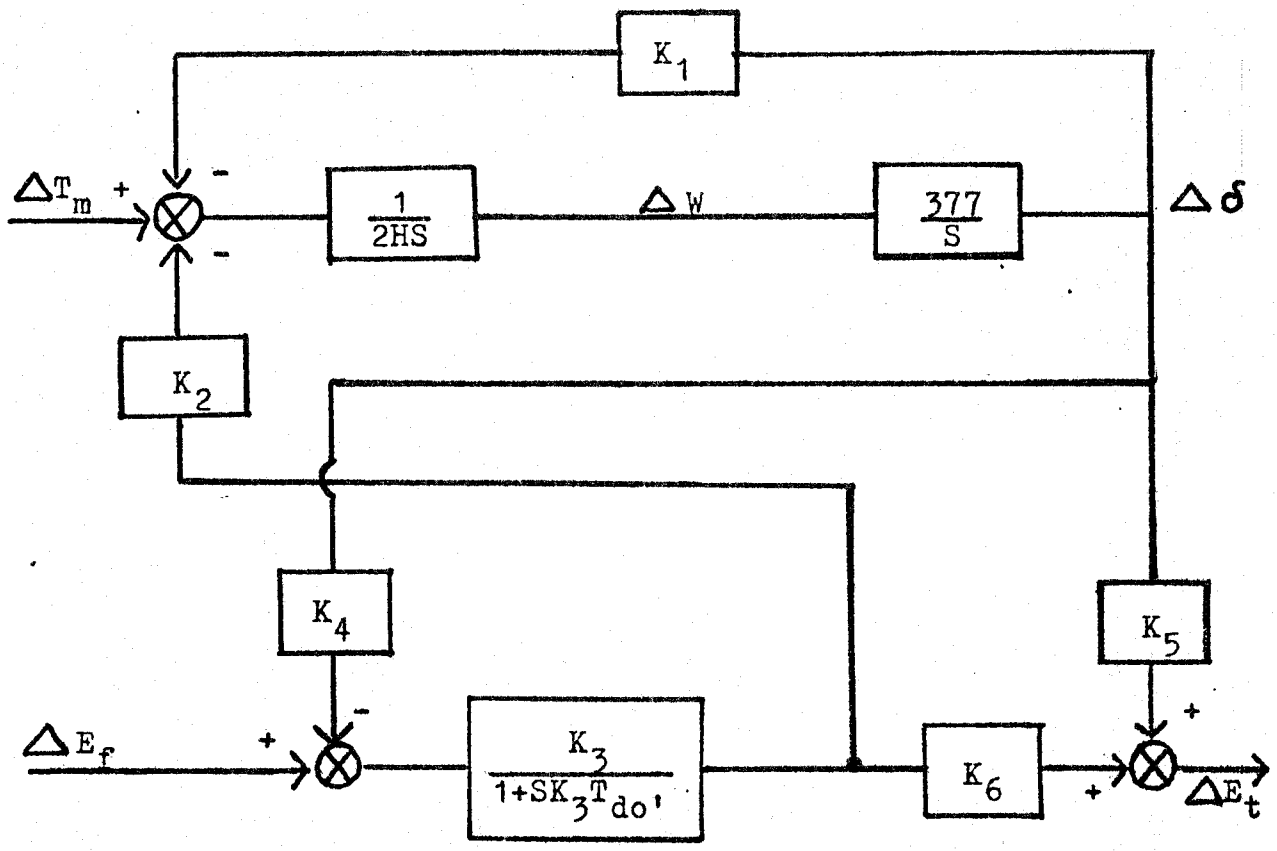

Figure 2.1 Heffron-Phillips Generator Model

E_{to} = Base terminal voltage

The transfer function 2.3 is identical to 2.2.

It has previously been concluded by the use of this model [13] that the performance of the voltage control system under load is very similar to its open circuit behaviour. It will be shown in this report that this is not the case.

The procedure used in this project to obtain a model of a loaded generator for voltage control studies is described next.

2.4 Modelling the Sundance 3 Generator using a Transient Stability Program

2.4.1 Outline of Procedure

In section 2.2, various methods of obtaining the transfer functions of a system were reviewed. The identification procedure used in this study will now be described.

The frequency response of the loaded machine chosen for study in this project was obtained by doing a Fourier analysis of the simulated machine input and output signals with the system disturbed by a properly designed noise signal. The required transfer functions were then obtained from the frequency response by well known graphical techniques.

A flow chart of the procedure is shown in figure 2.2. The names shown in the figure refer to computer programs that perform the tasks shown.

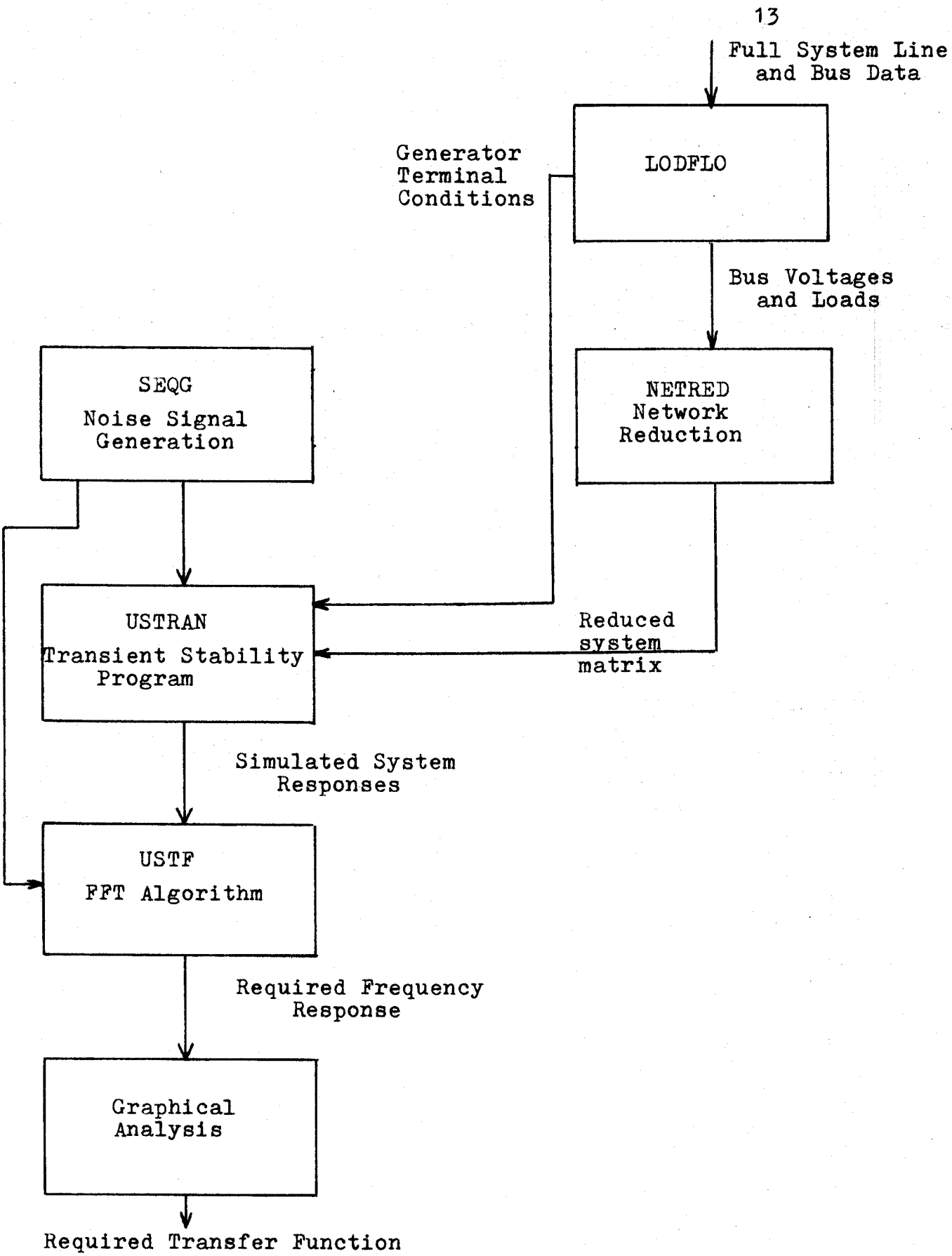

Figure 2.2 Flow Chart of Procedure to Obtain On-Line Machine Transfer Function

These programs are described in detail elsewhere [14], [15]. A brief outline is given here.

A Pseudo Random Binary Sequence (PRBS) of the required characteristics is generated by the program SEQG. A listing of the program SEQG1 in which slight modifications to the original program were made is given in Appendix III.

A transient stability program USTRAN is used to simulate system responses. This program which is based on the FACE [16], [17] simulation program can accommodate up to nine plants. Each plant can be fully modelled including the machine, voltage regulator, exciter, turbine and governor. Large systems can be accommodated by the use of a network reduction program, NETRED. This program eliminates all but the main busses of a system and produces the matrix of admittances seen by a small number of selected generators.

The loadflow program is required for the calculation of initial system conditions needed by the network reduction and transient stability programs.

The simulated responses calculated by USTRAN with the system disturbed by the noise signal are analysed by the program USTF. This program utilizes a Fast Fourier Transform algorithm to transform the discrete time domain signals to the frequency domain. The program output is the system frequency response over the required range.

Straight line asymptotic approximations are then used to fit a transfer function to the frequency response plot.

2.4.2 Application to Sundance 3 Generator

The plant selected for study in this project was Calgary Power's Sundance thermal generating plant. This plant now consists of two coal fired units. A third 375 MW unit presently being installed is scheduled for commissioning in the spring of 1976. By 1978, the plant will have 5 units producing a total of 1725 MW.

Extensive work has already been done on the modeling of the Sundance 3 Unit [15] in relation to the tuning of a power stabilizer. This will be installed as part of the static Automatic Voltage Regulator. The AVR is described in detail in Chapter three.

The parameters used for the simulated noise signal in the identification of pertinent generator transfer functions will now be described.

The noise signal used was generated by the subroutine SEQG1. The required parameters were selected as follows:

a) Selection of the clock period:

The system bandwidth was estimated at 15 Hz. It is desirable to set the first node of the noise signal frequency spectrum at 2.5 times the system frequency, i.e. $f_c = 2.5\, f_{syst}$

$= 2.5 \times 15$ Hz $=$ 37.5 Hz.

or $F_c \approx 40$ Hz

The clock period is thus set at

$$CLPER = \frac{1}{f_c}$$

$$CLPER = \frac{1}{40} = .025 \text{ sec}$$

b) Selection of filter frequency

This is set at one half of f_c.

$$FFILT = \frac{f_c}{2} = 20 \text{ Hz}$$

c) Selection of IDIM, NINT and T

The number of input points, IDIM, to the program USTF must be a binary number. USTF also requires four samples for each clock period. Therefore, if IDIM is set at:

$$IDIM = 2048 = 2^{11}$$

then $NINT = IDIM/4 = 512$

The period of the noise signal is then:

$$T = NINT \times CLPER$$

$$= 512 \times .025$$

$$= 12.8 \text{ seconds}$$

With this period length, the lower frequency limit of the signal is:

$$f_o = \frac{1}{T} = .078 \text{ Hz}$$

$$= .5 \text{ Rads/sec.}$$

Since this is low enough for the present identification purposes, the above selection of the value of

IDIM is considered acceptable.

The noise signal is to be used with the simulation program USTRAN in which the integration time normally used is .00125 sec. This corresponds to 10,240 integration steps during one 12.8 sec. PRBS period. The value of IDIM is modified to provide one input value for each integration step. If IDIM is set at

$$IDIM = 10,240$$

there will be one input value for each integration step of USTRAN and every 5th point can be used in USTF. This provides the required 2048 points for USTF.

d) Selection of filter integration time

The step size of the integration routine used in the implementation of the filter should be small compared to the filter time constant.

We specify:

$$\Delta t_f = \frac{T_f}{10}$$

Where Δt_f = integration step size

T_f = filter time constant

$$= \frac{1}{2\pi \, FFILT} = \frac{1}{40\pi}$$

$$\therefore \Delta t_f = \frac{1}{400\pi}$$

The minimum number of integration steps in one PRBS period is therefore

$$NFILT = \frac{T}{\Delta t_f} = 12.8 \times 400\pi = 16,085$$

Computation is simplified if NFILT is made a multiple of IDIM. The number of filter integration steps is therefore increased to

NFILT = 20,480 = 2 x IDIM

In this way, as the binary sequence is filtered, the value at every second integration step is stored for output.

e) Selection of lead-in time:

When periodic signals are used to identify a system, it is necessary to allow enough time for all transients to die out before any measurements are made. Previous tests on this identification process have indicated that a lead-in time of 1/4 period is sufficient. This value is used here:

ALDN = .25

Summarizing the selected parameters for the generation of the PRBS, we have

CLPER = .025
NINT = 512
IDIM = 10,240
FFILT = 20.
NFILT = 20,480
ALDN = 0.25

The noise sequence was generated and stored on a disc file prior to applying it to the simulated power system.

The Alberta Power system was then simulated with

the transient stability program USTRAN. The noise signal was injected at the reference node of the AVR where the power stabilizer signal would normally be applied. This is illustrated in fig. 2.3. The program was run for 16 seconds of simulated time. The reduced admittance matrix of the Alberta Power System was available from previous studies done on the system with the Sundance 3 generator operating at full load. The discrete time output signals required for later use by the USTF program, i.e. terminal voltage, field voltage and field current were stored on disc files.

The two frequency response plots obtained from the USTF program, i.e. V_t / E_f and I_f/ E_f are shown in figure 2.4 and figure 2.5.

These graphs are characterized by a resonant peak which occurs at about 11 Rads/Sec. in both cases. This is marked by a pronounced dip or increase in phase angle at that frequency. This feature is non existant in the traditional machine models discussed in section 2.2. This fact is quite important because, as will be seen later, this resonance is the cause of the oscillatory response of the generator terminal voltage when the machine is loaded.

The D.C. gain shown on these plots was obtained from a step response test done on the simulated system. The recommended practice [18] for obtaining the small signal gain of a system is to do two step response tests, one with

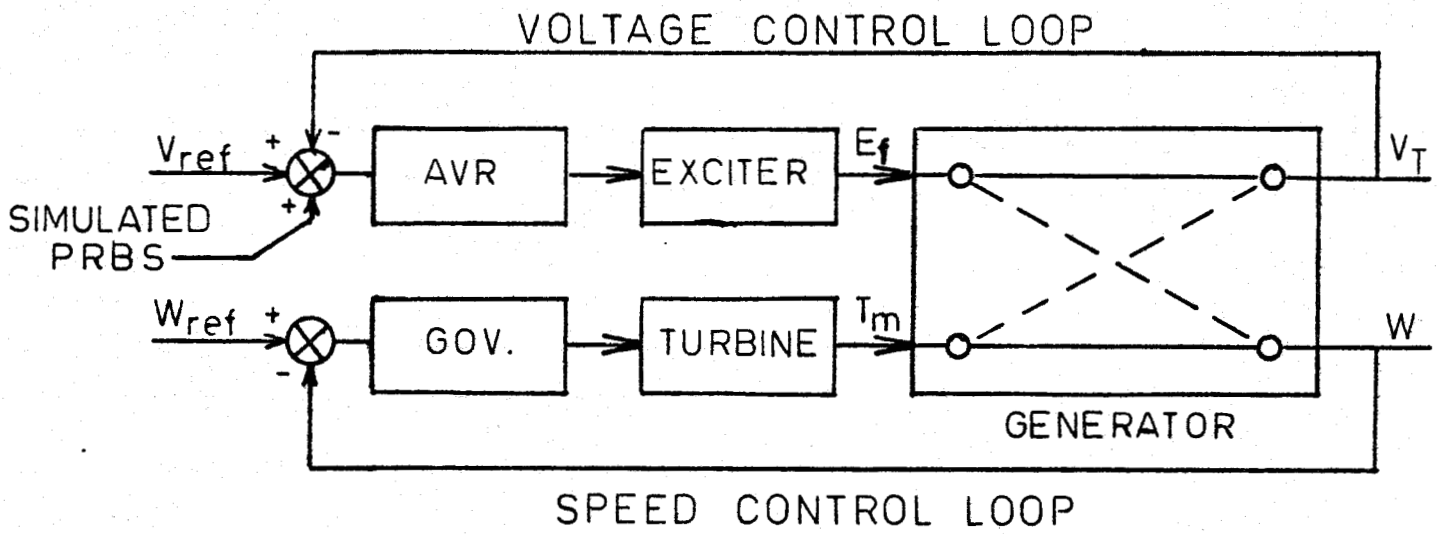

Figure 2.3 **Block diagram of generator control system**

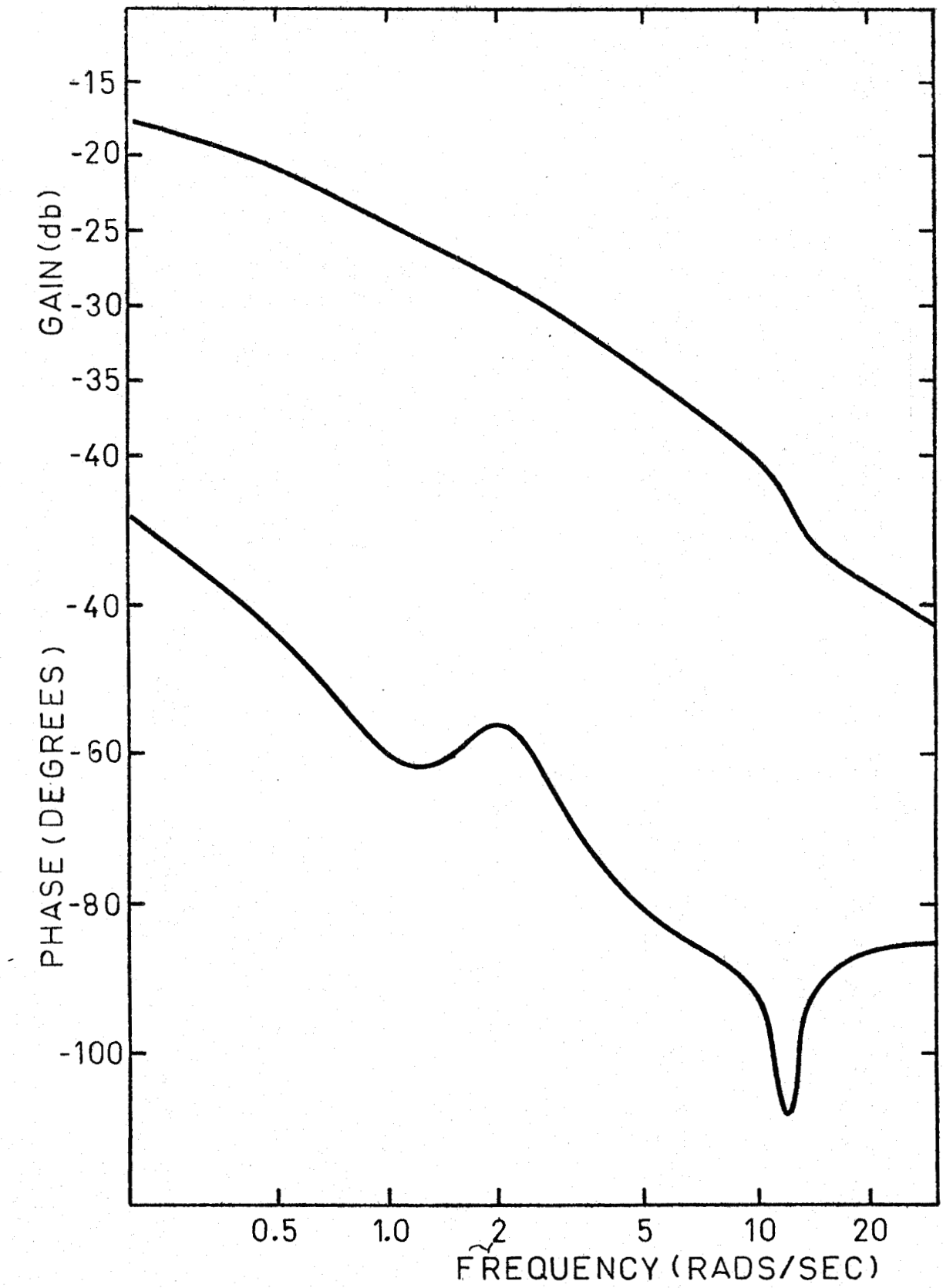

Figure 2.4 Frequency response of Sundance 3 generator leading to the transfer function V_t / E_f

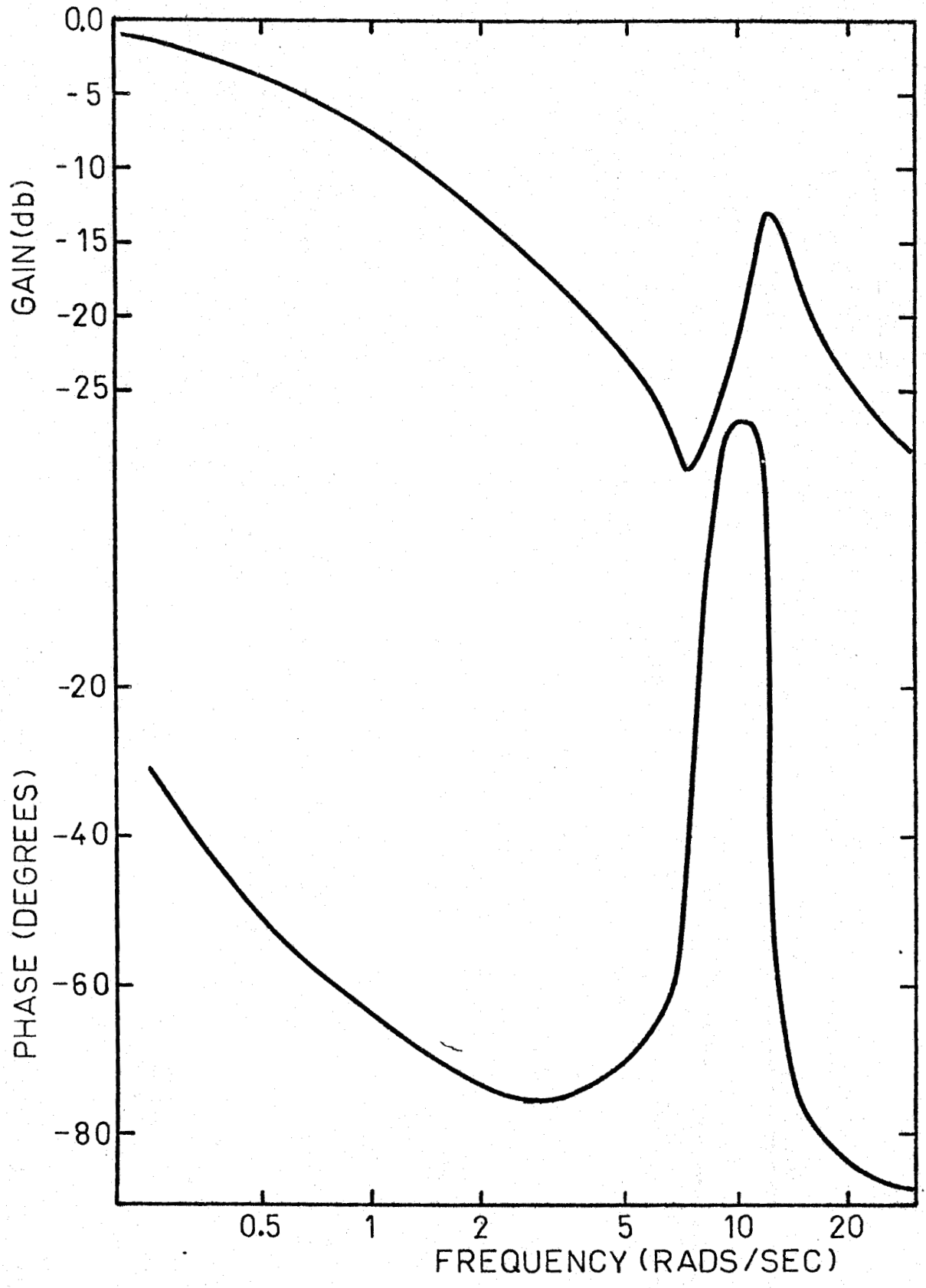

Figure 2.5 Frequency response of Sundance 3 generator leading to the transfer function I_f / E_f

a positive .01 P.U. disturbance and one with a negative .01 P.U. disturbance. The system small signal gain is the slope of the straight line joining the two new steady state operating points. As an approximation to this, one step response test only was done with a disturbance of .001 P.U. This permitted a saving in computing time. The program was run for 12 seconds of simulated time.

The transfer functions V_t / E_f and I_f / E_f shown in figure 2.6 were obtained graphically from the frequency response plots of figure 2.4. As a first approximation, the graphs were fitted with asymptotes. The frequency

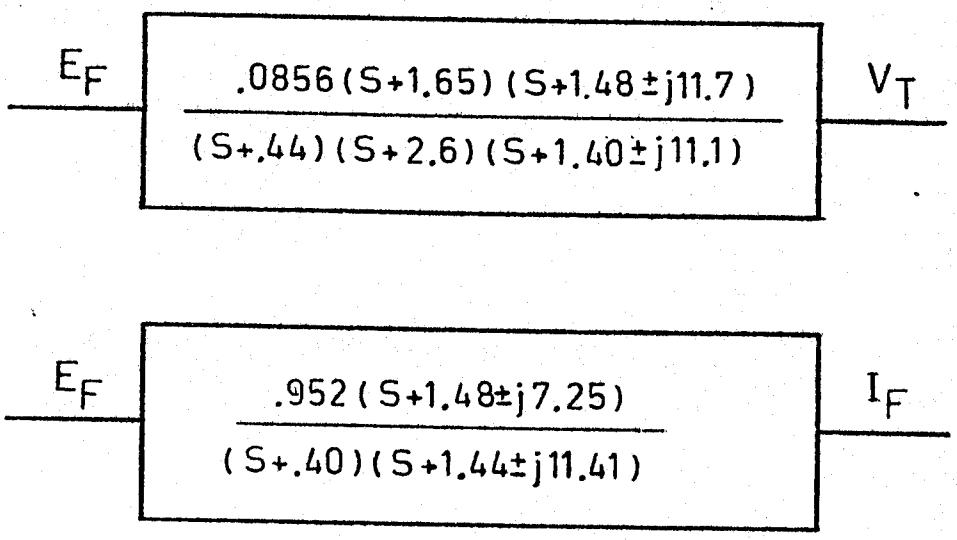

Figure 2.6 Sundance 3 full load generator transfer functions

response of the transfer function corresponding to this approximation was then calculated. This was compared with the original Bode plot. Adjustments were then made to the transfer function to get as close a fit as possible.

Figures 2.7 and 2.8 show the frequency response of the approximated transfer functions superimposed on the originals. The transfer function for I_f / E_f produced quite a close fit. In the case of V_t / E_f some error in phase remained in the 2 Rad/Sec. range. This could have been corrected by the addition of a second set of complex poles and zeros to the transfer function. However, the resonance at 12 Rads/Sec. was considered the dominant feature. This assumption was proven correct by step response tests that were carried out on the model. These are described in the following section.

2.4.3 Evaluation of the Machine Model

The Sundance 3 generator on-line model described in the preceding section was tested by comparing the step response of the reduced order system to that obtained from a USTRAN simulation where the system is modelled in detail.

A state space model of the Sundance 3 voltage control system was derived, including the AVR, the exciter and the reduced order machine model obtained above. The excitation system model is described in detail in chapter 3. The same disturbance was used in both simulations. The

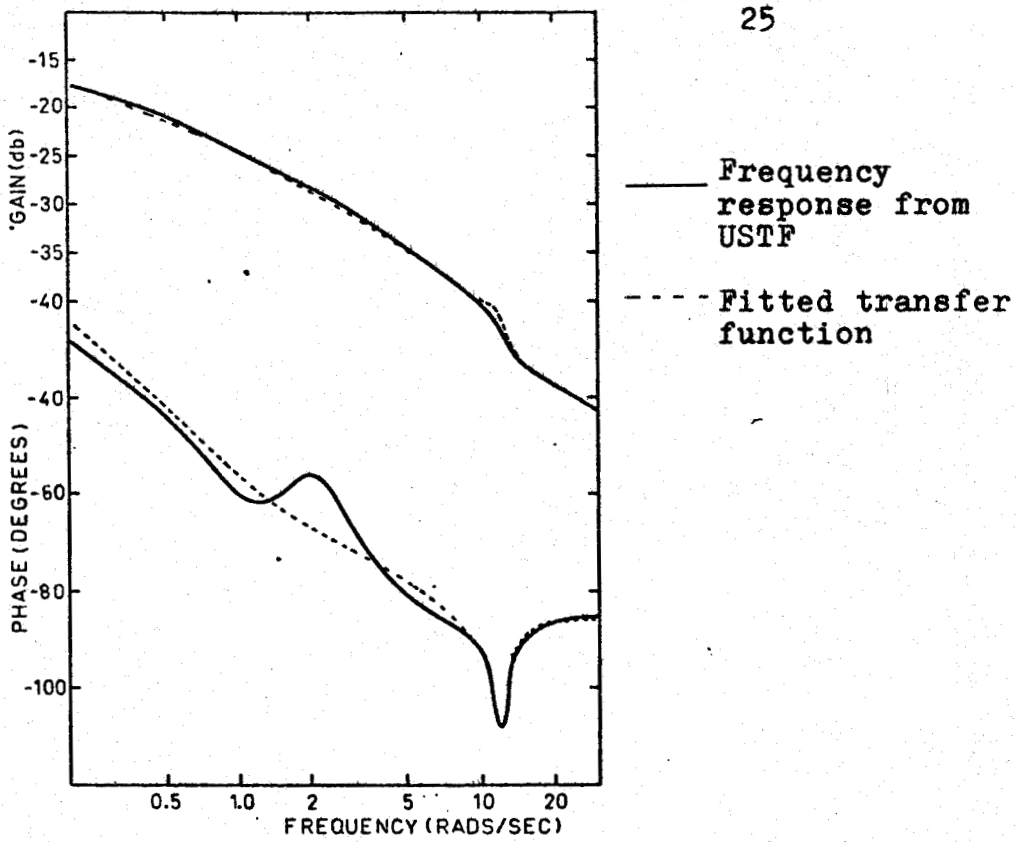

Figure 2.7 Sundance 3 V_t / E_f transfer function fit

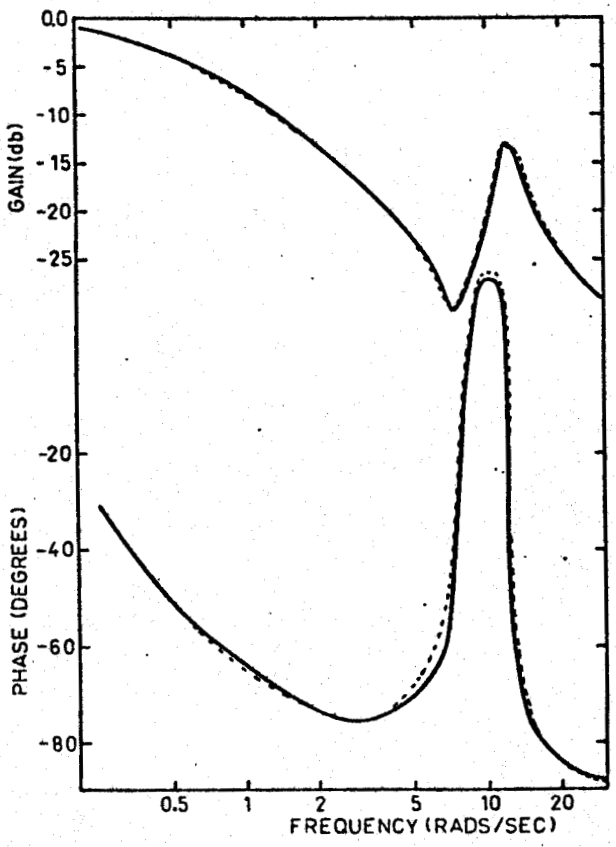

Figure 2.8 Sundance 3 I_f / E_f transfer function fit

integration routine and step size were also identical.

The responses obtained from the two simulations are shown in figure 2.9. The discrepancies between the responses are largely due to errors in the damping factors of the complex poles and zeros of the machine model. Because of the light damping of the roots, these could only be measured to an accuracy of ±25% on the Bode plots. However, for the purposes of this study, the model was considered quite acceptable.

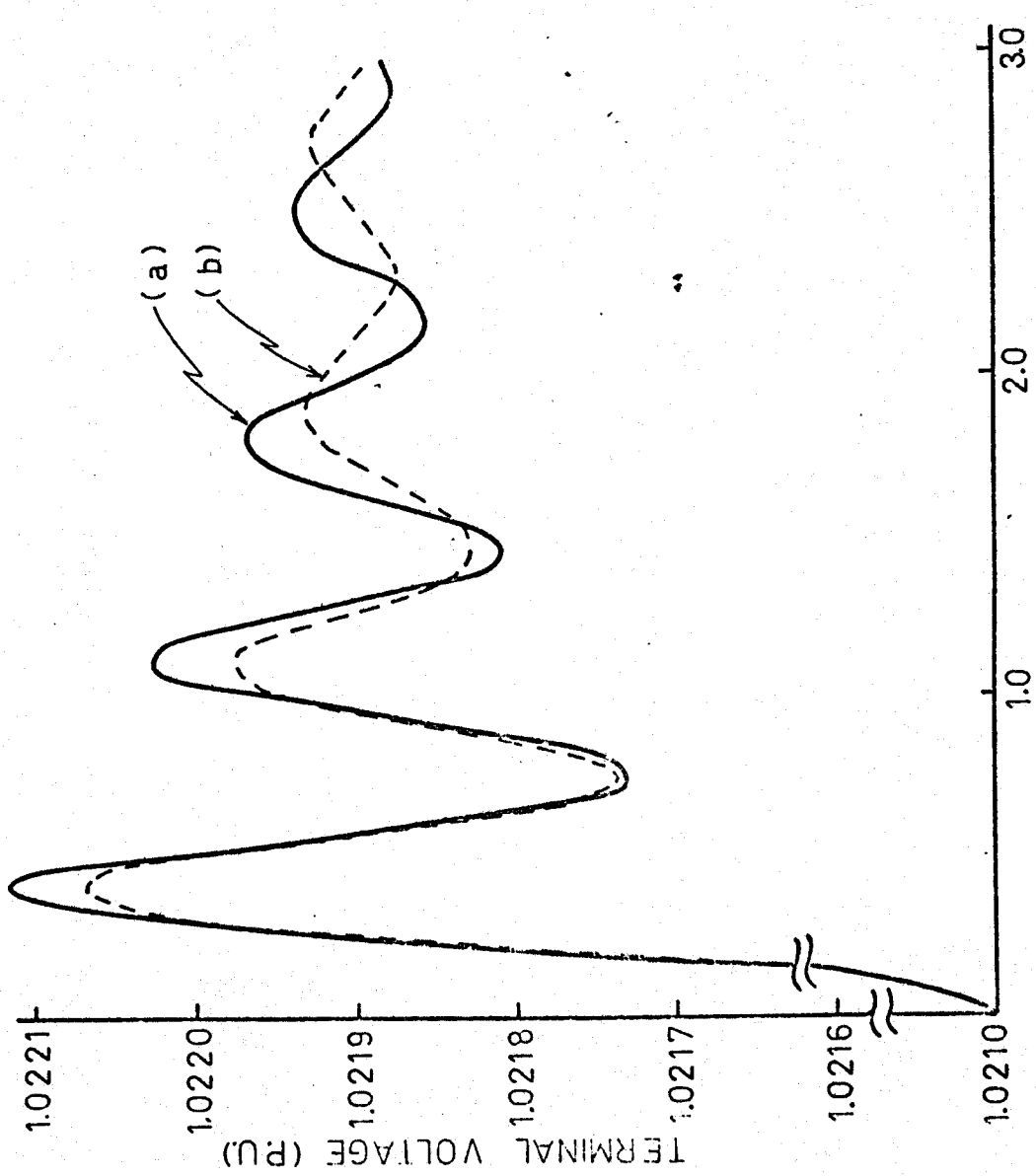

Figure 2.9 Comparison of full load step response from the reduced order model and from USTRAN simulations.
a) Reduced order model simulation
b) USTRAN simulation

3. TUNING THE SUNDANCE 3 AVR USING EXISTING HARDWARE

3.1 Introduction

In the previous chapter, a model describing the behaviour of the Sundance 3 generator under full load conditions was developed. This model can now be used to tune the static AVR that will be installed at Sundance.

This chapter begins with the description of the Sundance excitation system and of its model.

This model, along with an open circuit model of the generator is then used to calculate settings for the AVR which provide good response under open circuit conditions. This is the procedure normally followed for AVR tuning and the results serve as a basis of comparison for other settings.

The next step is to use the on-line generator model to find improved AVR settings. No modifications to the excitation system are made and all settings are kept within the range provided by the equipment. The possible improvements in on-line performance are illus-

trated by time domain responses. Finally, the effect of AVR settings on power oscillations is examined.

3.2 The AVR and Exciter Models

The excitation system that will be used at Sundance 3 consists of an electronic AVR and a thyristor bridge exciter. The block diagram of the system shown in figure 3.1 shows its dominant features. The AVR consists of a rectifier, a voltage setting rheostat and a series of amplifiers which act as summing junctions for other signals and as series compensators. The exciter consists of four parallel thyristor bridge units. One only is shown on the diagram. Each of the units has a field current feedback path which is included to force equal load sharing by the four bridges.

A model of this excitation system has been developed by Calgary Power and is shown in figure 3.2. The values of the constants are listed in table 3.1.

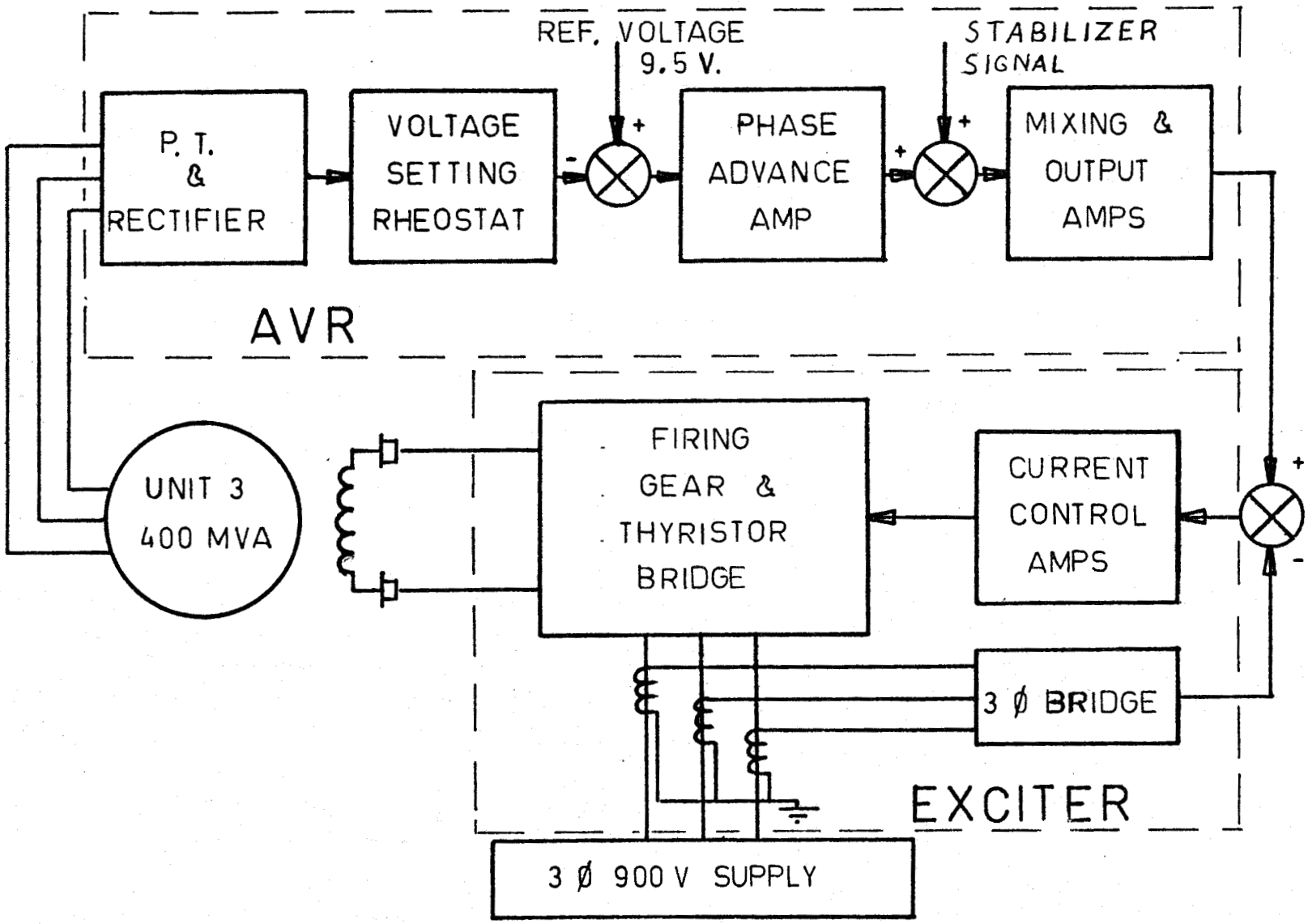

Figure 3.1 Sundance 3 voltage control system

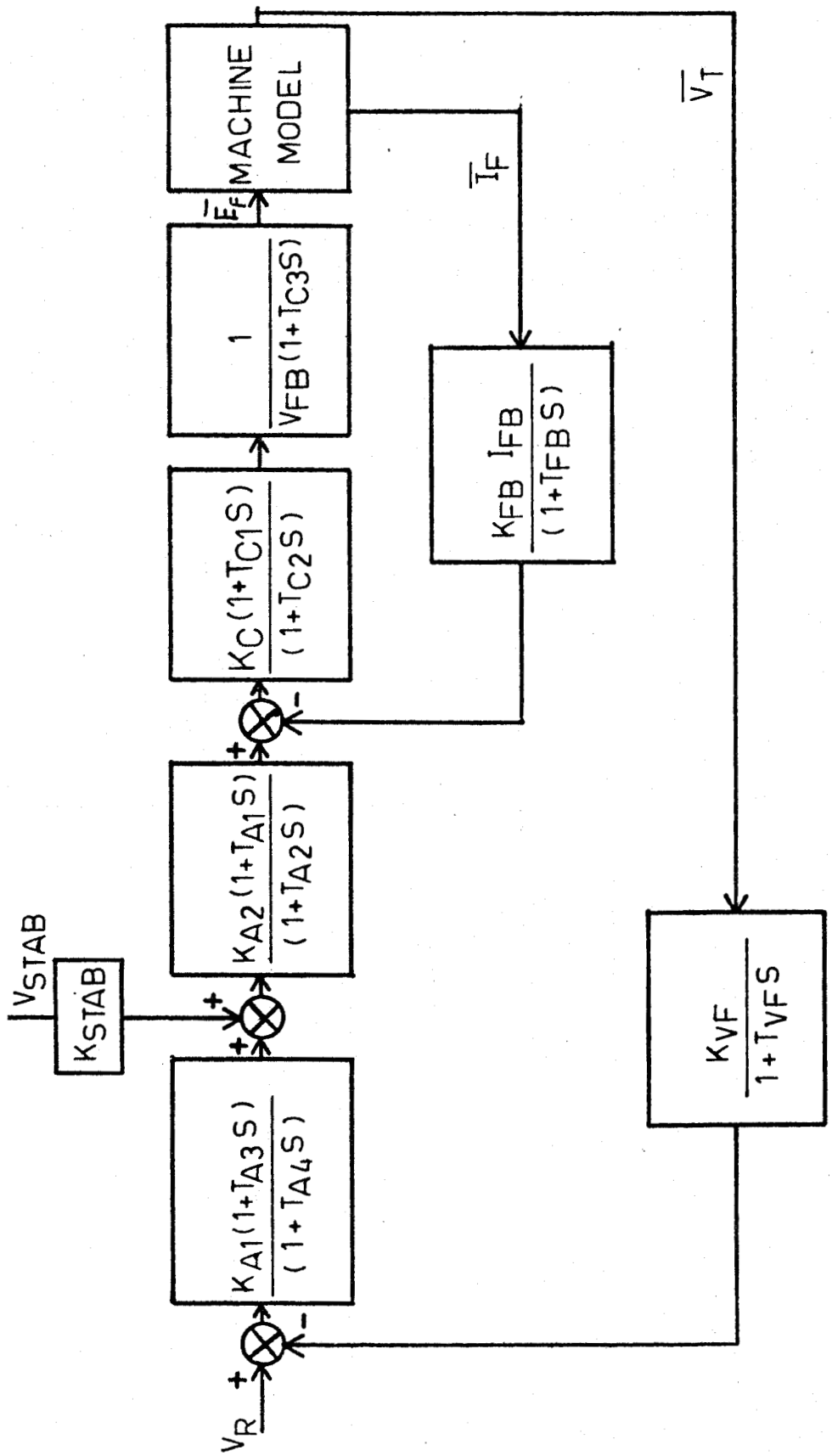

Figure 3.2 Sundance 3 voltage control system model

Variable	Value
K_{A1}	0.851
K_{A2}	2.0
K_C	11137.5
K_{FB}	0.0 to .00303
K_{STAB}	0.0
K_{VF}	132.59
I_{FB}	1500.
V_{FB}	139.2
T_{A1}	0.0875 to 2.5875
T_{A2}	1.0875 to 3.585
T_{A3}	0.039 to .2813
T_{A4}	0.039
T_{C1}	0.918
T_{C2}	10.0
T_{C3}	0.01
T_{FB}	0.01
T_{VF}	0.01

Table 3.1 Values of constants and variables of the Sundance 3 excitation system model (figure 3.2)

The two blocks containing the time constants T_{A1} to T_{A4} provide lead-lag compensation for the system. Their range of adjustment is given in table 3.1 and is illustrated on the S-plane in figure 3.3. The time constants of the lag compensator, T_{A1} and T_{A2}, are adjusted by the same rheostat and are therefore interdependant.

The two time constants are related by:

$$T_{A2} = T_{A1} + .9975$$

The input quantity shown as V_{STAB} is the power stabilizer signal. In these studies, the effect of the stabilizer was not considered. The constant K_{STAB} was therefore always zero.

The field current signal fed back to the exciter input is also variable. The range K_{FB} is given in table 3.1.

3.3 Tuning the AVR for Open Circuit Conditions

3.3.1 Introduction

It was stated in chapter two that it is standard procedure among equipment manufacturers and utilities to tune voltage regulators with the machine at open circuit. This is certainly the simplest method. The resulting settings have been found satisfactory in some cases, but in other cases have resulted in the need for the addition of a power system stabilizer to give added stability. (19)

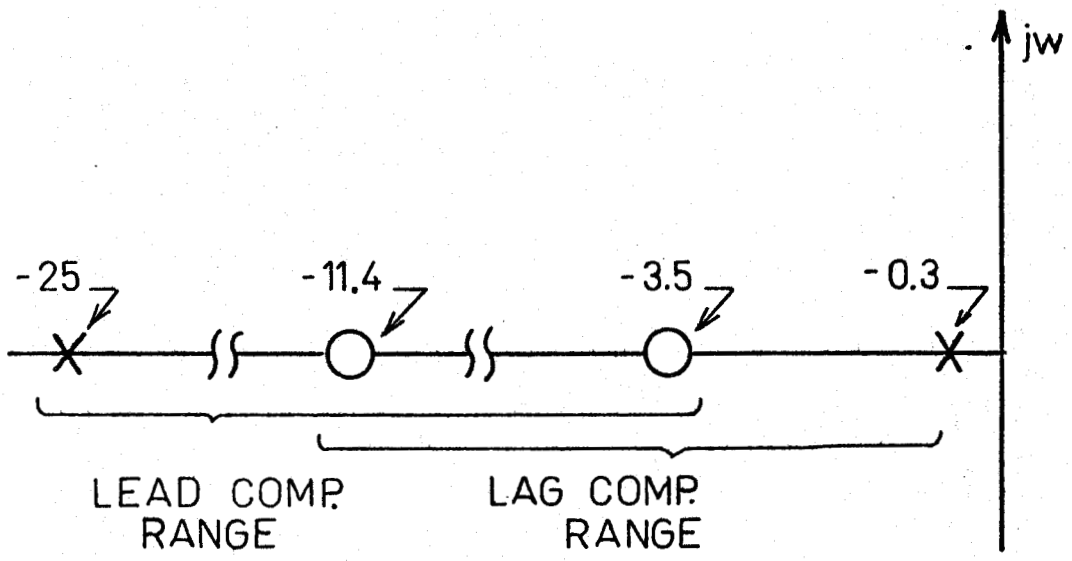

Figure 3.3 Range of adjustment of lead and lag compensators at Sundance

In this section, the Sundance 3 AVR is tuned using an open circuit model of the generator. This has two purposes. It serves as a verification of the settings provided by Calgary Power for the system. Secondly, it provides a basis of comparison for settings and responses that can be arrived at by tuning the system with an on-line model of the generator.

3.3.2 The Open Circuit System Model

The open circuit generator model is shown in figure 3.4(a). The gain is the per-unitized slope of the open circuit characteristic of the machine shown in figure 3.4(b).

An analog diagram of the combined AVR and generator models appears in figure 3.5. This diagram was used to derive a state space model of the system which was required for eigenvalue analysis and digital simution.

3.3.3 Tuning the lead lag compensator

The lead lag compensator of the system was tuned using root locus and eigenvalue search techniques. In this section, the root locus diagram of the open cir-

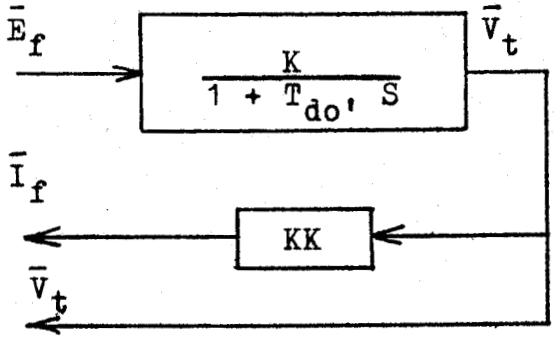

(a) Generator open circuit model

$K = .609$
$T_{do'} = 4.6$
$KK = \frac{1}{K} = 1.64$

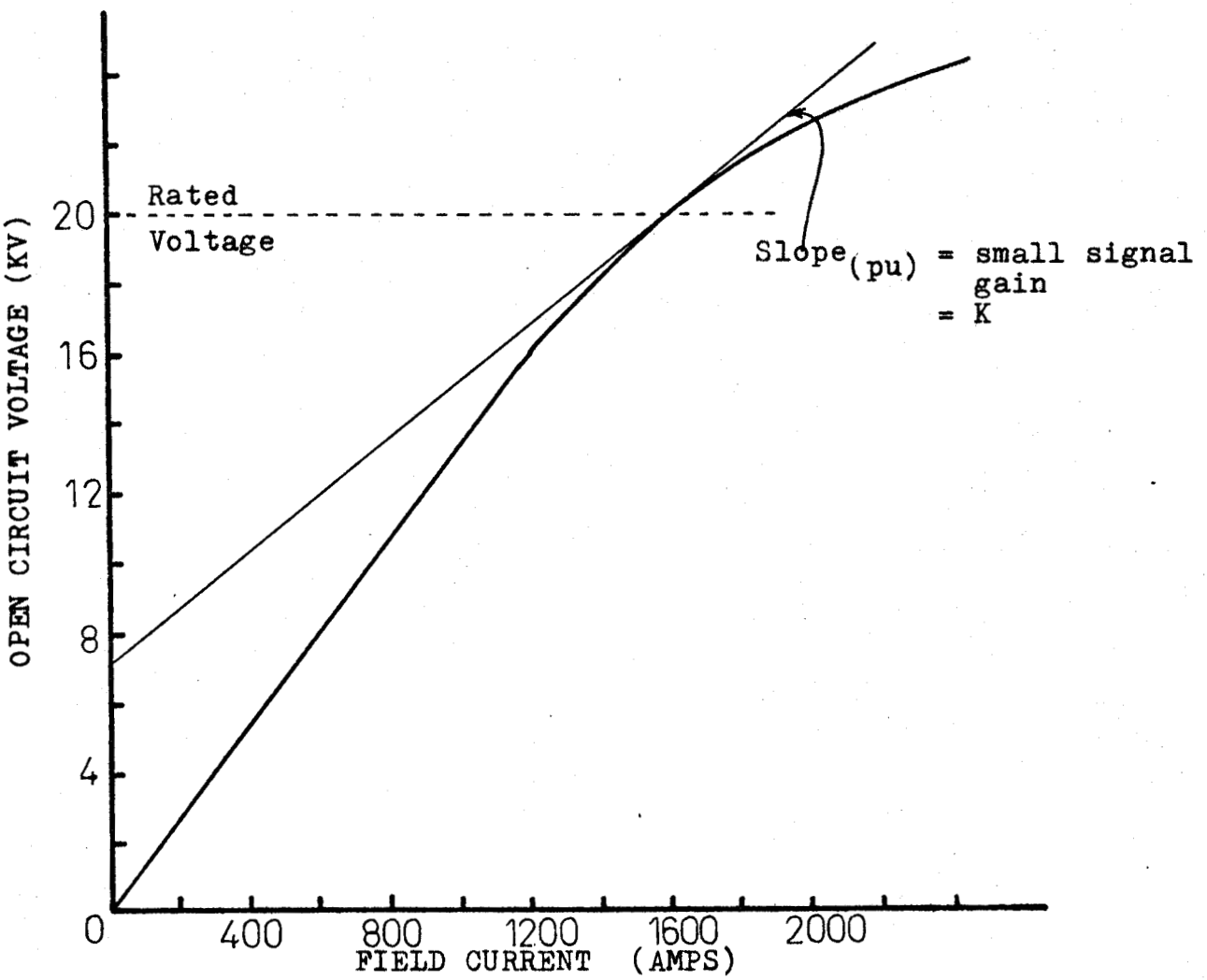

(b) Generator open circuit characteristic

Figure 3.4 Sundance 3 generator open circuit model

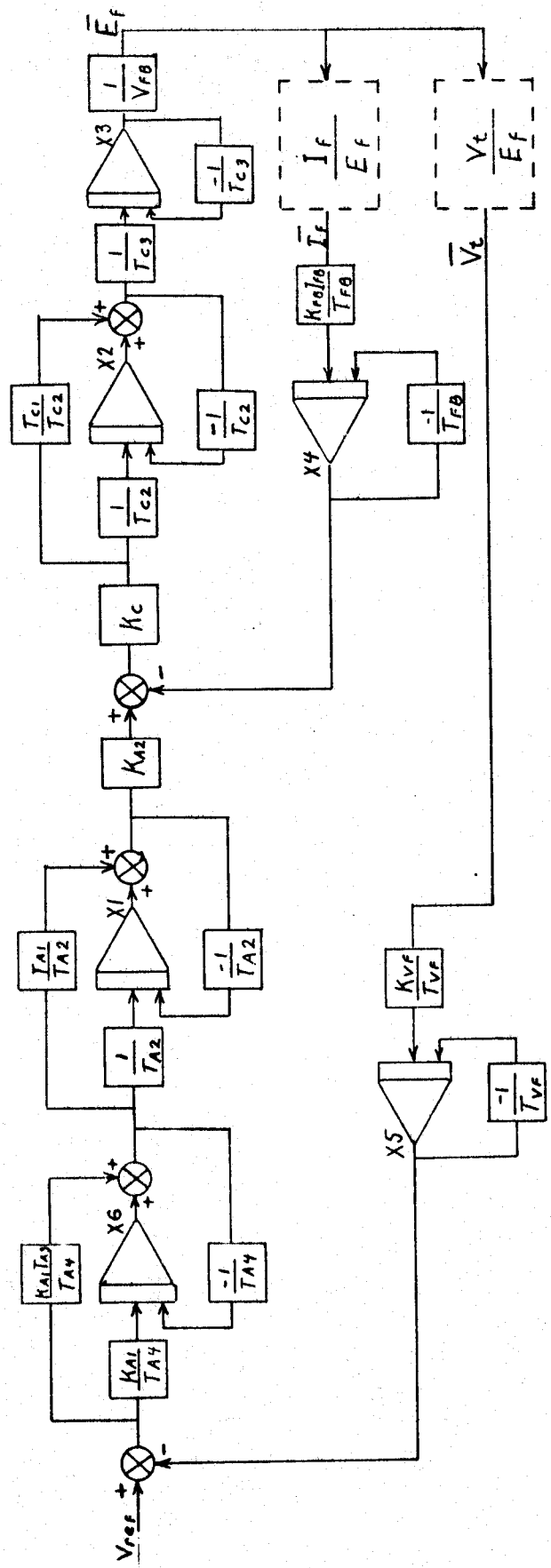

Figure 3.5 Analog circuit of Sundance 3 excitation system

cuit system is first shown to assess the possible influence of a lead-lag compensator. The compensator setting which provides the best location for the dominant system roots is then determined.

The programs used initially in this project to calculate the eigenvalues of the system "A" matrix were the two subroutines "HSBG" and "ATEIG" which are available as part of IBM's Scientific Subroutine Package. These provided fairly consistant results with occasional erroneous values. When one particular system condition produced a "shotgun pattern" effect instead of the usual smooth transition of eigenvalues for the variation of a system parameter, a second set of subroutines was used to verify results. These were the subroutines "EBALAF", "EHESSF" and "EIGRF" which are part of IBM's new IMSL [20] subroutine package. These cleared the problem for this particular system condition. It also became evident that there was a large error in the system high frequency roots calculated by the S.S.P. subroutines. All calculations done up to that point were re-done using the IMSL subroutines.

A root locus plot of the uncompensated system, i.e. with no lead-lag compensation, and with the machine open circuited appears in figure 3.6. This was calculated by finding the eigenvalues of the system matrix for various values of the gain K_{A1}. This gain is actually

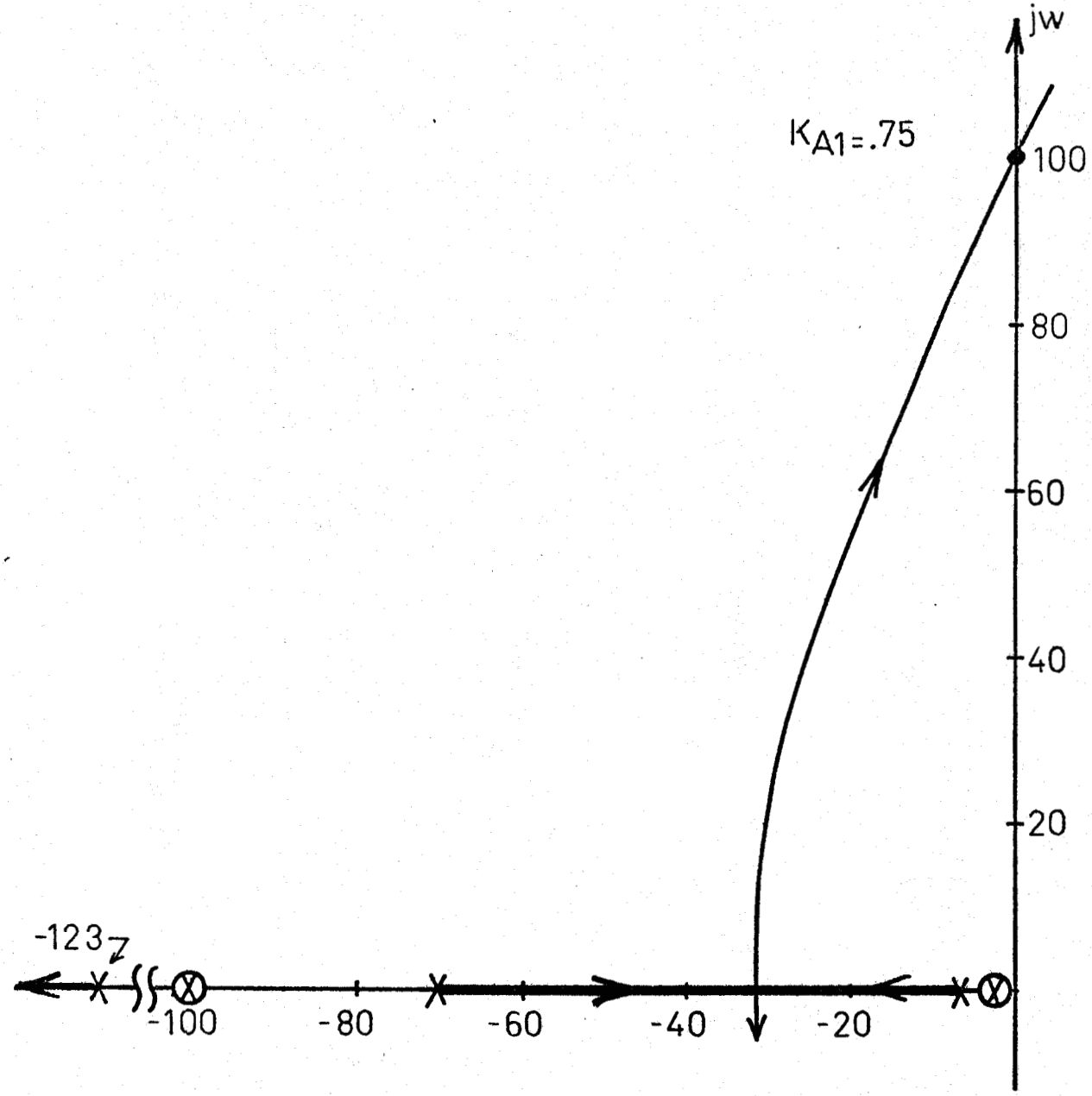

Figure 3.6 Root locus of open circuit system with no series compensation

Note: System gain is set at K_{A1}=0.851
∴System unstable with
no compensation

fixed to a value of .85 by the AVR hardware. It was varied here as a convenient means of analyzing the system for various gains. All other gain coefficients were fixed. The lead and lag compensators were rendered ineffective in this calculation by making their poles and zeros equal. The current feedback gain was set at the manufacturer's suggested setting of

$$K_{FB} = .00267$$

All other gains and time constants were as listed in table 3.1. The power stabilizer signal was set equal to zero.

The root locus diagram shows that the system complex roots cross into the right hand plane for values of $K_{A1} > .75$.

Therefore, series compensation is required to make the system stable at its set gain value ($K_{A1} = .85$).

It appears that lag compensation would be most useful in this case as this would cause the system complex roots for a given value of the gain K_{A1} to move down along the complex pole branches.

If a lag compensator of the form

$$\frac{1+ T_{A1} S}{1+ T_{A2} S} \qquad T_{A2} > T_{A1}$$

is introduced, it has no effect on the system steady state gain. In root locus form, this compensator is

$$\frac{T_{A1}}{T_{A2}} \frac{\left(S+\frac{1}{T_{A1}}\right)}{\left(S+\frac{1}{T_{A2}}\right)} .$$

The system root locus gain is thus reduced by the factor T_{A1} / T_{A2}. If the angle contribution of the lag compensator is small, the shape of the root locus diagram will not be affected. The system root (closed loop pole) corresponding to a fixed value of DC gain (indicated by K_{A1}) will then move downwards along the complex pole path to a new position corresponding to the new root locus gain.

Lead compensation could also be of some use in this case. The angle contribution of a lead compensator would tend to draw the complex root branch to the left, thus increasing damping. A lead compensator would however counteract the desirable reduction of root locus gain introduced by a lag compensator.

These influences of the lead and lag compensators on the dominant system roots are shown in figure 3.7. This illustrates the location of the system complex roots as the compensation is varied. In this case, the system gain is constant with K_{A1} set at the value fixed by the hardware:

$$K_{A1} = .851$$

Each of the branches numbered 1 to 5 corresponds to one of the lead compensator settings shown in the figure. The system root moves along the branches in the direction shown as the lag compensation is decreased, that is, as the lag compensator pole and zero are moved closer together.

The damping factor of these complex roots is defined by:

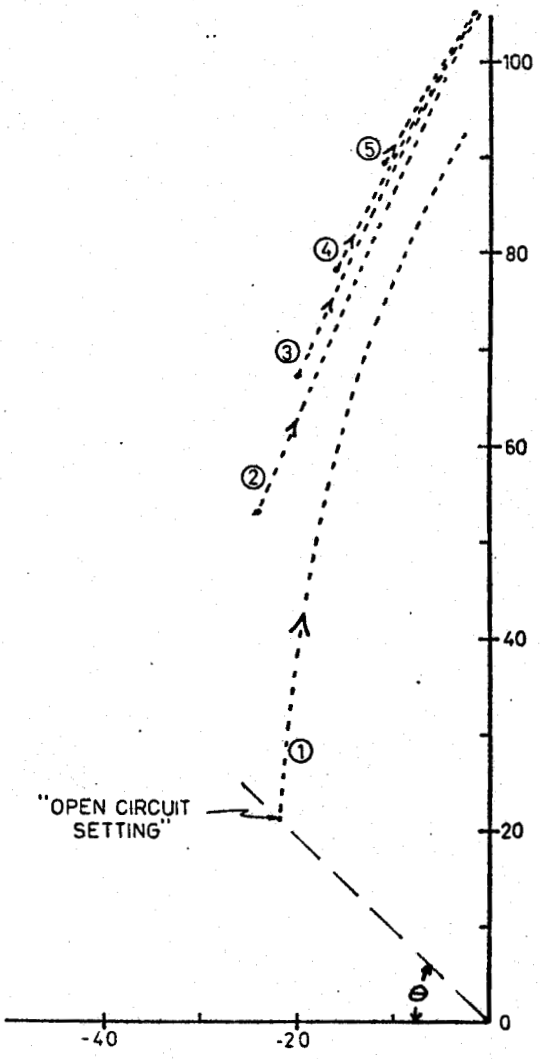

Figure 3.7 Open circuit dominant eigenvalue trajectories for variation of lead-lag compensation. (Arrow indicates direction of root for decreasing amount of lag compensation).

(1) $\frac{1 + .039\ S}{1 + .039\ S}$

(2) $\frac{1 + .1\ S}{1 + .039\ S}$

(3) $\frac{1 + 16\ S}{1 + .039\ S}$

(4) $\frac{1 + .22\ S}{1 + .039\ S}$

(5) $\frac{1 + .28\ S}{1 + .039\ S}$

The trajectories correspond to the above lead compensator settings.

$$\zeta = \cos \theta$$

where θ is the angle shown in figure 3.7. It gives a direct indication of the oscillatory nature of the time response. A very small damping factor indicates a very oscillatory response (for $\zeta = 0$, the response is purely oscillatory, with no damping). If the imaginary part of the complex root is reduced to zero, the damping factor is 1.0. For this case, the time response of the system to a step disturbance is non oscillatory with no overshoot but with a longer rise time.

In this system, the best root location occurs with minimum lead and maximum lag compensation, that is, with the lead compensator set at:

$$\frac{1 + T_{A3} S}{1 + T_{A4} S} = \frac{1 + .039 S}{1 + .039 S}$$

and the lag compensator at:

$$\frac{1 + T_{A1} S}{1 + T_{A2} S} = \frac{1 + .0875 S}{1 + 1.0875 S}$$

The system dominant roots are at $22. \pm j21.$ and have a damping factor of 0.7. The time domain response with this setting should therefore be excellent.

These settings are identical to those suggested by Calgary Power. The previous analysis therefore verifies the present tuning procedure for AVR's.

It is interesting to examine the root locus diagram of the compensated system with the above settings. This is shown in figure 3.8. Note that no significant

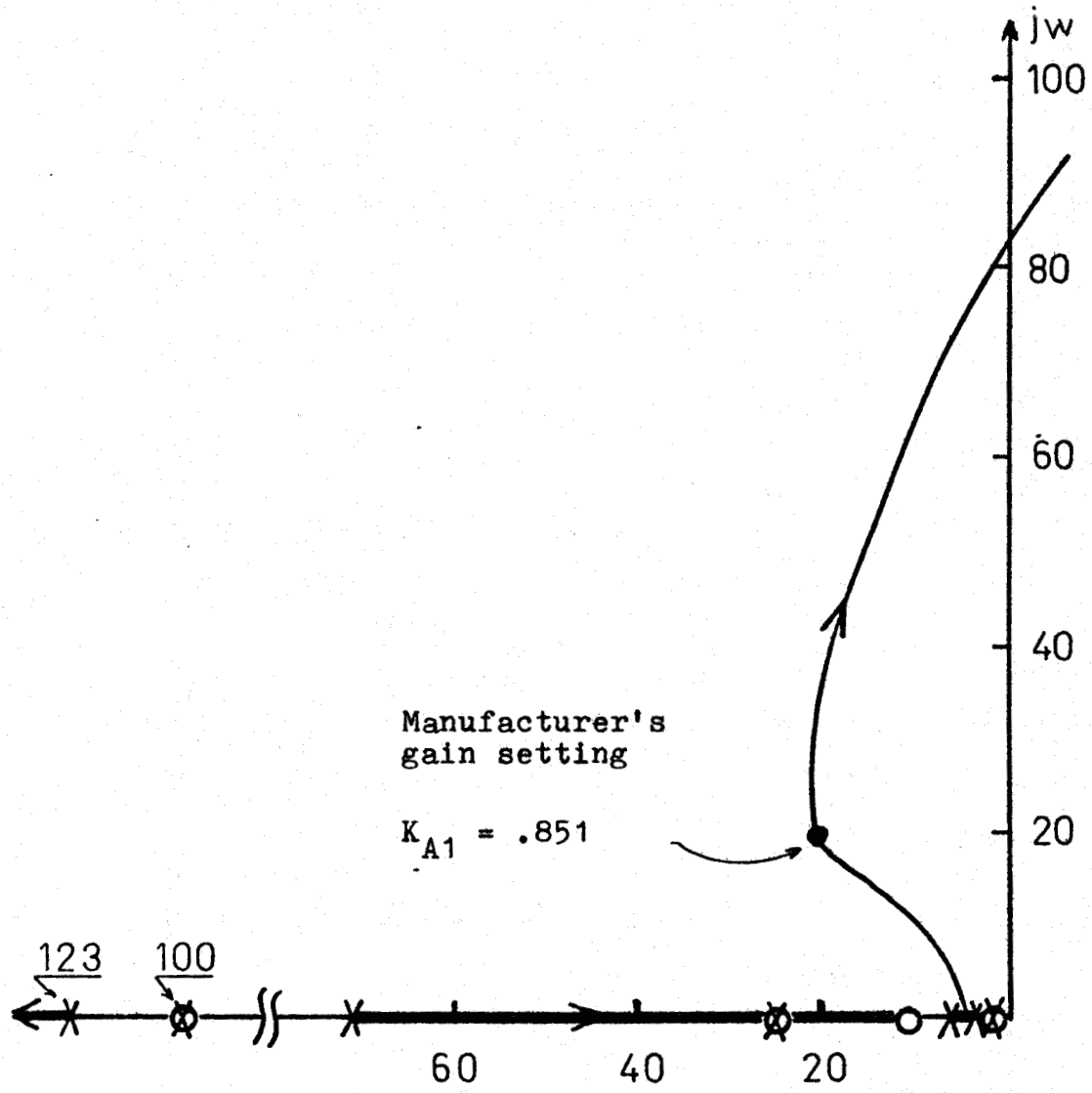

Figure 3.8 Root locus of open circuit system with lag compensation

improvement in response could be achieved with a change in system gain.

3.3.4 Adjusting the Current Feedback

The question of the effect of the amount of current feedback in the exciter now arises. The current feedback gain K_{FB} has a range of settings of:

$$0.0 < K_{FB} < .003$$

The manufacturer's suggested setting is

$$K_{FB} = .00267$$

Figure 3.9 shows the effect on the dominant system roots of variations in K_{FB}. The series compensator setting is as previously determined. It can be seen from the figure that a modification of the manufacturer's suggested setting for K_{FB} would not result in an appreciable benefit.

3.3.5 Time Domain Performance

The state space model derived to find the eigenvalues of the system can also be used to run digital time domain simulations of the system response.

Figure 3.10 shows the response of the system to a .01 PU step voltage signal disturbance introduced at the machine terminals. The lead lag settings used were those found in the previous section and the current feedback was as suggested by the manufacturer. In the simulation, the initial conditions were all set to zero. This explains the .0097 PU steady state level of the response. As was expected the response is smooth with some overshoot but

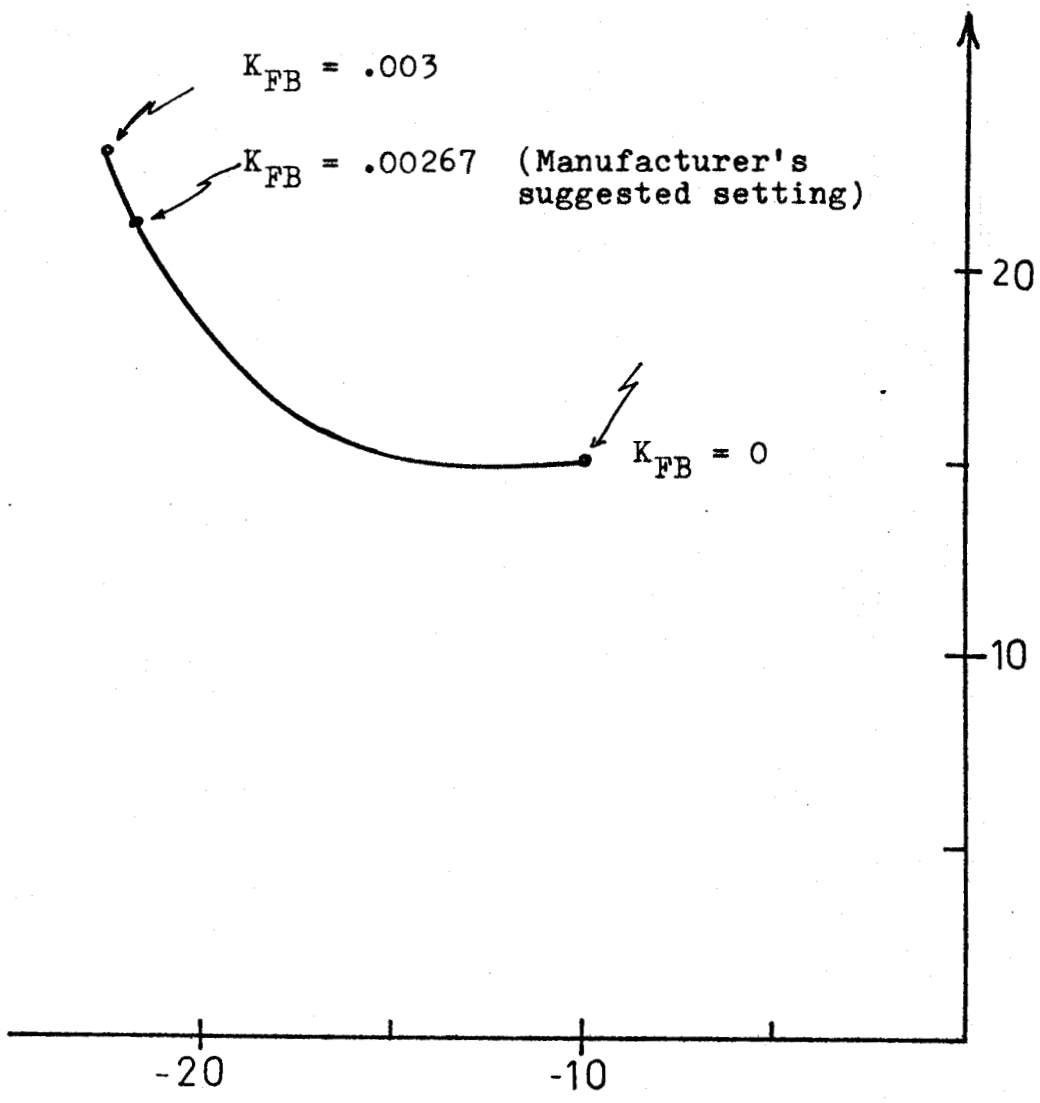

Figure 3.9 Effect of current feedback on dominant open circuit system root.

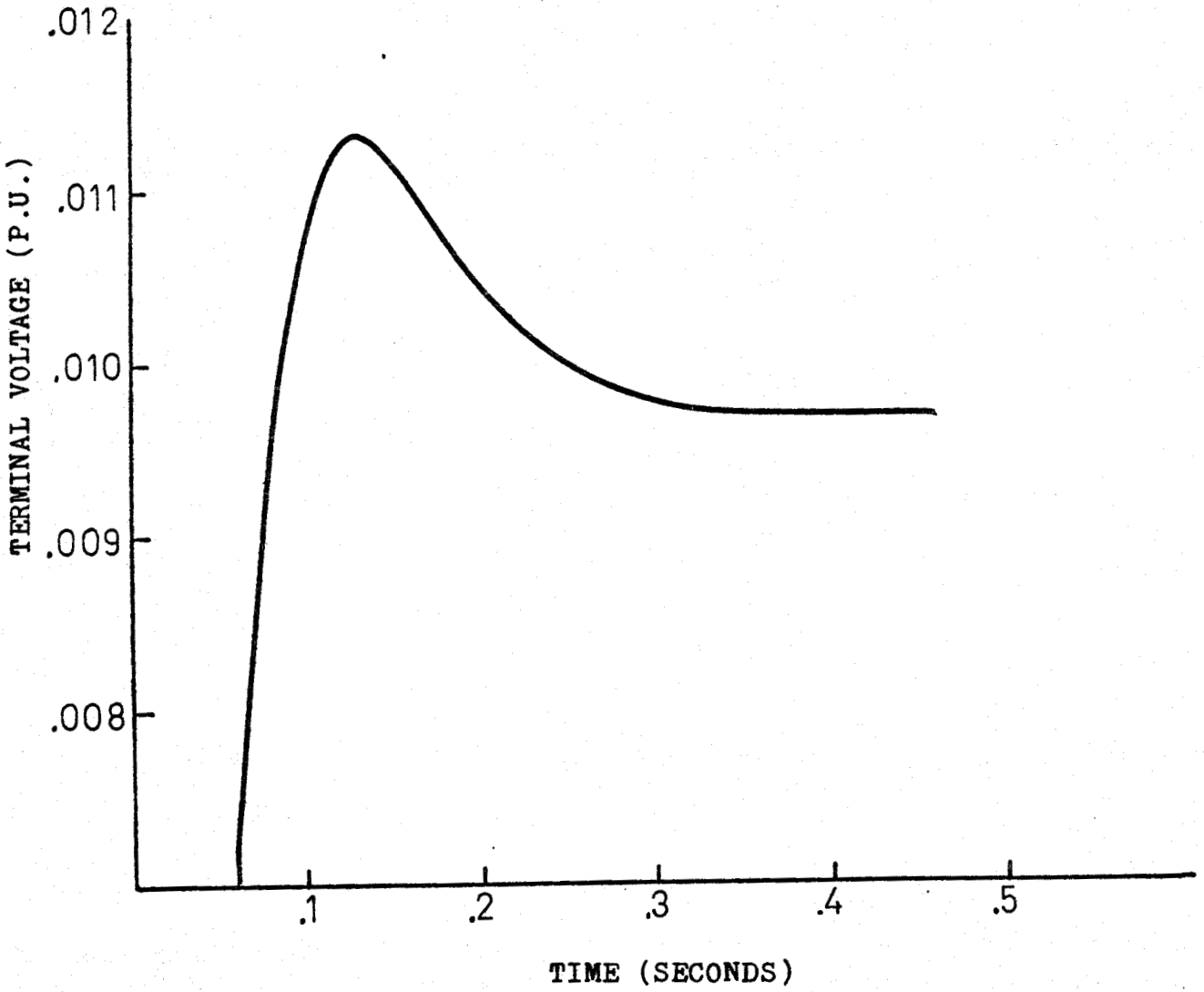

Figure 3.10 Voltage step response of open circuit system with "open circuit settings"
Voltage shown is change from steady state

with no oscillations occurring.

This section has established the "base case" settings of the AVR, that is, those settings that will provide the best system response with the machine open circuited. These settings will also be referred to as the "open circuit settings". The next step is the tuning of the AVR for best operation at full load.

3.4 Tuning the AVR for On-Line Conditions

3.4.1 Introduction

With the on-line generator model developed in chapter 2 for the Sundance plant, it is possible to go beyond the normal procedure of tuning the AVR for open circuit conditions only. In this section, the state space model of the on-line system is used to determine AVR settings which improve the system performance with the machine fully loaded without adversely affecting the open circuit operation.

3.4.2. The On-Line System Model

In order to obtain a state space model of the loaded machine, an analog circuit is first developed.

The machine transfer functions found in chapter 2 was put in the general form:

$$\frac{K(b_{n-1}\ S^{n-1} + b_{n-2}\ S^{n-2} + \ldots + b_1\ S + bo)}{S^n + a_{n-1}\ S^{n-1} + \ldots + a_1\ S + a_o}$$

That is:

$$\frac{V_t}{E_f} = \frac{.08557\ (S^3 + 4.6\ S^2 + 144.1\ S + 229.7)}{S^4 + 5.84\ S^3 + 135.1\ S^2 + 384.5\ S + 143.5}$$

$$\frac{I_f}{E_f} = \frac{.952\ (S^2 + 2.96\ S + 54.76)}{S^3 + 3.275\ S^2 + 133.4\ S + 52.9}$$

The corresponding analog circuits are shown in figures 3.11 and 3.12. As in the circuit shown previously, the summers and integrators do not invert the signal.

These two circuits are combined with the analog model of the excitation system shown in figure 3.5. This results in a 13th order system for which the state equations can be written directly.

3.4.3 Tuning the lead lag compensator:

The procedure used to tune the AVR in this case is the same as was used for open circuit conditions. The only difference is the model used for the generator.

A root locus diagram of the Sundance 3 voltage control system with the generator fully loaded appears in figure 3.13. This illustrates the closed loop root locations as the system open loop gain is varied from zero to infinity. The series compensator and current feedback settings are as determined in section 3.3 for best open circuit operation.

The dominant roots of this system are determined by the relative location of the roots and by their resi-

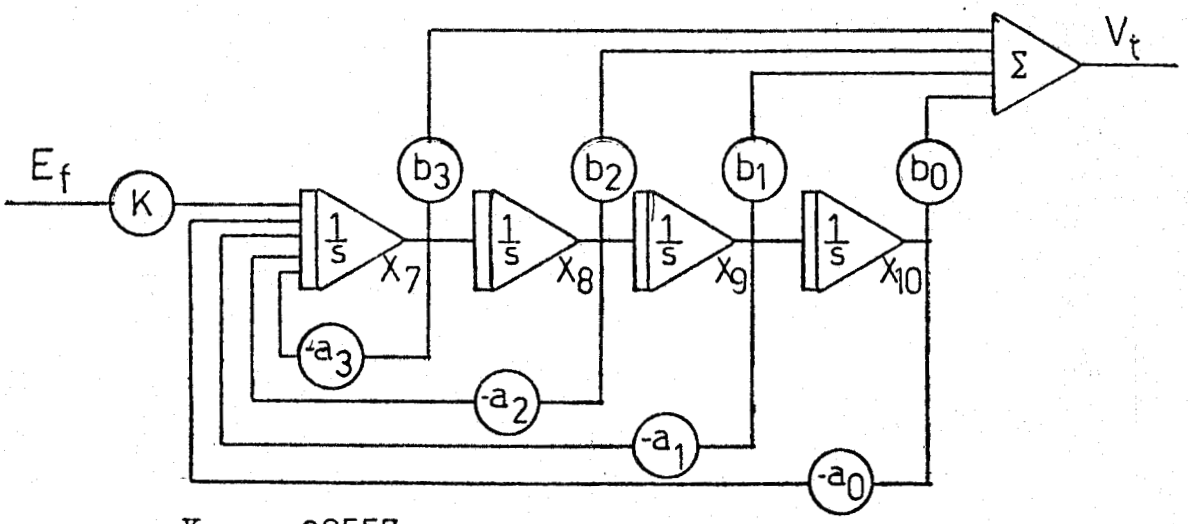

$K = .08557$

$a_o = 143.5$
$a_1 = 384.5$
$a_2 = 135.1$
$a_3 = 5.84$

$b_o = 229.7$
$b_1 = 144.1$
$b_2 = 4.6$

Figure 3.11 Analog circuit of V_t / E_f

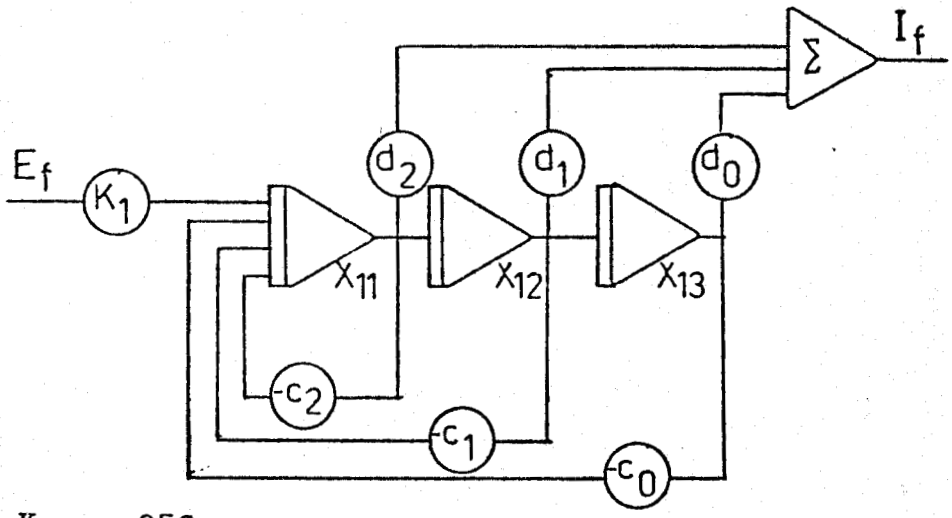

$K_1 = .952$
$C_o = 52.9$
$C_1 = 133.4$
$C_2 = 3.275$

$d_o = 54.76$
$d_1 = 2.96$
$d_2 = 1.0$

Figure 3.12 Analog circuit of I_f / E_f

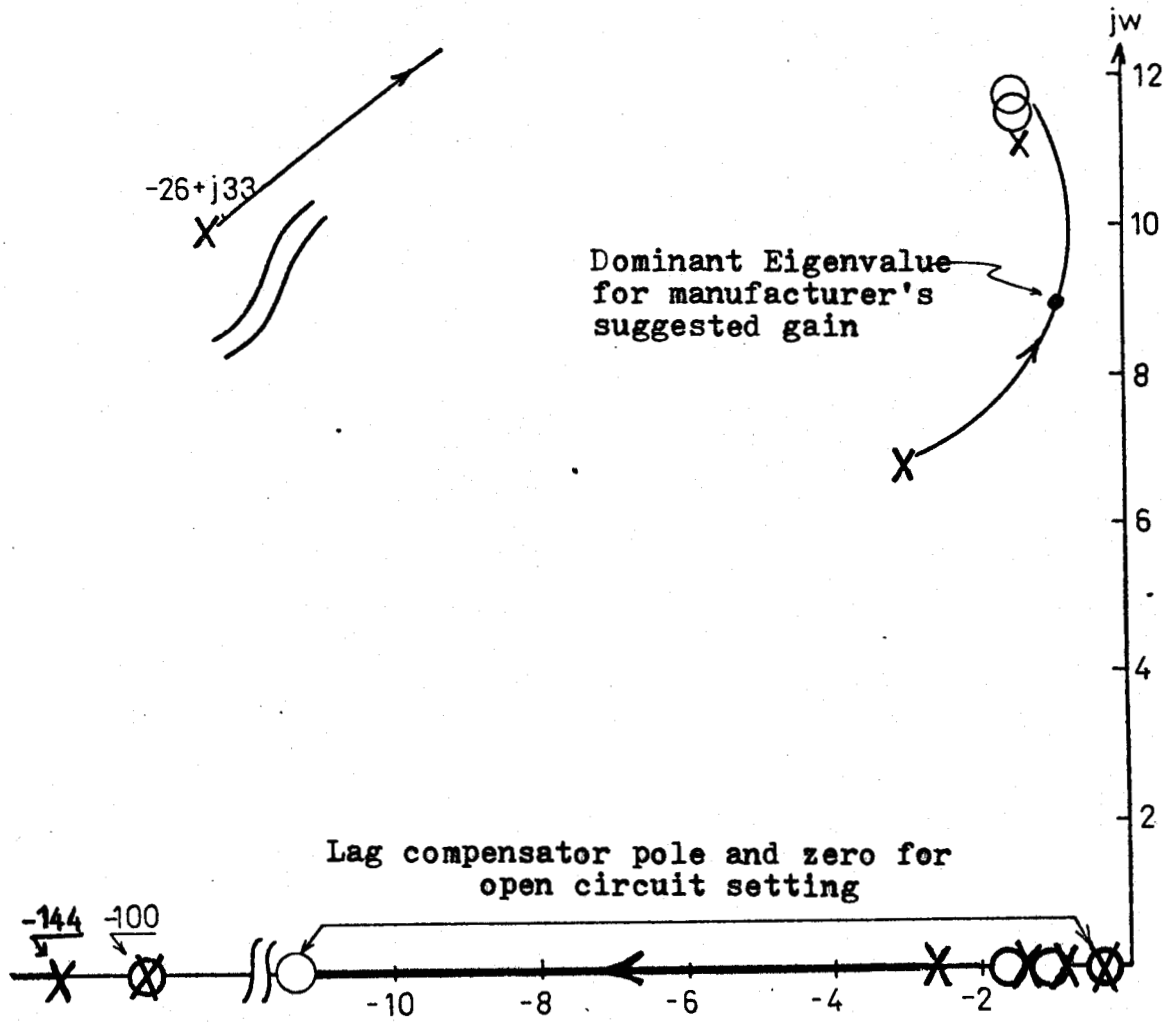

Figure 3.13 Root locus of on-line system with open circuit settings

dues. Roots that are far from the imaginary axis contribute components that have very small time constants in the system real time response. These roots are therefore negligible. The relative magnitude of the component contributed to the time response by a root is determined by the residue at that root. Residues can be calculated graphically on an S plane plot of the system closed loop poles and zeros. For any given configuration, the magnitude of the residue at a pole is given by:

$$\frac{\pi \text{ (Distances from closed loop zeros to the pole)}}{\pi \text{ (Distances from the other closed loop poles to the pole)}}$$

From this, it can be seen that if a system closed loop zero is very close to a pole, the residue at that pole will be very small. The effect of that pole on the system time response will be correspondingly small.

Figure 3.14 is a closed loop pole zero plot of the Sundance voltage control system with the on-line machine model. The dominant roots of this system can be easily determined. The poles far to the left, including the one at $-7.7 \pm j0.$, contribute fast decaying time domain components. The poles on the real axis close to the origin and the complex pole pair at $-1.4 \pm j11.1$ have very small residues due to the nearby zeros. The dominant roots of this system are therefore the complex pair of roots at $-.9 \pm j\ 8.9$. This pair of roots has a very small damping factor ($\zeta = 0.1$) and it can be expected that the time domain response of the system will be quite oscillatory.

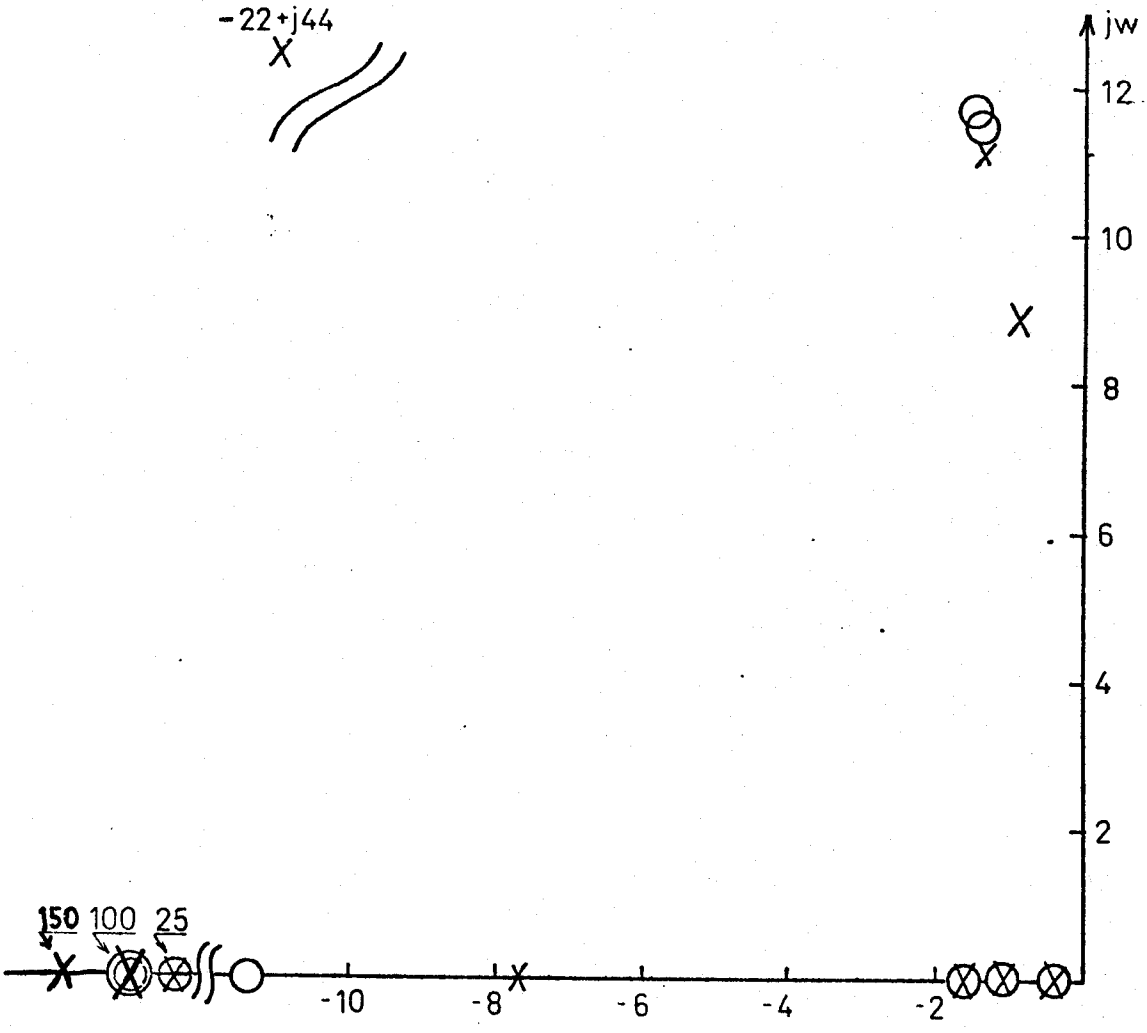

Figure 3.14 On-line system closed loop poles and zeros

The root locus diagram of figure 3.13 can now be used to illustrate how the dominant system roots can be influenced. One method of increasing the damping factor of the dominant root is to reduce the system gain. This would draw the root down towards the open loop pole at $(-3.1 \pm j7)$. The AVR gain is usually determined by the requirement to drive the field voltage to ceiling for a given voltage error. If possible, it is desirable to set the AVR for better on-line operation without modifying the system gain.

The lead-lag compensator can be used to some advantage here. The angle contribution of a lead compensator would tend to draw the locus of the dominant system root to the left. The reduction of the "root locus gain" caused by lag compensation would also draw the root down along its path.

The effect on the dominant root of varying the lead and lag compensator settings over the physically available range is shown in figure 3.15. Each of the branches numbered 1 to 5 is the locus of the root for a given lead setting as the lag compensator angle contribution is decreased. The first point on path #3 is selected as the best setting. At this point the damping factor is increased to 0.18. The compensator settings corresponding to this point are:

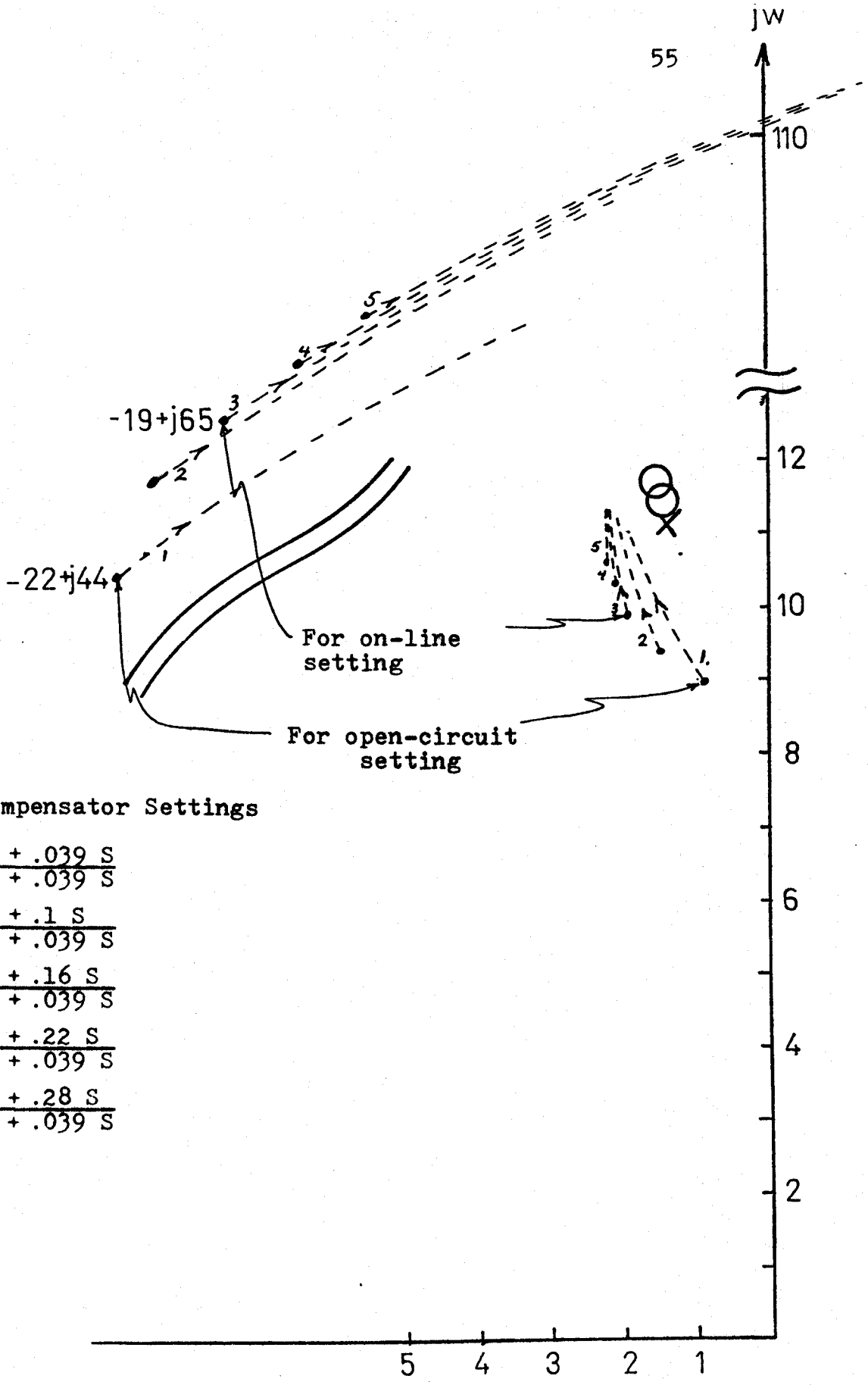

Lead Compensator Settings

1 $\frac{1 + .039\ S}{1 + .039\ S}$

2 $\frac{1 + .1\ S}{1 + .039\ S}$

3 $\frac{1 + .16\ S}{1 + .039\ S}$

4 $\frac{1 + .22\ S}{1 + .039\ S}$

5 $\frac{1 + .28\ S}{1 + .039\ S}$

Figure 3.15 On-line system eigenvalue trajectories for variation of lead lag compensation. Each trajectory shown is for a fixed lead setting; the eigenvalues move in the direction shown as lag compensation is decreased.

$$\text{lead:} \quad \frac{1+T_{A1}S}{1+T_{A2}S} = \frac{T_{A1}\left(S+\frac{1}{T_{A1}}\right)}{T_{A2}\left(S+\frac{1}{T_{A2}}\right)} = \frac{25.6\ (S+6.3)}{6.3\ (S+25.6)}$$

$$\text{lag:} \quad \frac{1+T_{A3}S}{1+T_{A4}S} = \frac{T_{A3}\left(S+\frac{1}{T_{A3}}\right)}{T_{A4}\left(S+\frac{1}{T_{A4}}\right)} = \frac{.9\ (S+11.4)}{11.4\ (S+.9)}$$

Thus the amount of lag compensation that was used for the "open circuit setting" is unchanged but some lead compensation is added.

Before going on to the resulting time domain performance of the system, the effect of current feedback must be examined.

3.4.4 Effect of Current Feedback

The effect of varying the current feedback gain K_{FB} on the system dominant roots is shown in figure 3.16. The range of settings determined by the hardware is:

$$0.0 < K_{FB} < .003$$

The manufacturer's suggested setting is

$$K_{FB} = .00267$$

No improvement in the damping factor of the dominant system root can be achieved by modifying the suggested current feedback setting. This is the case for both the open circuit setting and the on-line setting of the lead-lag compensator. However, as the value of K_{FB} is reduced, the dominant roots migrate towards the system closed loop

zeros. The residue at the system roots is therefore reduced, thus improving the system response.

It was mentioned earlier that the field current feedback is required to insure equal load sharing by the four thyristor bridges. A reduction in the value of K_{FB} aimed at improving the dynamic response of the system results in a slower return to equal load sharing by the bridges after a disturbance. These two factors must therefore be considered in arriving at a setting for K_{FB}.

The time domain performance of the system for the settings determined in this section will now be examined. In all simulations the value of K_{FB} is kept at the manufacturer's suggested setting.

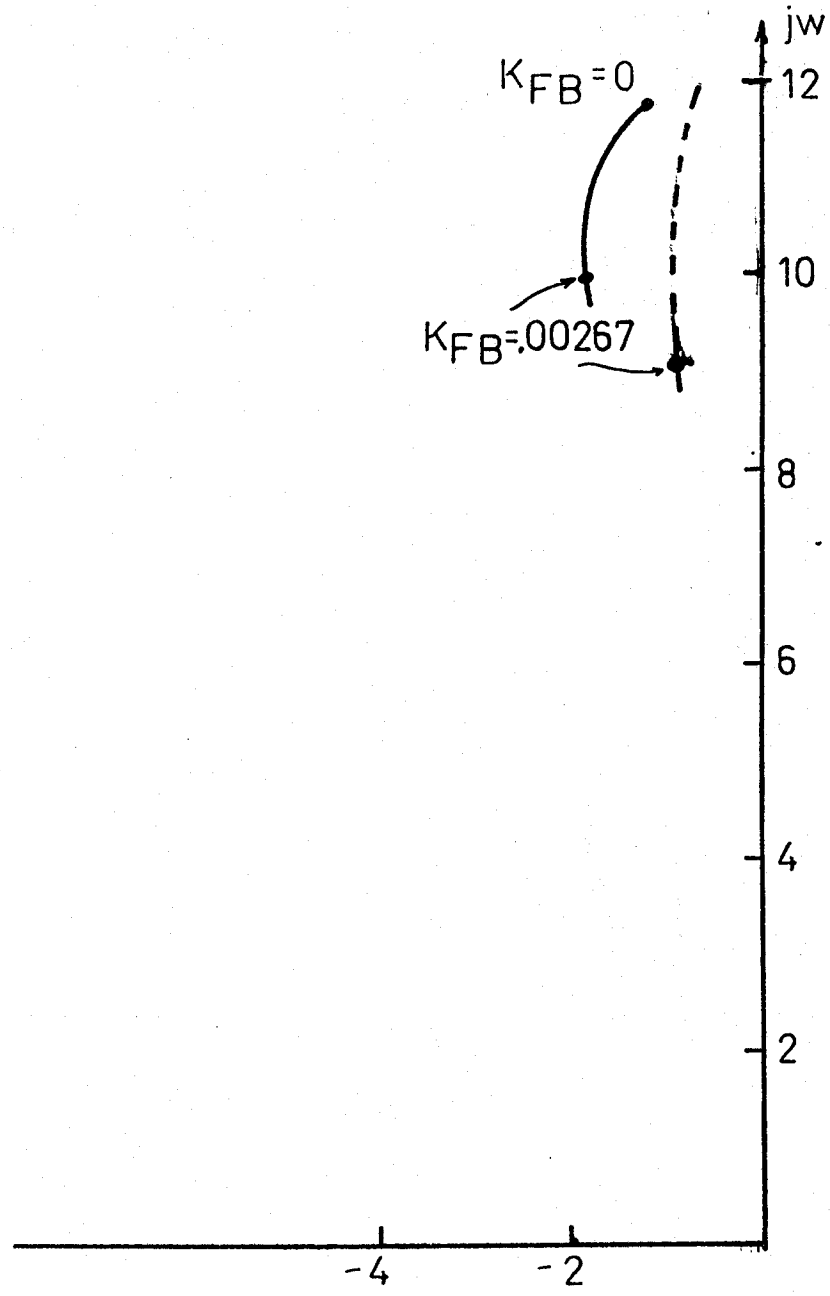

Figure 3.16 Effect of Current feedback on dominant on-line system eigenvalue

_____ with "on-line" lead lag setting

- - - - with "open circuit" setting

3.4.5 System Time Domain Performance

The time domain responses of the on-line system were obtained using the 13th order model derived earlier and also with a simulation of the Alberta Power System using the transient stability program USTRAN. The system was also simulated at open circuit conditions using the reduced order model.

The terminal voltage response to a .01 PU voltage step disturbance with the machine fully loaded is shown in figure 3.17. This is the result of a simulation of the 13th order model with a disturbance introduced at the terminals of the machine and with all initial conditions set to zero. The two curves shown in the figure correspond to the two AVR settings obtained when the system is tuned for best open circuit operation and for best on-line operation. The damping is significantly increased in the second case. One performance evaluation criterion that can be used is the time required for the response to settle to $\pm 5\%$ of the steady state level. For the open circuit setting this time is:

$$T_{SS} \text{ (open cct)} = 1.9 \text{ Sec.}$$

and for the on-line setting it is:

$$T_{SS} \text{ (on-line)} = 0.8 \text{ Sec.}$$

The settling time of the terminal voltage is therefore reduced to less than half of its original value if the AVR is tuned to on-line conditions.

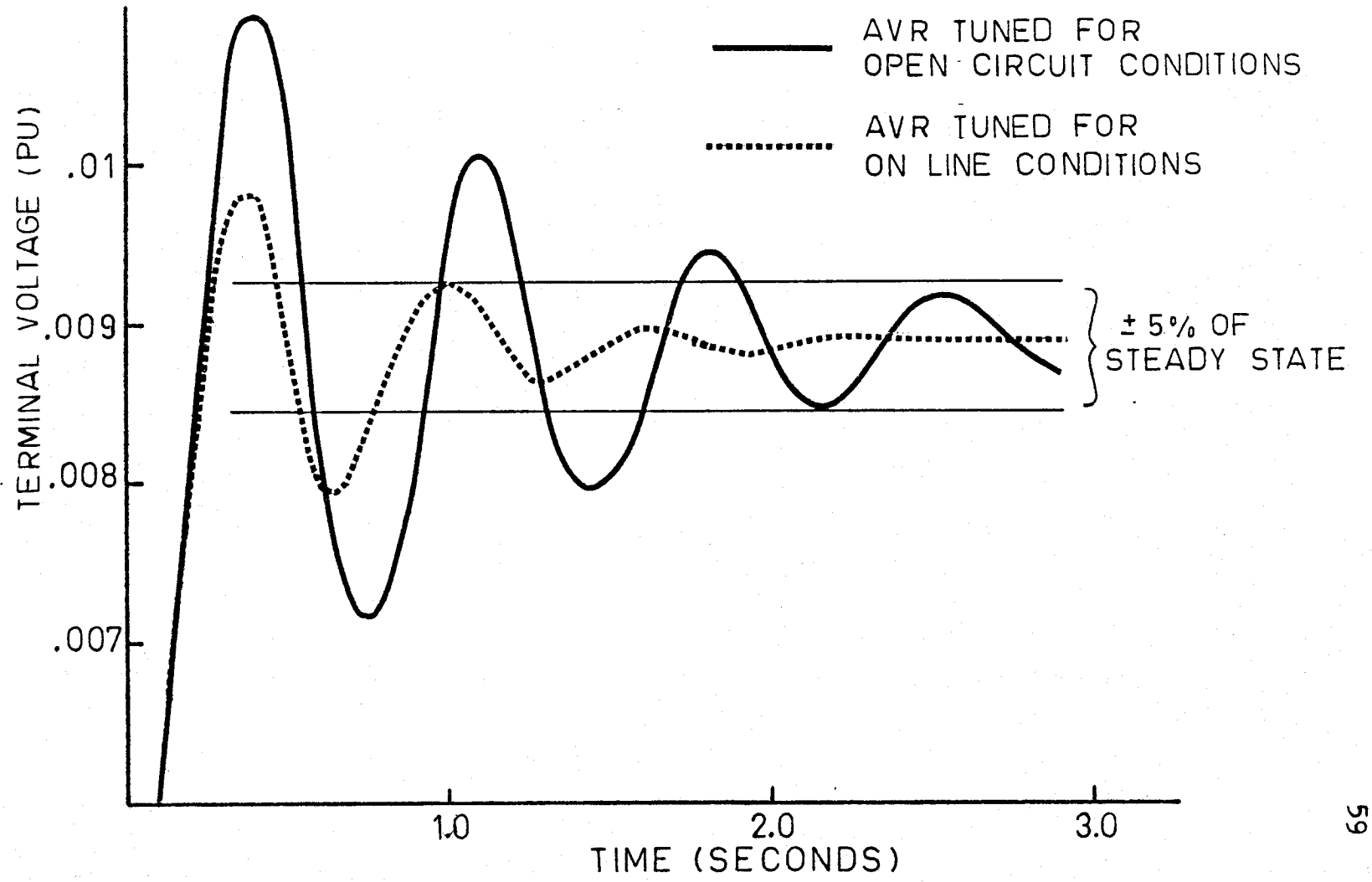

Figure 3.17 **Full load voltage step response with on-line lead lag compensator setting**
Voltage shown is change from steady state

In the real world, a generating unit is rarely subjected to step changes in reference voltage. A more realistic test of the new settings was carried out by simulating the response to a line outage of the Calgary Power system with the USTRAN transient stability program. In this way the disturbance introduced at Sundance is essentially a sudden change in power demand.

There is a second important advantage of using the USTRAN program to test the new setting of the AVR. In the design procedure, a single-input single-output model of the Sundance system was assumed in order to permit the use of conventional control theory. A generator, with its speed and voltage controls, is actually a complex multiple input multiple output system. The detailed models used in the USTRAN program take this into account. Thus, testing the new settings with the transient stability program verifies that the simplifying assumption made for design purposes is acceptable.

The responses obtained are shown in figure 3.18. As in the reduced order model simulations, the damping is improved significantly with the on-line setting. In order to measure the settling time of the response, a convenient band to use in this case is $\pm 0.2\%$ of steady state voltage. With this specified band, the settling time is reduced to one third of its original value, i.e. from 5.4 seconds to 1.8 seconds.

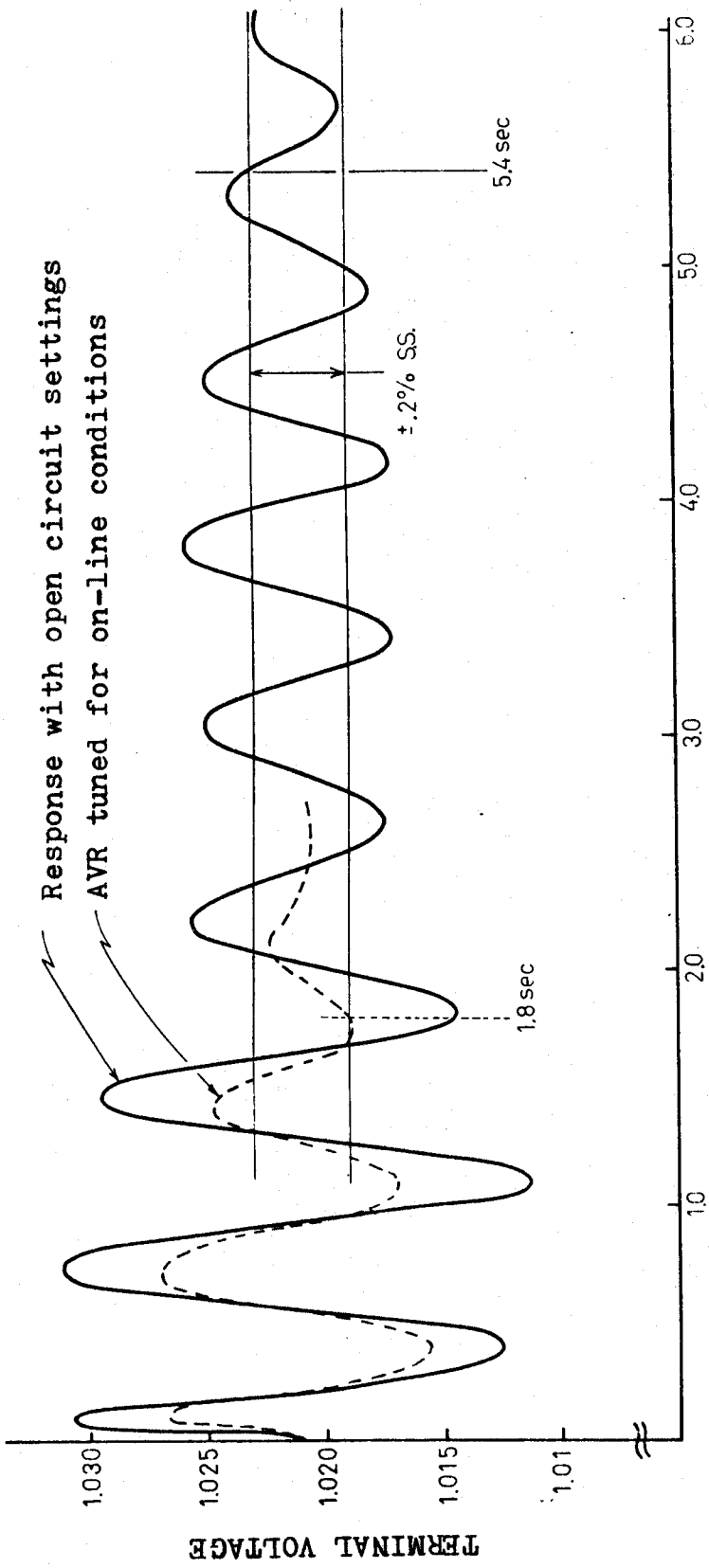

Figure 3.18 Full load voltage response after a line outage with on-line lead lag settings

There remains to verify that the system is still stable when the machine is open circuited. The open circuit responses shown in figure 3.19 were obtained from a simulation of the 7th order model used in section 3.3. Again, a .01 P.U. terminal voltage disturbance was used with all initial conditions set to zero.

The response of the system with the AVR tuned for on-line conditions is much more oscillatory. However the rise time is shorter. Also, if the settling time to ± 5% of steady state is again used as a performance criterion, the system performs much better with on-line settings. The least that can be said is that the open circuit performance with on-line settings is quite acceptable.

3.4.6 Effect on Power Oscillations

The studies described up to this point have been aimed at improving the damping of terminal voltage oscillations of a fully loaded machine. Changes in the voltage control loop of a generator are bound to have an effect on the speed control loop. It is worthwhile, and even necessary, to verify the effect of changes in the AVR on the damping of power oscillations in the system.

The real power oscillations at the Sundance 3 unit caused by a line outage in the system are shown in figure 3.20. These curves were calculated by a USTRAN simulation of the Alberta Power System.

It appears that the standard procedure of tuning

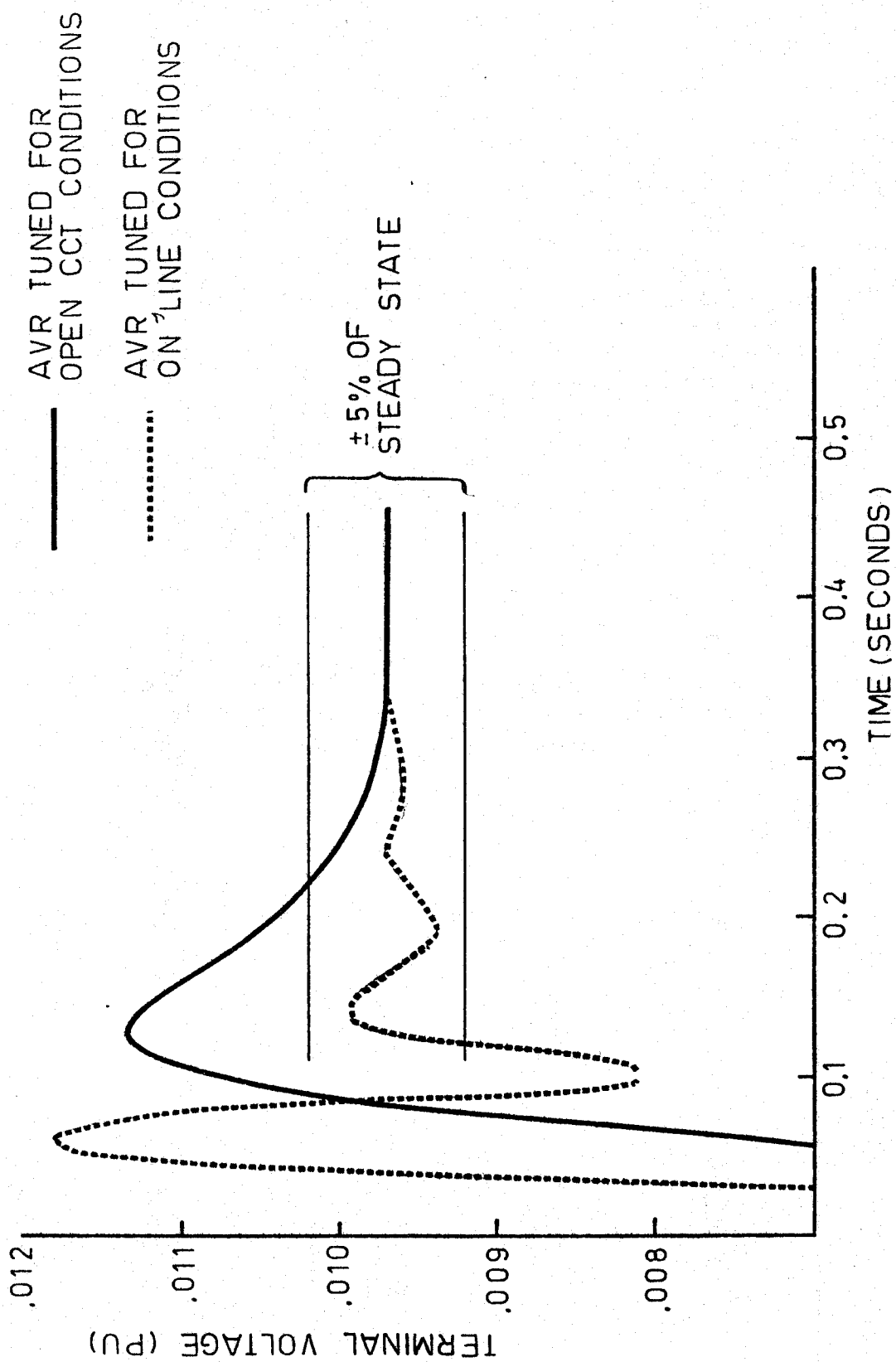

Figure 3.19 Open circuit step response with on-line lead lag settings

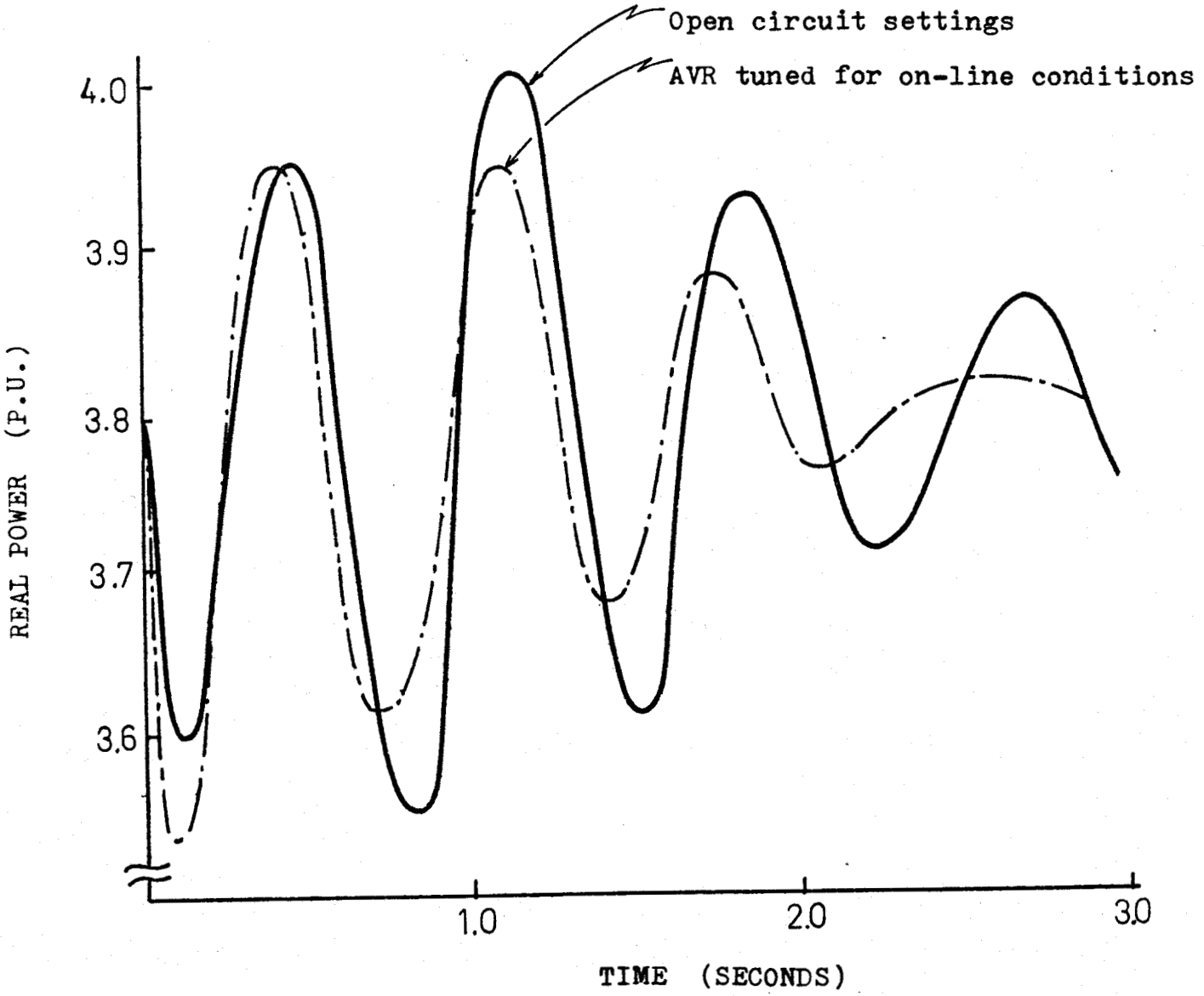

Figure 3.20 Full load real power oscillations after a line outage with on-line lead lag settings

AVR's for open circuit conditions has in this particular case an adverse effect on machine power oscillations. This is demonstrated by the increased damping resulting from the on-line tuning of the AVR.

The effect of the different AVR settings on the system performance where a power stabilizer is included has not been studied. It is strongly suspected however that the effect of on-line AVR settings would once again be beneficial when used in conjunction with a properly tuned power stabilizer.

It has been demonstrated in this chapter that it is possible to improve the dynamic performance of a generator by tuning its excitation system for on-line conditions rather than for open circuit conditions. At this point, it is worthwhile to note that although significant improvement in system performance has been achieved without modifying the existing hardware, there are definite limits to what can be done. This is best seen on the eigenvalue plot of figure 3.15. The dominant root location has been improved but no amount of lead lag compensation could provide further improvement.

Other forms of compensators are available that have the potential of providing much greater improvement than was shown here. These compensators are investigated in the next chapter.

4. TUNING THE SUNDANCE 3 AVR USING COMPLEX COMPENSATORS

4.1 Introduction

In chapter three, an attempt was made to improve the on-line dynamic performance of the Sundance 3 voltage control system. Although lead-lag compensation was capable of significantly improving system response, it was pointed out that there are definite limits to the possible improvement. The purpose of the lead-lag compensation was to improve the dominant system root locations, that is, to improve the damping factor of those roots. However, it was not possible to move the dominant roots by a large amount because of the configuration of the root locus diagram of the system.

In such a case, there exists another method of improving system response. With this method an attempt is made to reduce the residue of the dominant root so that the root will have less effect on the system time response. To do this, a series compensator that has a pair of complex zeros at the same location as the system dominant roots, is introduced.

Such a compensator has been used by Raczkowski et al [21], [22], [23]. They have shown that a complex

root compensator can be used effectively to raise the steady state stability limit of a generating plant. In this chapter an investigation of the effects of a complex compensator added to the Sundance 3 AVR is described. The emphasis here is placed on the possible improvement in on-line performance of the voltage control system.

Two possible root configurations for the complex compensator are discussed. These are first described in general terms. Then, for each case, the compensator is tuned for the Sundance plant and the resulting time domain performances, both at full load and at open circuit, are given.

4.2 General Description

The transfer function of a complex compensator is:

$$\frac{Y}{X} = \frac{K(1 + C_1 S + C_2 S^2)}{(1 + C_3 S + C_4 S^2)}$$

Its poles and zeros can be real or complex conjugate pairs. A compensator with such a transfer function can be implemented by a bridged-T network (24) such as the one shown in figure 4.1. It can also be implemented with an active network such as the analog circuit of the compensator shown in figure 4.2.

As mentioned earlier the advantage of such a compensator is that its zeros can be placed directly over

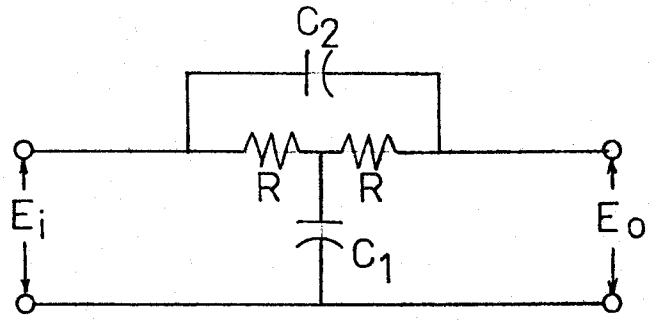

$$\frac{E_o(S)}{E_i(S)} = \frac{RC_1RC_2S^2 + 2RC_2S + 1}{RC_1RC_2S^2 + (RC_1+2RC_2)\,S + 1}$$

Figure 4.1 Bridged-T network implementation of complex compensator

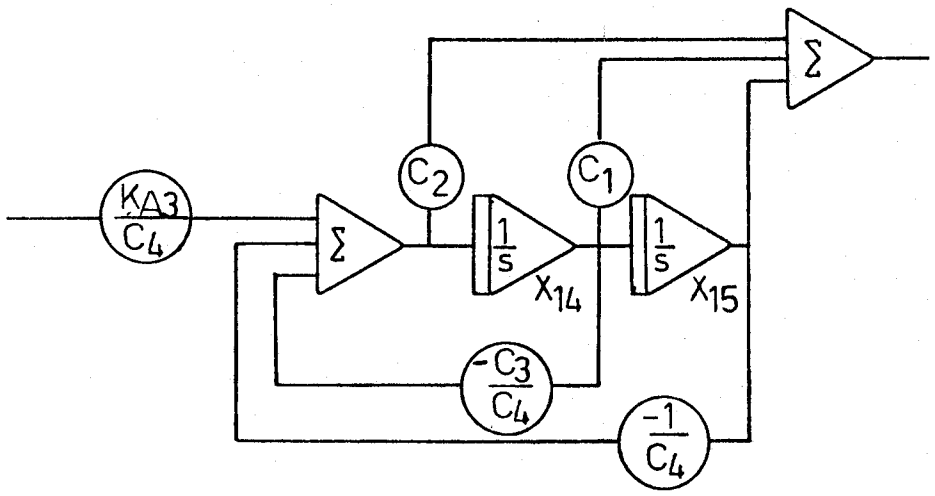

Figure 4.2 Analog circuit of complex compensator

Note: Amplifiers do not invert signal

the plant dominant roots. If the plant model and compensator settings are accurate, the actual plant dominant roots are essentially cancelled at the operating point studied. With a system such as the one studied here, there are two approaches that can be used in setting the location of the compensator poles. These are illustrated in figure 4.3. The locus of the dominant root of the Sundance voltage control system for variation of the open loop gain appears in figure 4.3(a). This was determined in the previous chapter. In figure 4.3(b), the complex compensator is added and set so that its complex zeros are on the system open loop poles. The compensator poles are then placed somewhere to the left, resulting in a modified form of the root locus. The dominant system roots now lie somewhere on the new branch shown. Their specific location can be adjusted by varying the system gain or by adding real root compensation.

The second method of setting the complex compensator is shown in figure 4.3(c). In this case, the compensator poles and zeros are placed over the system zeros and poles. In this way the closed loop poles are fixed at one location for all values of system gain. The residue at both sets of poles is thus made very small. This reduces the effect of both pairs of roots on the time response.

It should not be forgotten that there still exists a system root at the locations shown, although it

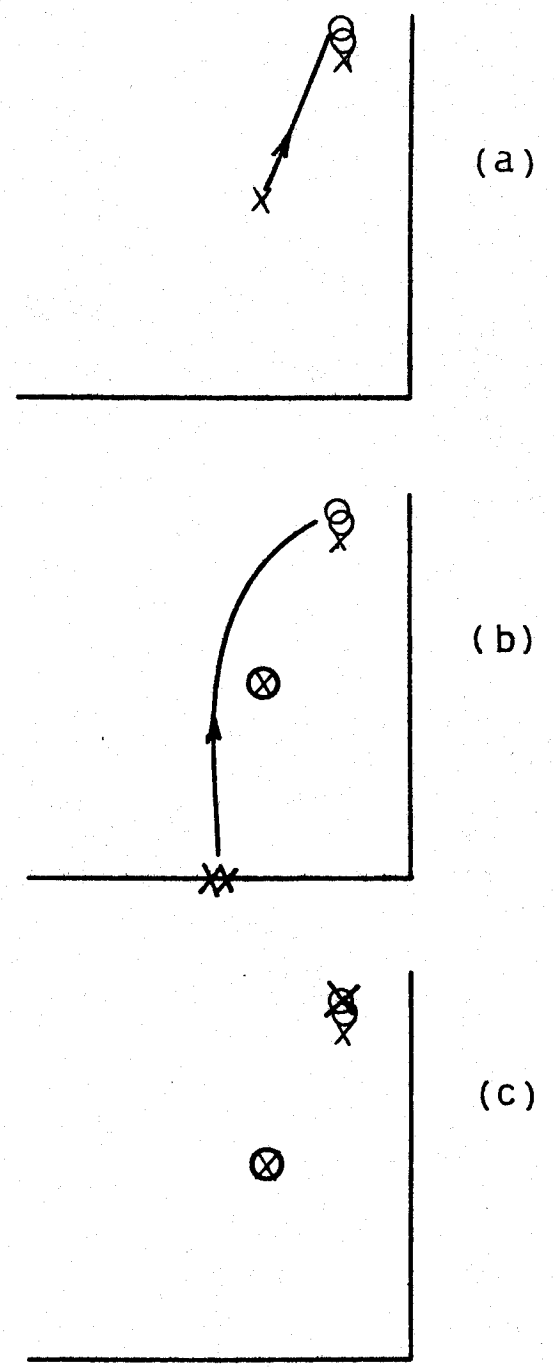

Figure 4.3 Root locus showing effect of complex compensator on Sundance dominant roots.
a) Uncompensated System
b) Effect of complex compensator #1
c) Effect of complex compensator #2

is mathematically cancelled by a zero. In practice, it is impossible to cancel a root completely because of the errors involved in calculating its location and because of the inaccuracy of the physical implementation of the compensator. Furthermore, the roots of some systems can change with time or with varying operating conditions. For these reasons, a system that has a root in the right hand half of the S plane cannot be made stable by cancelling the pole with a compensator zero.

The two design approaches discussed above for setting the complex compensator will now be described in more detail in relation to their application to the Sundance plant. They will be referred to simply as the type 1 and type 2 complex compensators.

4.3 The Type 1 Complex Compensator

4.3.1 Description

The complex compensator which achieves a system configuration of figure 4.3(b)is referred to here as the type 1. In this case, the compensator poles can be made a complex conjugate pair somewhere to the left of the system zeros, or they can be placed on the real axis.

In evaluating this compensator for use with the Sundance AVR, lead lag compensation was maintained as part of the system. This was done for two reasons. Firstly, for some settings of the complex compensator, (when the

poles are too far to the left) the system becomes unstable because of a high frequency root crossing into the right hand plane. This root was shown earlier in figure 3.13. When this occurs, lag compensation is required for stable operation. Secondly, lead-lag compensation can be useful in improving the location of the complex poles introduced by the compensator.

The lead lag compensator used has the form:

$$\frac{(1 + T_{A1} S)}{(1 + T_{A2} S)} \qquad \frac{(1 + T_{A3} S)}{(1 + T_{A4} S)}$$

The range of adjustment of the time constants was made similar to the range available with the lead lag compensator to be installed at Sundance. That is:

$$.0875 < T_{A1} < 1.11$$

$$T_{A2} = 1.11$$

$$.039 < T_{A3} < .28$$

$$T_{A4} = .039$$

Note that here again, the gain of the compensator is 1.0 so that the system D.C. gain is not affected.

4.3.2 Tuning the system

The tuning of the system involves the determination of the best combination of complex compensator parameters and of lead lag compensator time constants. The system gain was not altered.

The selection of the complex compensator zeros is a simple matter. The general form of the compensator being:

$$\frac{K\ (1+C_1\ S+C_2\ S^2)}{(1+C_3\ S+C_4\ S^2)}$$

the numerator coefficients are:

$K = 1.0$

$C_1 = 0.11$

$C_2 = 0.018$

so that the zeros are at $-3 \pm j\ 6.8$, on the system open loop poles.

An eigenvalue search was used to determine the other required settings. The Sundance voltage control system state space model was modified by adding the state equations derived from the analog circuit of figure 4.2. The complex compensator poles were placed in turn at the following positions:

$-10 \pm j\ 12$

$-10 \pm j\ 6$

$-5 \pm j\ 6$

$-10 \pm j\ 0$

$-7 \pm j\ 0$

$-4 \pm j\ 0$

For each of these settings, the lead lag compensation was varied over the range given earlier. The system dominant roots, which are now the roots introduced by

the complex compensator, were monitored.

Figure 4.4 is an example of the effect of lead lag settings with the complex compensator poles set on the real axis. When the complex compensator poles were made complex pairs, the dominant system roots were less dampened than those shown here. The root location of the best on-line setting when the system has lead lag compensation only, (no complex compensation), is shown for comparison. In the figure, the paths numbered one to three correspond to the following lead settings:

(1) $\frac{1 + .039S}{1 + .039S}$

(2) $\frac{1 + .07S}{1 + .039S}$

(3) $\frac{1 + .28S}{1 + .039S}$

For each path, the direction indicated is for increasing lag compensation, i.e. increasing angle contribution.

The setting that produced the best damping factor for the dominant root occurred with the complex compensator poles at $-4.0 \pm j0.0$. The lead and lag compensator settings were:

lead: $\frac{1 + .28S}{1 + .039S}$ lag: $\frac{1 + .2S}{1 + 1.1S}$

With this setting, a considerable amount of lead has been added to the system. This has the effect of increasing the high frequency gain of the system, making it more susceptible to noise problems. Such considerations

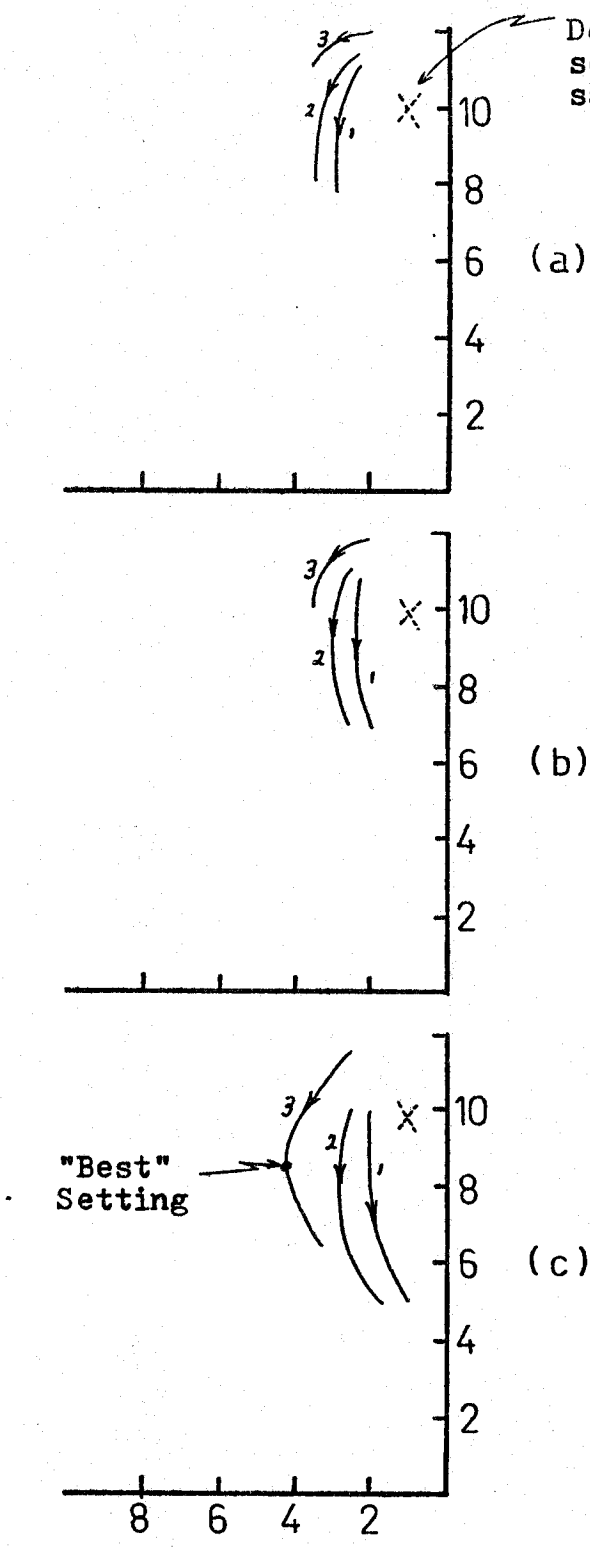

1 - Lead:
$$\frac{1 + .039\ S}{1 + .039\ S}$$

2 - Lead:
$$\frac{1 + .067\ S}{1 + .039\ S}$$

3 - Lead:
$$\frac{1 + .28\ S}{1 + .039\ S}$$

(Arrow indicates direction of root for increasing lag)

Figure 4.4 Effect of Type 1 Complex and lead-lag compensators on dominant eigenvalue
a) Complex compensator poles at $-10 \pm j\ 0$
b) Complex compensator poles at $-7 \pm j\ 0$
c) Complex compensator poles at $-4 \pm j\ 0$

are important and must be given serious thought before implementation. However, at the stage of preliminary studies such as this, the main purpose is to establish whether readjustment of existing AVR hardware, or the addition of slightly more sophisticated feedforward controllers could give additional damping.

For the above setting, the system eigenvalues are:

Real Part	Imag. Part	Damping Factor	Notes
-4.2	± j 8.8	0.43	Dominant Root
-3.1	± j 6.8	0.41	Cancelled by compensator zero
-1.4	± j 11.1	0.12	Cancelled by plant zero
-21.5	± j 70.	0.29	"High frequency" Root
-0.4			
-1.1			
-1.6			
-3.6			
-5.1			
-100.			
-172.			

TABLE 4.1 Eigenvalues for the best setting of the type 1 complex compensator

The high frequency roots of the system, at $-21.5 \pm j\ 70$, are well to the left and cause no problems. The damping factor of the dominant roots, at $-4.2 \pm j\ 8.8$, has been increased to 0.43. Recall that the dominant root damping factor was 0.1 for the "open circuit setting" and 0.18 for the "on-line" setting of the existing Sundance AVR. Thus an improvement in the system time response, compared to the response with lead lag compensation only, is expected.

4.3.3 System Performance

The time domain response of the terminal voltage of the fully loaded machine to a .01 P.U. voltage step disturbance is given in figure 4.5. This response was obtained from a simulation of the reduced order model of the system. All initial conditions were set to zero. The settling time to a $\pm$ 5% band is now 0.6 seconds. This compares with 0.8 seconds for the lead lag compensated system set for on-line conditions, and 1.8 seconds for the same system set for open circuit conditions.

As in the previous chapter, a more realistic evaluation of the effect of the type 1 complex compensator was made by simulating the system with the transient stability program where all machines, controllers and the transmission system are represented in detail. As before, the disturbance was a line outage. Results are shown in figure 4.6. The system response with lead lag compensation

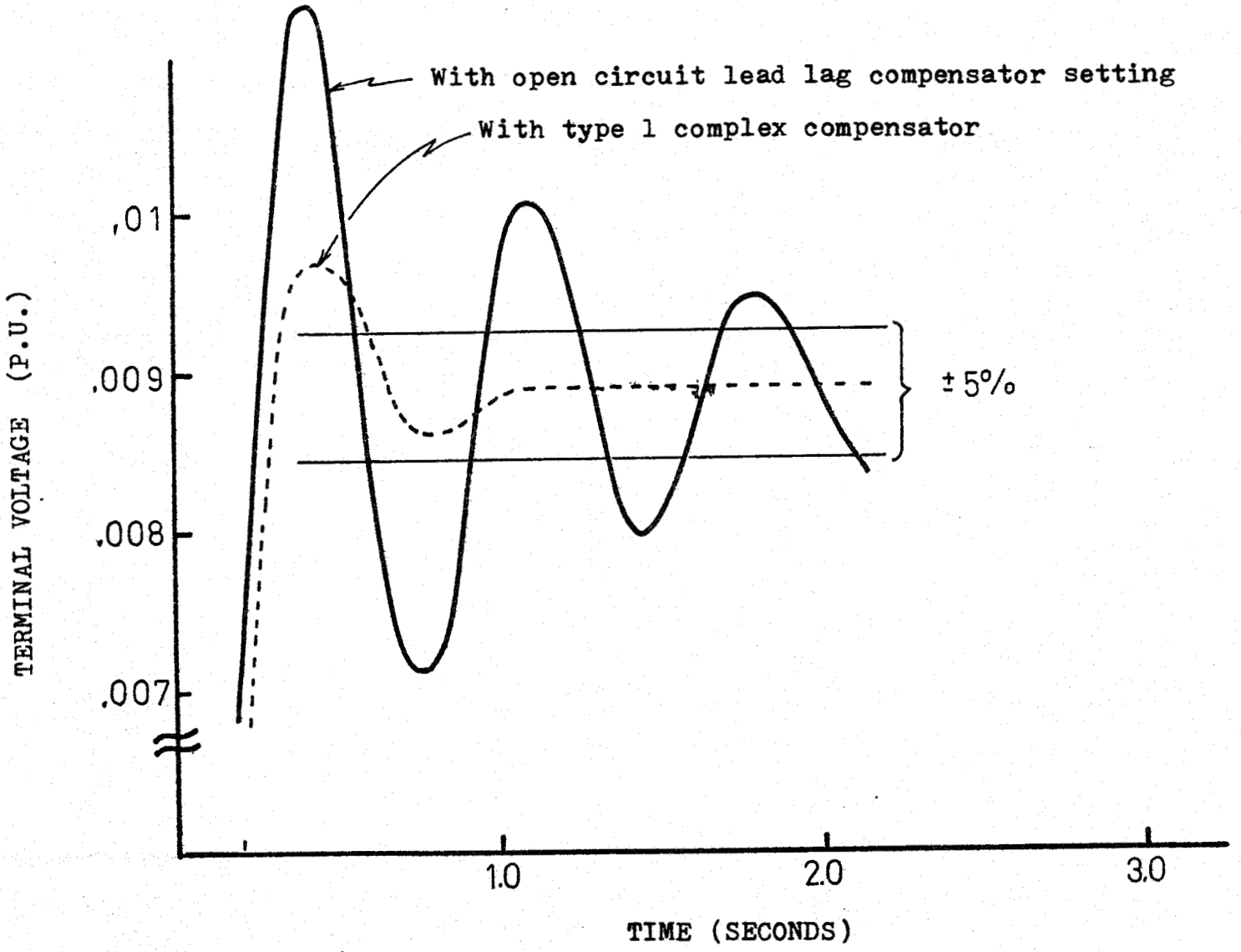

Figure 4.5 Full load terminal voltage step response with type 1 complex compensator

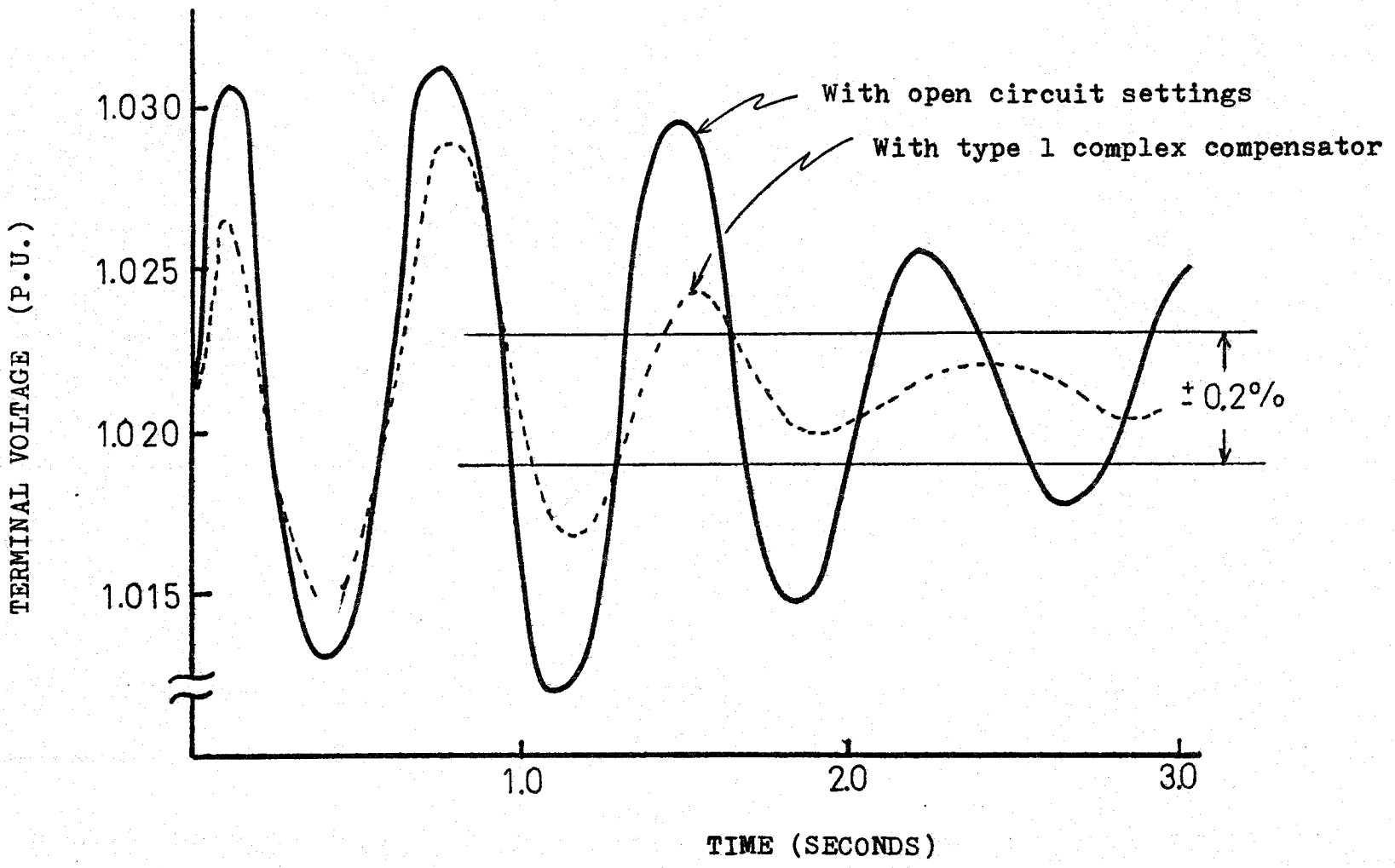

Figure 4.6 Full load voltage response after line outage - with type 1 complex compensator

only, set for open circuit operation, is also shown for comparison.

The settling time of the complex compensated system to ± 0.2% of the steady state voltage level is 1.6 seconds. Thus, the addition of this complex compensator significantly improves the system response. However, this improvement is almost identical to that achieved by setting the existing Sundance excitation system for on-line conditions. In that case, a settling time of 1.8 seconds was achieved. (see figure 3.18).

Because the complex compensator introduces a new complex pole pair in the system, the effect of the compensator at open circuit conditions must be evaluated. The open circuit voltage step response shown in figure 4.7 was calculated using the reduced order model. Although the response is much more oscillatory than with the open-circuit settings, the settling time to a ± 5% band is not greatly affected.

4.4 The Type 2 Complex Compensator

The strategy used in setting the type 2 complex compensator for the Sundance excitation system is very simple. The compensator poles and zeros were placed over the system zeros and poles respectively. This is shown on the root locus diagram of figure 4.3 (c).

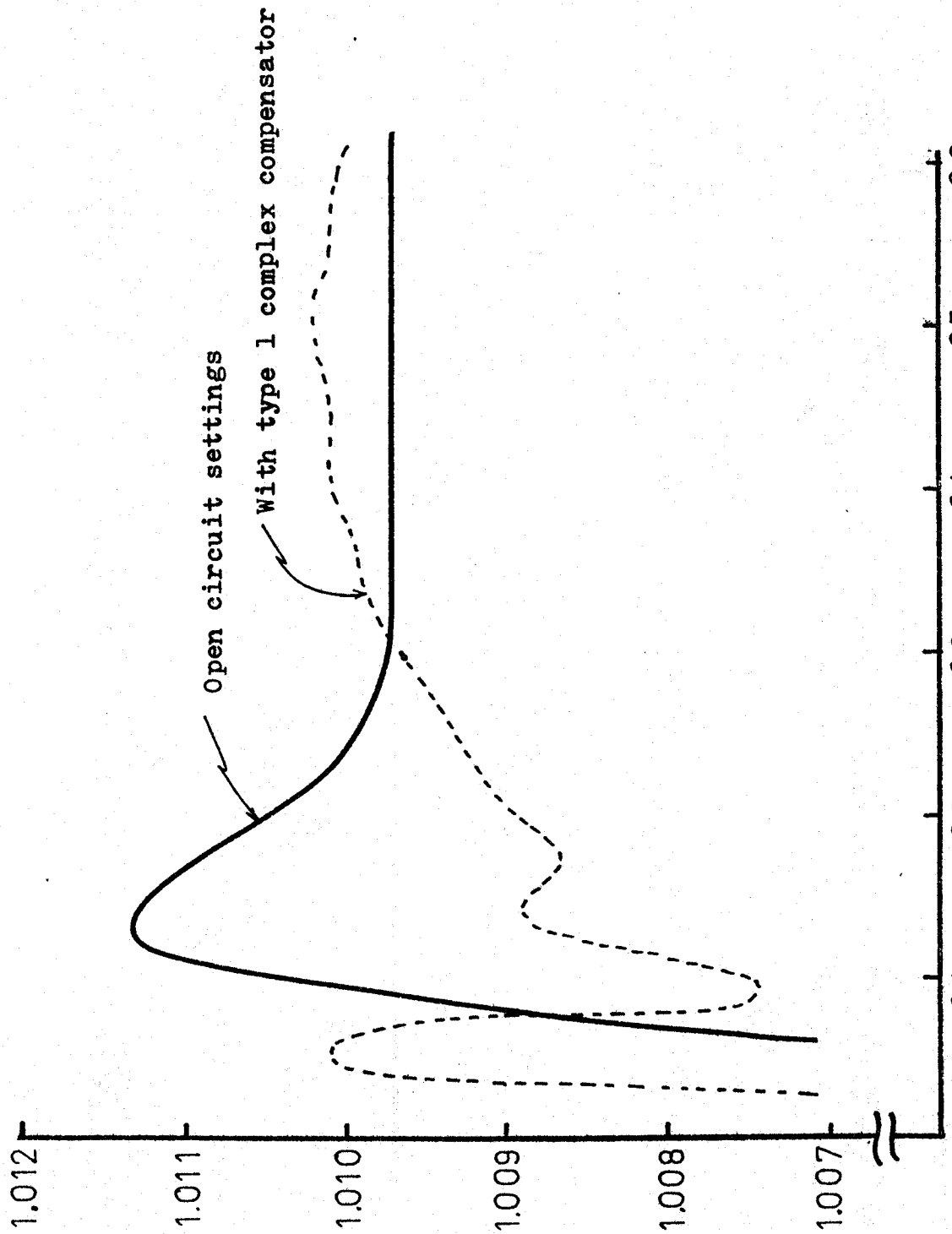

Figure 4.7 Open circuit voltage step response with type 1 complex compensator

Because of the possible instability due to the high frequency root mentioned earlier, it was necessary to maintain maximum lag compensation. Lead compensation was not required. In this way the high frequency root was kept at $-16 \pm j\ 54$. This has a small damping factor but the time response component due to this root decays quickly and is negligible in the overall response.

This compensator greatly improved the full load terminal voltage step response of the machine. The reduced order model simulation of the on-line system shown in figure 4.8 shows a settling time 0.3 seconds with the complex compensator. This improved damping was confirmed by a USTRAN simulation of the detailed system. The result of this simulation, shown in figure 4.9 shows a terminal voltage settling time of 0.9 seconds when the type 2 complex compensator is used. This compares with 5.4 seconds for the existing system with "open circuit settings", and with 1.6 seconds when the type 1 complex compensator is used.

With the machine open circuited, the compensator introduces a large amount of oscillation as can be seen in figure 4.10. The system is still quite stable however, and this performance could be considered acceptable. If not, it would be a simple matter to switch the complex compensator into the circuit only at a predetermined load level.

4.5 Effects on Power Oscillations

It was seen in the previous chapter that setting

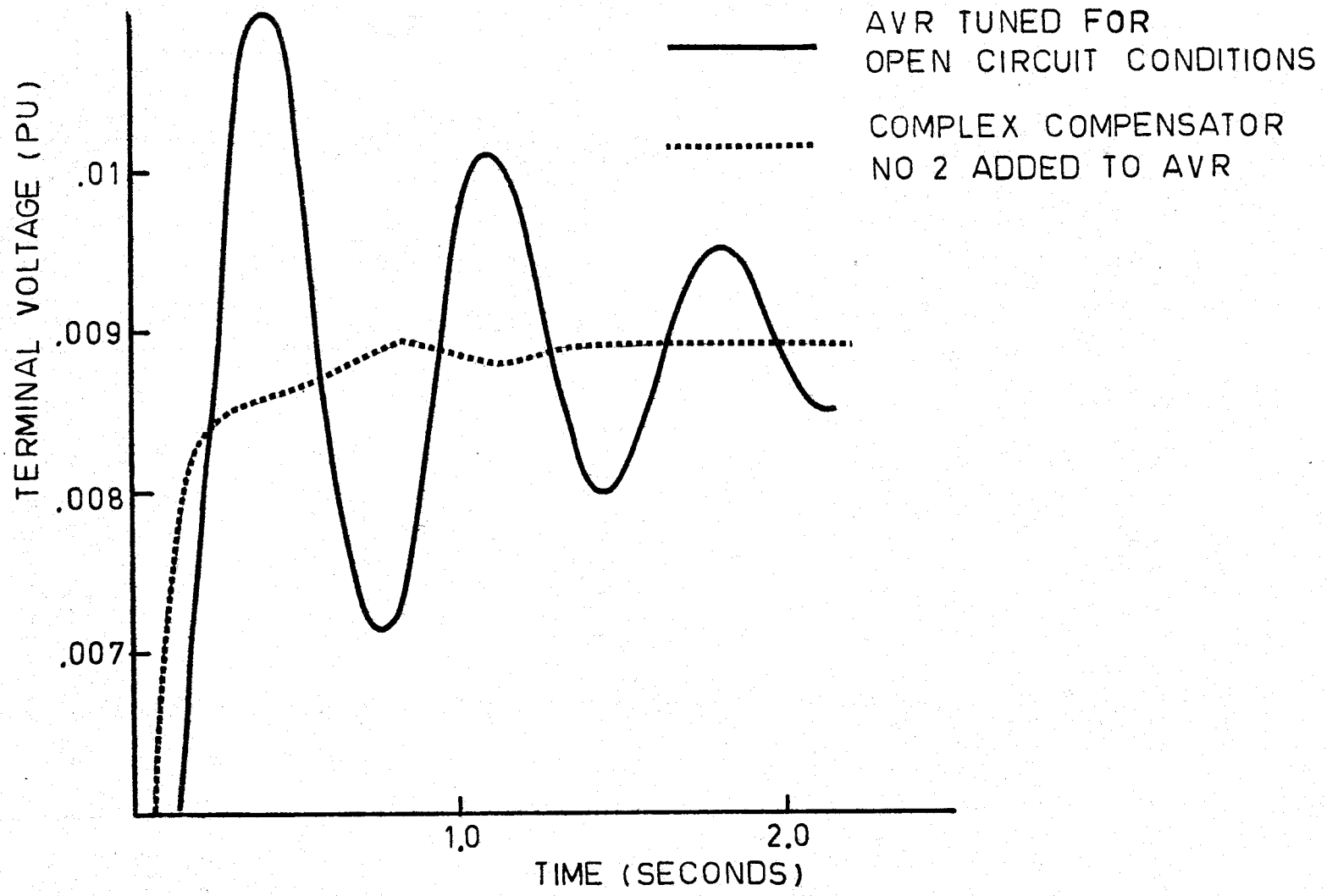

Figure 4.8 **Full load voltage step response with type 2 complex compensator**

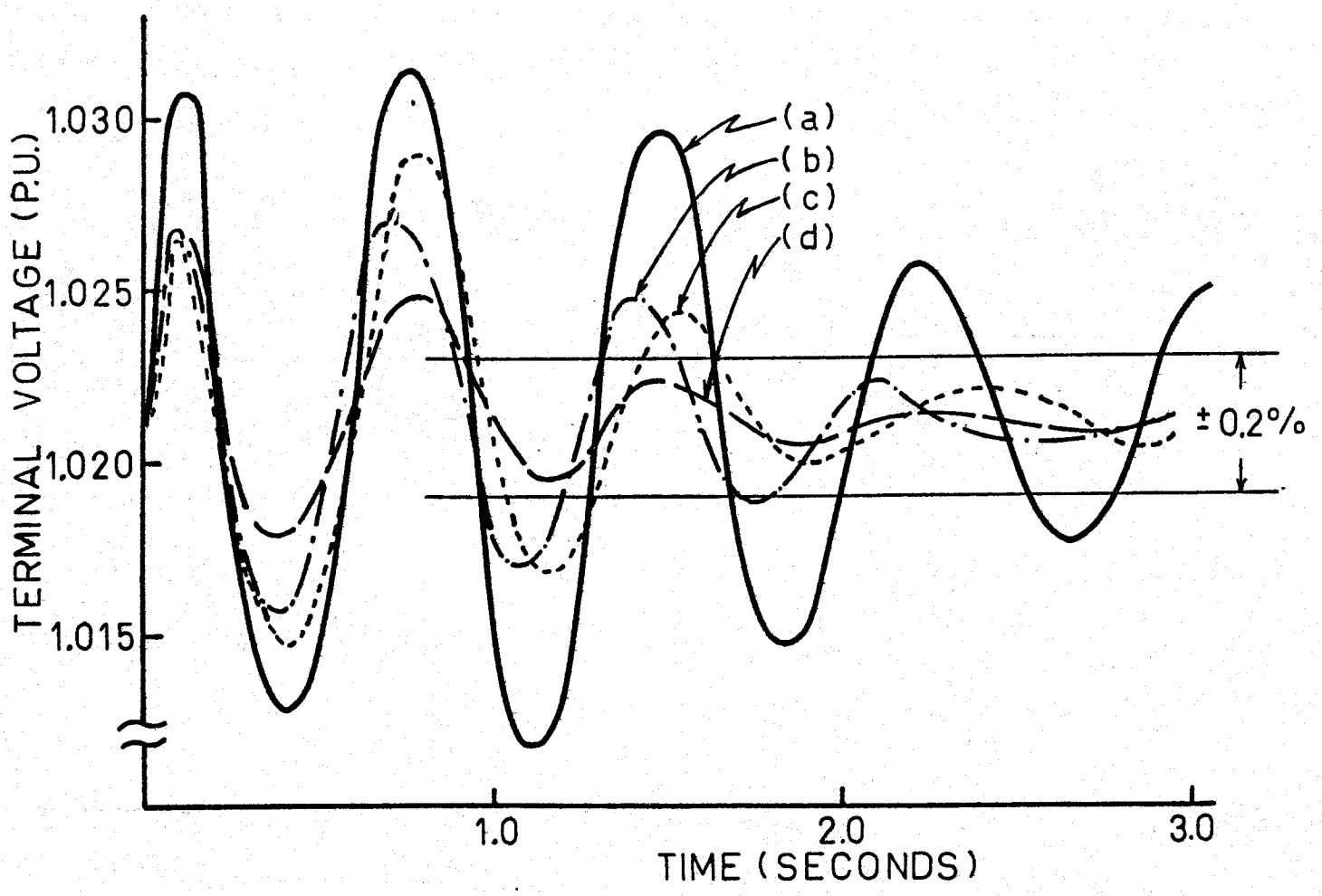

Figure 4.9 Full load terminal voltage response after line outage - comparison of 4 cases
a) Base case: existing hardware (lead lag compensation) with open circuit settings
b) Existing hardware with on-line setting
c) Type 1 complex compensator
d) Type 2 complex compensator

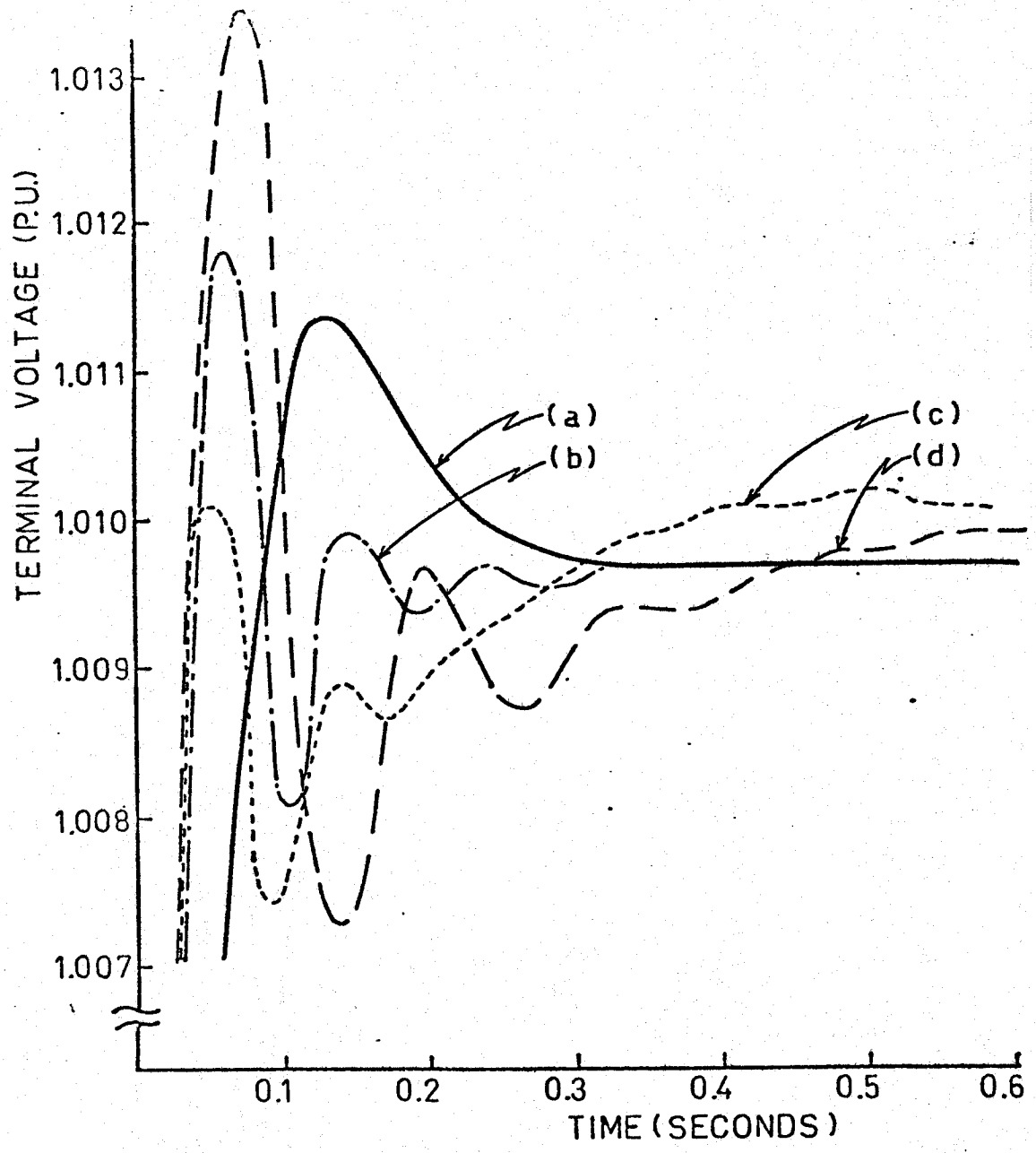

Figure 4.10 Open circuit voltage step response; comparison of 4 cases
a) Base Case: existing hardware (lead lag compensation) with open circuit settings
b) Existing hardware with on-line settings
c) Type 1 complex compensator
d) Type 2 complex compensator

the Sundance excitation system to improve the terminal voltage response in the dynamic range also had a beneficial effect on the damping of power oscillations. Figure 4.11 illustrates that the same phenomenon occurs when complex compensators are used. The increased damping of power oscillations as compared to those obtained with AVR "open circuit settings" is significant.

At this point it would be useful to summarize the results of improvements to the Sundance excitation system. The settling times of the generator terminal voltage for various conditions are tabulated below. Both the results of the reduced order model simulations and the USTRAN simulations are given. Since the magnitudes of the disturbances used and the size of band specified were different for the two simulation methods, the settling times shown for each specific condition are quite different.

The proportional reductions in settling times for the various compensation techniques calculated by the two methods are similar. This illustrates the accuracy of the reduced order model of the generator. This also demonstrates that a relatively small error was introduced by assuming a single-input single-output system for design purposes.

The design procedure in this and the preceding chapters utilized a full load model of the generator. Test-

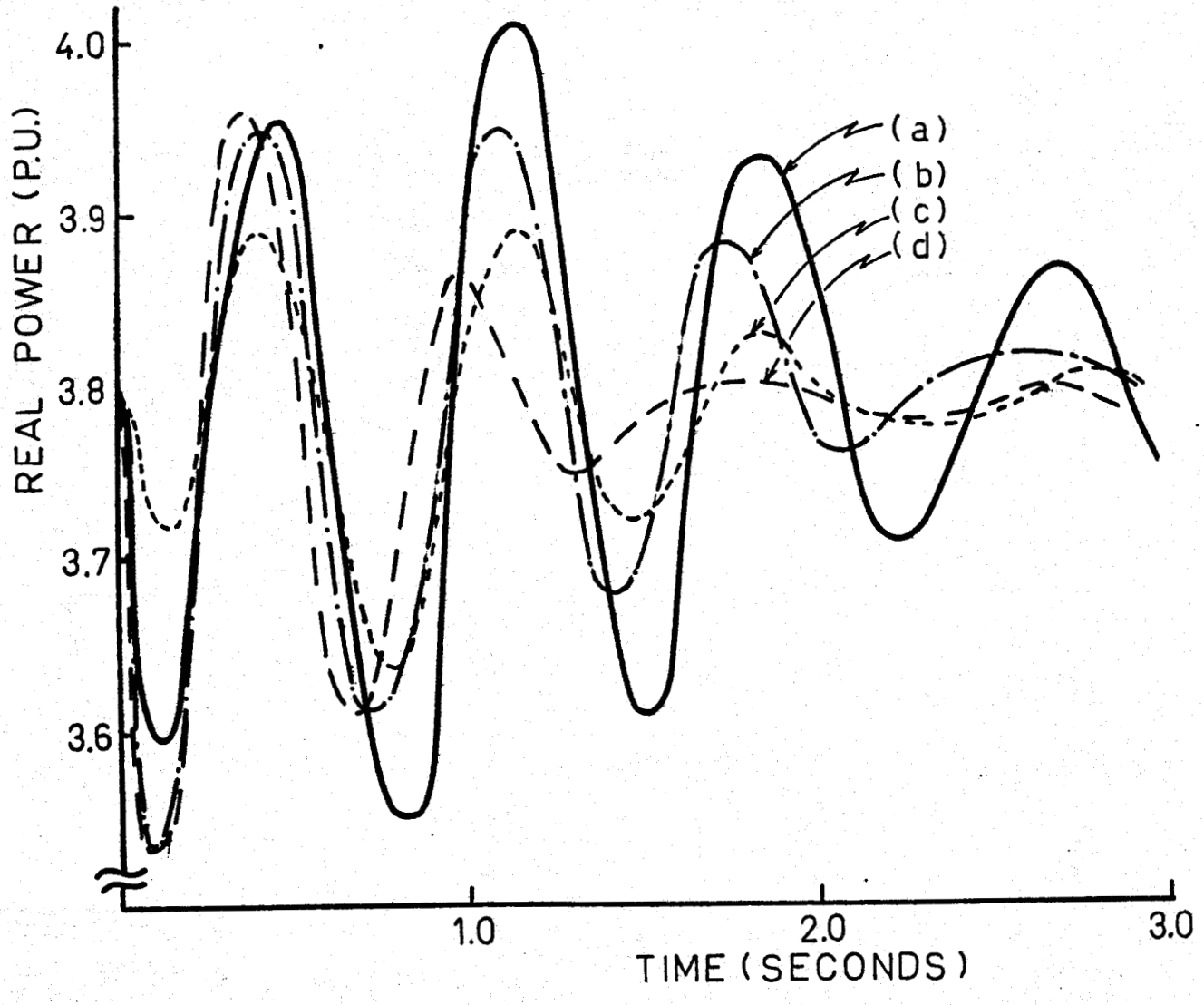

Figure 4.11 Power oscillations after line outage; comparison of 4 cases. Cases (a) to (d) as in figure 4.10

Compensation Used	Reduced order model simulation Time to ± 5% of steady state	USTRAN simulation Time to ±.2% of steady state
Existing system tuned for open circuit operation	1.8 seconds	5.4 seconds
Existing system tuned for on-line operation	0.8 seconds	1.8 seconds
Lead lag plus complex compensator #1	0.6 seconds	1.6 seconds
Lag plus complex compensator #2	0.3 seconds	0.9 seconds

TABLE 4.2 Settling times of terminal voltage with machine at full load.

ing of resulting settings was also done with the generator at full load. Since any change in loading affects the response of a generator, a study of system performance at other than full load conditions is required. This aspect is investigated in the following chapter.

5. EFFECTS OF LOAD VARIATIONS

5.1 Introduction

In previous chapters, an attempt was made to improve the on-line performance of the Sundance voltage control system by readjusting the existing real root compensators and by adding complex compensation. Since it is at full load that a generator's time response tends to be most oscillatory, the compensators were tuned using a full load model of the Sundance generator.

Theoretically, different compensator "best settings" could be calculated for each possible loading condition. Furthermore, the tuning of some compensators is very sensitive to changes in system conditions. This is the case where complex pole cancellation is used. With changes in system conditions, it is possible for the compensator to introduce a new oscillatory mode to the system, thus hindering, rather than improving damping. For these reasons, an assessment of system performance at various loading conditions is important.

In this chapter, a model of the Sundance generator at 60% load is obtained by reapplying the identification procedure which utilizes a noise signal applied to a simulation of a detailed model of the power system. This

was described in detail in chapter 2.

The roots of the system at this loading condition are then compared with those of the fully loaded system in order to assess the sensitivity of the various forms of compensated systems to load changes. This sensitivity is illustrated by simulations of the system at reduced load.

5.2 Model of the Sundance Generator at Reduced Load

5.2.1 Use of reduced admittance matrix for load flow analysis

One of the preliminary steps in the identification procedure described in chapter two is the determination of the generator initial terminal conditions for use in the transient stability program. For the identification of the full load generator model, these were obtained from a load flow run of the 360 bus model of the Calgary Power system. The admittance matrix of this high order system was then reduced to 9th order for use in the transient stability program.

A new load flow run was required to obtain the terminal conditions with the Sundance generator at reduced load. This could have been done using the 360 bus system or using a lower order model in which the less important busses had been neglected. The method selected however, was to run a load flow using the reduced order admittance

matrix previously obtained with the network reduction program. This 9th order matrix gives the driving point and transfer admittances between the nine major generators of the Calgary Power system. In the reduction process, all loads are transformed to constant impedances. In this way the behavior of the system as viewed from the terminals of the nine selected machines is almost identical to that which would be obtained by maintaining the 360 bus model. Some error is introduced by the reduction process and by the inherent assumption of constant voltages at the load buses when the loads are transformed to constant impedances.

Thus, the use of the reduced admittance matrix in the load flow had the advantage of reducing computation time while introducing minor errors associated with the assumption of constant impedance loads.

The generation at the Sundance 3 unit was reduced to 222 MW, or about 60% of its rated load. The generation removed from Sundance was added to the other eight plants of the system in order to maintain the same total generation. The reactive power generation at Sundance 3 calculated by the load flow program was 74 MVAR. This compares to 93 MVAR when the generator was at full load.

5.2.2 Identification Results

The identification procedure used to obtain the

frequency response of the generator was described in chapter two. A noise signal was generated using the same parameters as before. This was injected as a disturbance into the transient stability program where the initial terminal conditions had been appropriately modified. The simulated responses were stored for later analysis by the USTF program. The resulting Bode plots leading to the transfer functions V_t/E_f and I_f/E_f are shown in figures 5.1 and 5.2. The plots for the reduced load case are superimposed on the frequency response obtained for the full load model. As expected, the resonant peaks at 60% load are reduced considerably.

The transfer functions fitted to the Bode plots are given below.

$$\frac{V_t}{E_f} = \frac{.107\left(1+\frac{S}{1.63}\right)\left[1+\frac{.5}{11.2}S\left(\frac{S}{11.2}\right)^2\right]}{\left(1+\frac{S}{.6}\right)\left(1+\frac{S}{2.45}\right)\left[1+\frac{.4}{11.2}S\left(\frac{S}{11.2}\right)^2\right]}$$

$$\frac{I_f}{E_f} = \frac{.986\left[1+\frac{.6}{8.5}S\left(\frac{S}{8.5}\right)^2\right]}{\left(1+\frac{S}{.56}\right)\left[1+\frac{.44}{11.2}S\left(\frac{S}{11.2}\right)^2\right]}$$

The order of these transfer functions is the same as was used for the full load model. The gains given here were obtained from a step response test of the simulated system.

The accuracy of the fit of the above two transfer functions is illustrated in figures 5.3 and 5.4. As

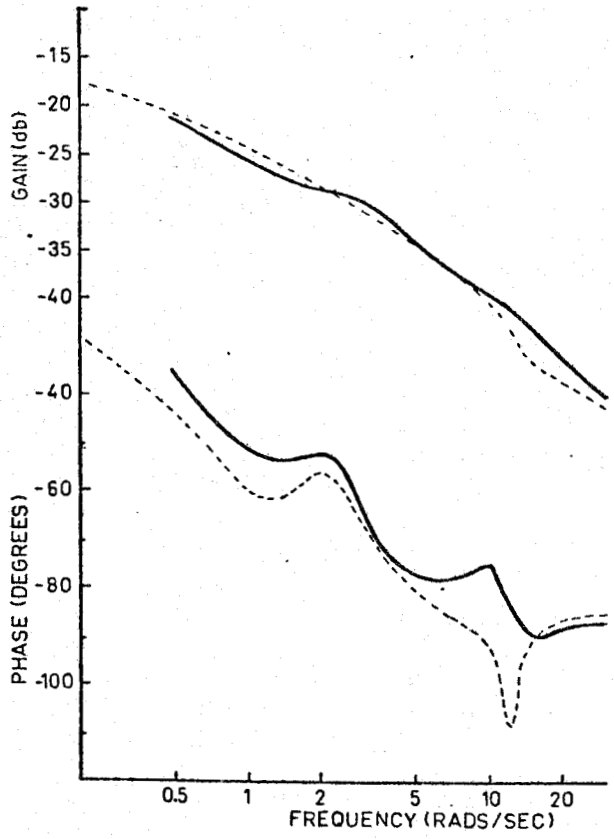

Figure 5.1 Bode plot of V_t / E_f obtained from USTF

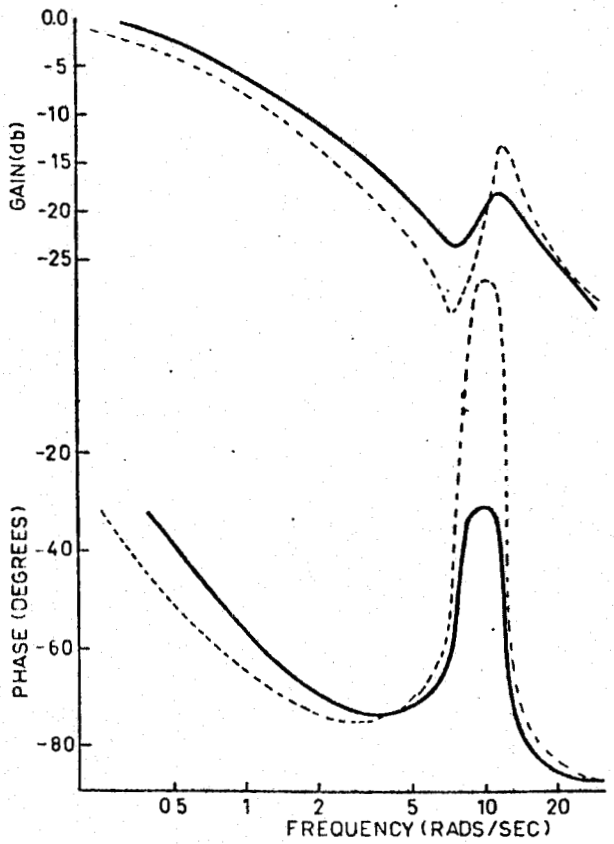

Figure 5.2 Bode plot of I_f / E_f obtained from USTF

——— 60% load
- - - - - - Full load

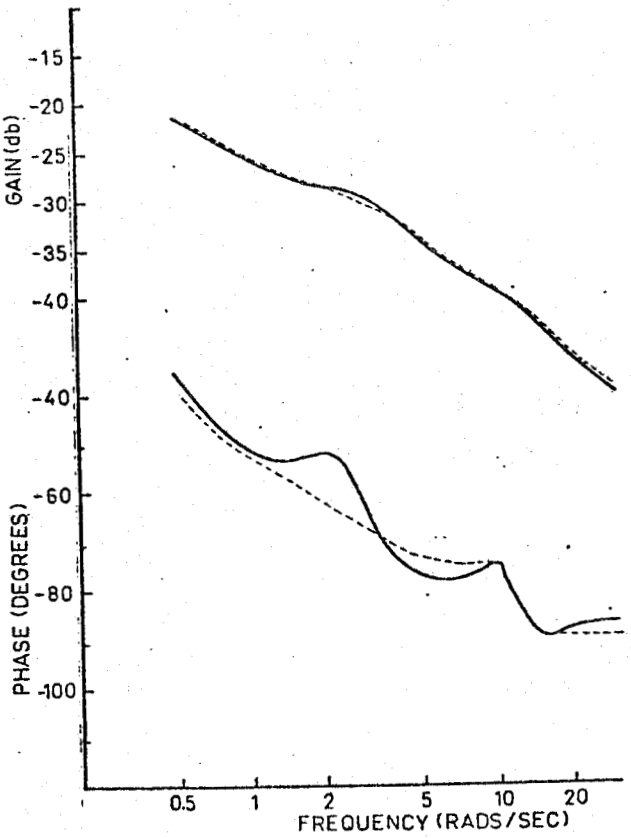

Figure 5.3 Bode plot of fitted transfer function for V_t / E_f

——— Response obtained from I.D.
- - - - - - - Fitted transfer function

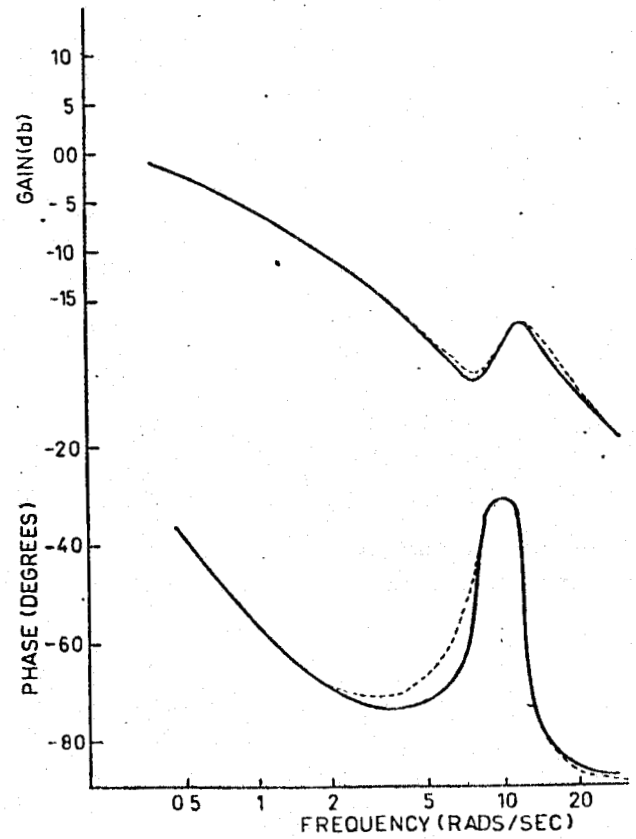

Figure 5.4 Bode plot of fitted transfer function for I_f / E_f

in the full load case, some error occurs in the phase of V_t/E_f at the 2 radian/sec. range. The validity of the model was tested by comparing the step response of the reduced order system with the response obtained from a USTRAN simulation of the detailed model. In both cases, a .1% step disturbance was applied to the reference voltage input point. The results of this test, illustrated in figure 5.5, indicate that the reduced order model of the generator is sufficiently accurate.

These voltage responses also illustrate the increase in damping at lighter load. To illustrate this, the full load response of the same system is superimposed.

The main open loop poles and zeros of the Sundance 3 voltage control system as calculated with the 60% load generator model, and with the excitation system model previously used, are shown in figure 5.6. The poles and zeros of the full load system are shown for comparison. Also shown are the branches of the root locus diagram that link these poles and zeros. The exact location of these branches depends of course on the lead lag compensation used. If complex compensation is used, the branches are altered completely.

It is not surprising that under lighter loading conditions the system roots move to the left. This is consistant with the increase in damping previously demonstrated by the time responses.

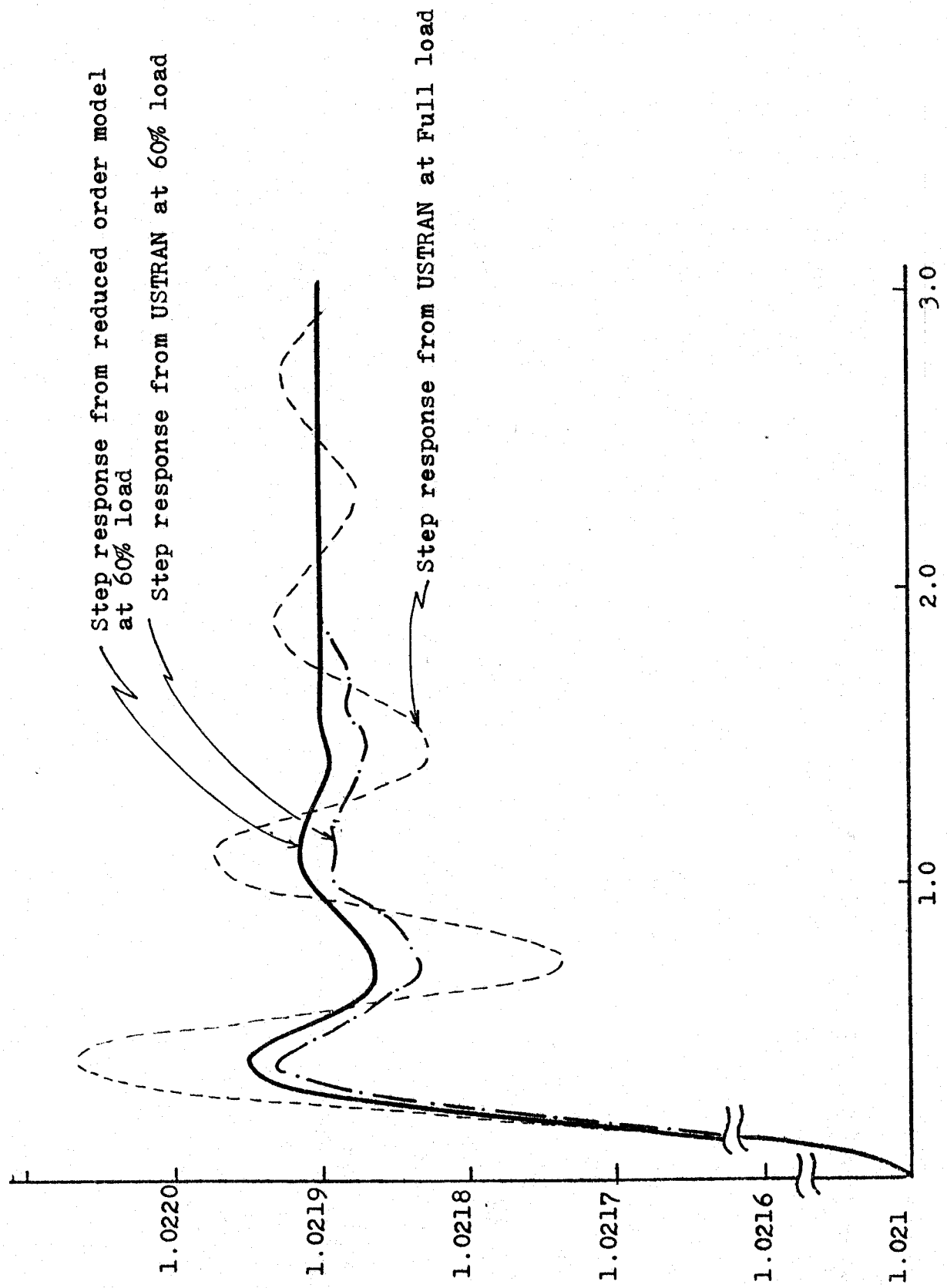

Figure 5.5 Comparison of 60% load generator model responses

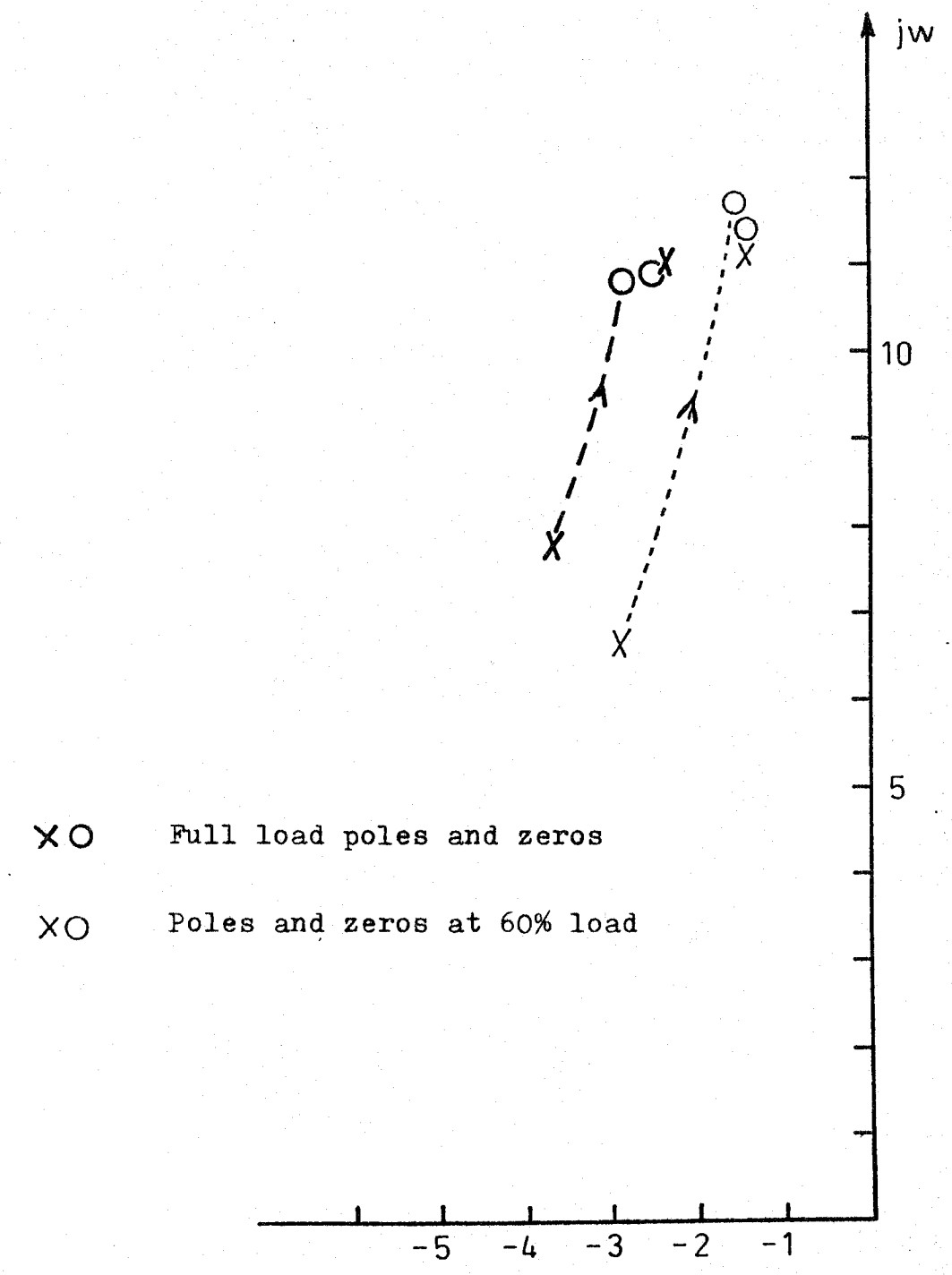

Figure 5.6 Main open loop poles and zeros at full load and 60% load

It is now possible to analyze this variation of the system roots in order to assess the effectiveness of various compensation techniques at other than full load conditions.

5.3 Performance of Compensated System at Reduced Load

5.3.1 Analysis in the S Plane

The pole zero plot of the system at 60% load shown in figure 5.6 can be used to predict the performance of the system at reduced loading conditions, and with the various forms of compensation previously applied.

In the case of lead lag compensation, it is recalled that the aim was to draw the branch of the root locus between the poles at $-3 \pm j\ 7$ and the zeros at $-1.5 \pm j\ 11.7$ towards the left, and to draw the root on this branch down towards the open loop pole. The form of the root locus diagram of the system does not change at lighter load. It is thus expected that the effect of lead lag compensation will also be beneficial at light load.

If a type 1 complex compensator is used, the effect of a load reduction is as shown in figure 5.7 (b). The compensator zeros placed to cancel the system complex poles now fall beside these poles. The residue at the poles increases thus causing the poles to contribute a larger oscillatory component to the time response. However, the second pair of complex roots which lies along the path

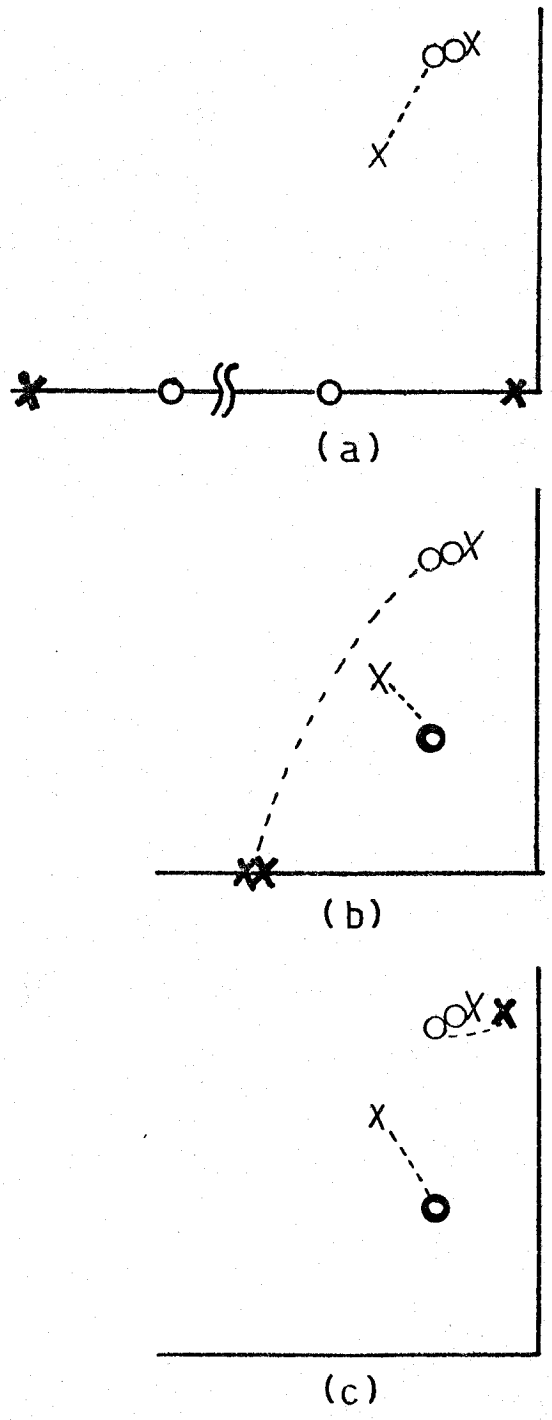

X O System poles and zeros

X O Compensator poles and zeros

Figure 5.7 Effect of load reduction on root locus of compensated system

a) Root locus at 60% load with lead lag compensator tuned for full load

b) Root locus at 60% load with type 1 complex compensator tuned for full load

c) Root locus at 60% load with type 2 complex compensator tuned for full load

from the compensator poles on the real axis to the system zeros continues to be beneficially affected by the lead lag compensation. (Recall that real root compensation was used in conjunction with the type 1 complex compensator.) Therefore, the performance of the system at half load depends on the new position of the plant poles and zeros and on the relative dominance of the two pairs of roots shown in figure 5.7 (b). The presence of the type 1 complex compensator could continue to be a benefit at reduced load but in some cases it could cause more oscillation. There is only a small chance that this could become serious because of the fact that the system is naturally less oscillatory at reduced load.

Figure 5.7 (c) illustrates the effect of a load reduction on the root locus of the system with which the type 2 complex compensator is used. As the system open loop poles and zeros move to the left, the cancelling effect with the compensator poles and zeros becomes less effective. Thus the original single dominant root of the uncompensated system is replaced with two dominant complex roots. It is quite possible that this could introduce additional oscillations in the system response at reduced load.

5.3.2 Simulation Results

The Sundance 3 voltage control system was simulated at reduced load and with the various forms of compen-

sation in order to verify the predicted behavior discussed above. These simulations were carried out using the reduced order model. This was considered sufficiently accurate because of the similarity of the step response previously obtained with this model, and that obtained from a USTRAN simulation (see figure 5.5). Furthermore, the primary aim here was simply to determine whether the response at reduced load becomes better or worse when compensation tuned for full load conditions is added.

The voltage step responses of the system at 60% load with the various compensator settings discussed in the previous two chapters are shown in figure 5.8.

In each case, the system was disturbed by injecting a .01 PU voltage step at the machine terminals. The response of the system with lead-lag compensation set for best open circuit operation is shown in each case for comparison.

An examination of the responses bears out the preceding analysis of the system root locus diagrams. With the on-line setting of the lead-lag compensator, damping is improved at this reduced load as it was at full load. This is also the case with the type 1 complex compensator. It appears in this case that the increased residue at the lower frequency system poles (at approximately $-3 \pm j\ 7$) does not have a serious effect on the response.

The predicted additional oscillation introduced by the type 2 complex compensator shows up clearly in

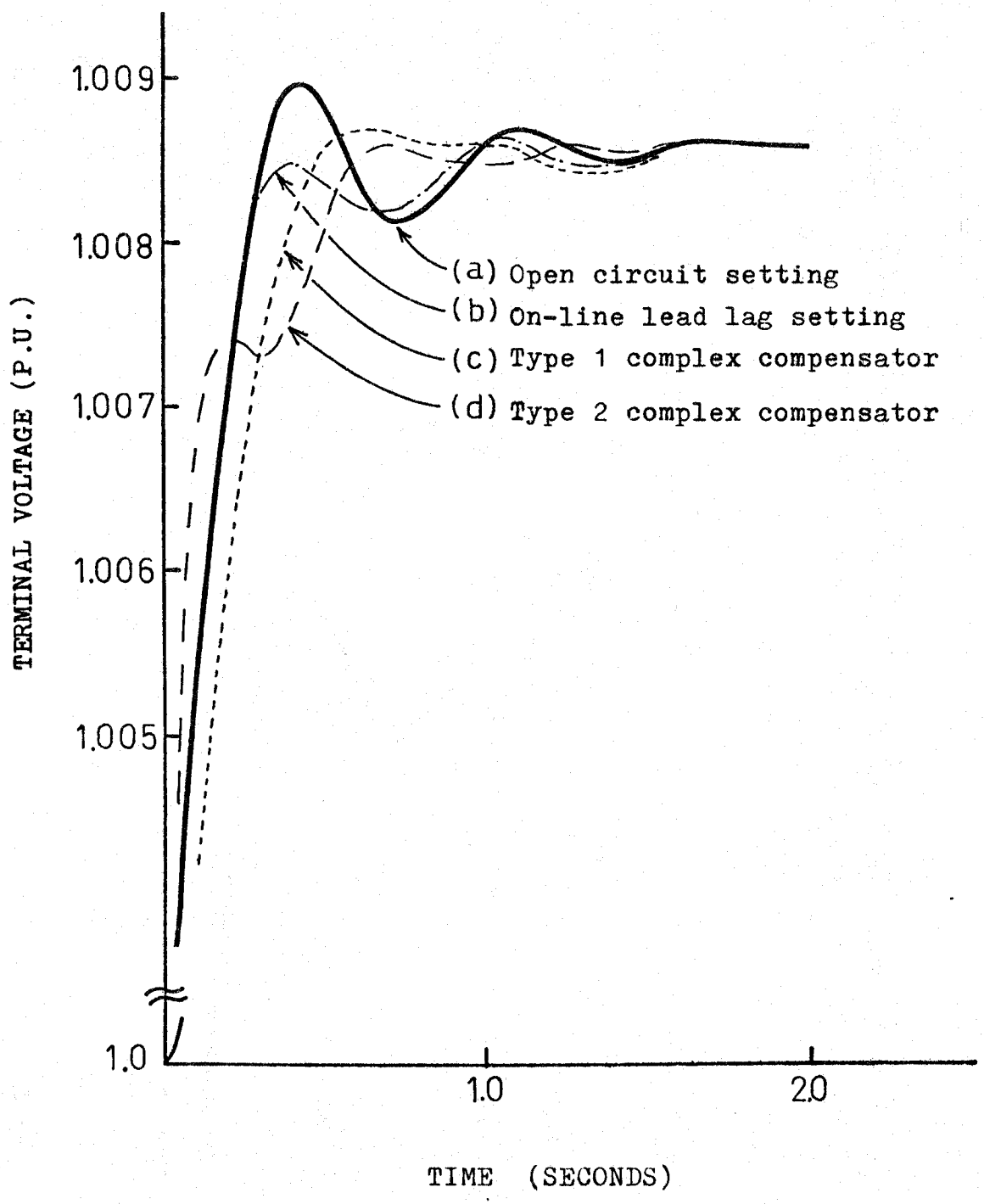

Figure 5.8 Step responses at 60%load

figure 5.8. This is caused by the compensator pole which is no longer cancelled by the system zero. For this particular case of 60% load, the overall response is not seriously affected; however it could be, at lighter loading.

The study presented in this chapter is by no means a complete analysis of the effects of load variations on the various forms of the compensated voltage control system. It does however, provide a good indication of the expected variation of system roots at other than full load conditions, and some insight into the effect of this variation on the various forms of compensation that can be used.

In the case of the existing Sundance AVR, no ill effects will result at reduced load from tuning the real root compensators for full load conditions. Before implementing a complex compensator however, an evaluation of its effects over a broader range of loads would be necessary.

6. TUNING A STATIC EXCITATION SYSTEM THAT HAS NO CURRENT FEEDBACK

6.1 Introduction

The studies described in the previous chapters of this report have been concerned with one particular installation, the Sundance 3 plant. Some of the features included with the excitation system at that plant, lead lag series compensation and field current feedback are slightly different than those used in the static systems produced by many other manufacturers. More commonly, static excitation systems are supplied with an adjustable gain only, and with no feedforward compensation.

In chapter three, it was demonstrated that, with an excitation system where field current feedback is included, it is possible to use real root compensation to improve the on-line performance of the voltage control system. In chapter four, complex compensation was added in an attempt to further improve the performance of that particular system. The question that arises at this point is one concerning the applicability of such simple series compensators to other forms of excitation systems. Two basic types come to mind: the first is the rotating excitation system, and the second is the "standard" static

system as it will be referred to here, where no field current feedback is included.

The second form was chosen as a suitable addition to the Sundance study for two reasons. Series compensators are most easily added to AVR's by the manufacturer before installation. Most new units now being brought on-line are equipped with static excitation systems. Furthermore, a comparison of the existing Sundance voltage control system with one using a "standard" static AVR provides an interesting evaluation of the present AVR's performance.

The chapter begins with a description of the model of the "standard" static excitation system. The accuracy of the generator on-line model used in previous chapters is then re-assessed for use here. Subsequent sections describe the application of the three forms of series compensation previously used, i.e. lead-lag and the two forms of complex compensation, to the Sundance plant in which a so-called "standard" static AVR is used.

6.2 "Standard" Static Excitation System Model

The commonly used model for a static excitation system is the IEEE Type 1S model shown in figure 6.1. In many studies, the derivative feedback is neglected. This was done here for expediency. The values of the model

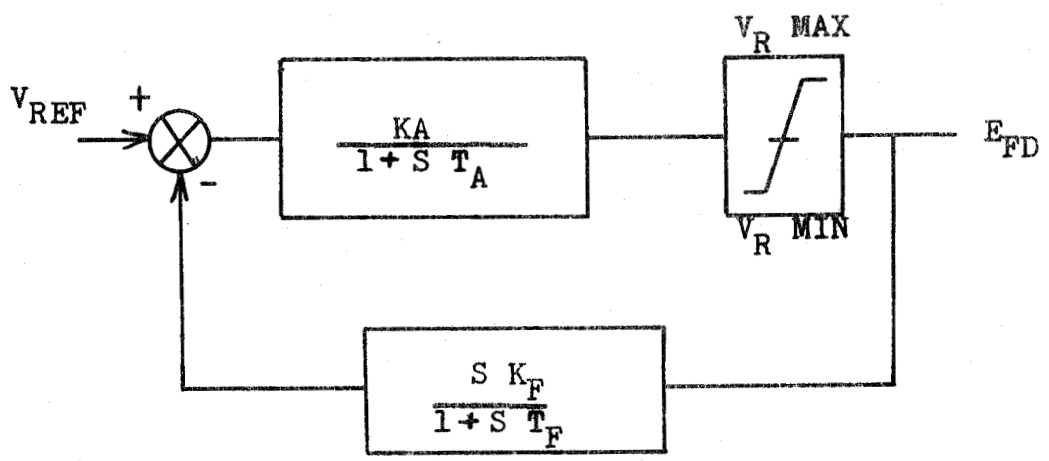

Figure 6.1 IEEE Type 1 S static excitation system model.

parameters are listed below:

K_A = 100

T_A = 0.02

$V_{R\ MAX}$ = 7.1 P.U.

$V_{R\ MIN}$ = -7.1 P.U.

K_F = 0

The field voltage limits shown are those of the present Sundance exciter. The gain was set so that a 0.05 P.U. error signal would drive the field voltage from normal op-

erating level to ceiling. Since the steady-state field voltage is 2.1 P.U., an increase of 5.0 P.U. causes the field voltage to reach the ceiling level. Such an increase is achieved for an error signal of .05 P.U. if the gain is set at 100. The time constant of 2 ms. is representative of static excitation systems.[25]

6.3 Generator Model Re-evaluation

Because of the removal of the current feedback from the excitation system only one of the transfer funcions previously used for the generator is required. This is V_t / E_f. In this section, the effect of the removal of the current feedback is investigated in the complex S plane. It is found that it is worthwhile to re-assess the validity of the on-line generator model. This re-evaluation is done by comparing once again the step response of the reduced order system with that calculated by the transient stability program.

Figure 6.2 shows the root locus diagram of the Sundance system with the "standard" static AVR and the on-line generator model. The complex poles and zeros shown are introduced by the V_t/ E_f transfer function. The dominant oscillatory mode of the system is caused by the closed loop root which lies on the branch between the complex pole and zero. It is recalled that in the previous case studied, the effect of this root was considerably

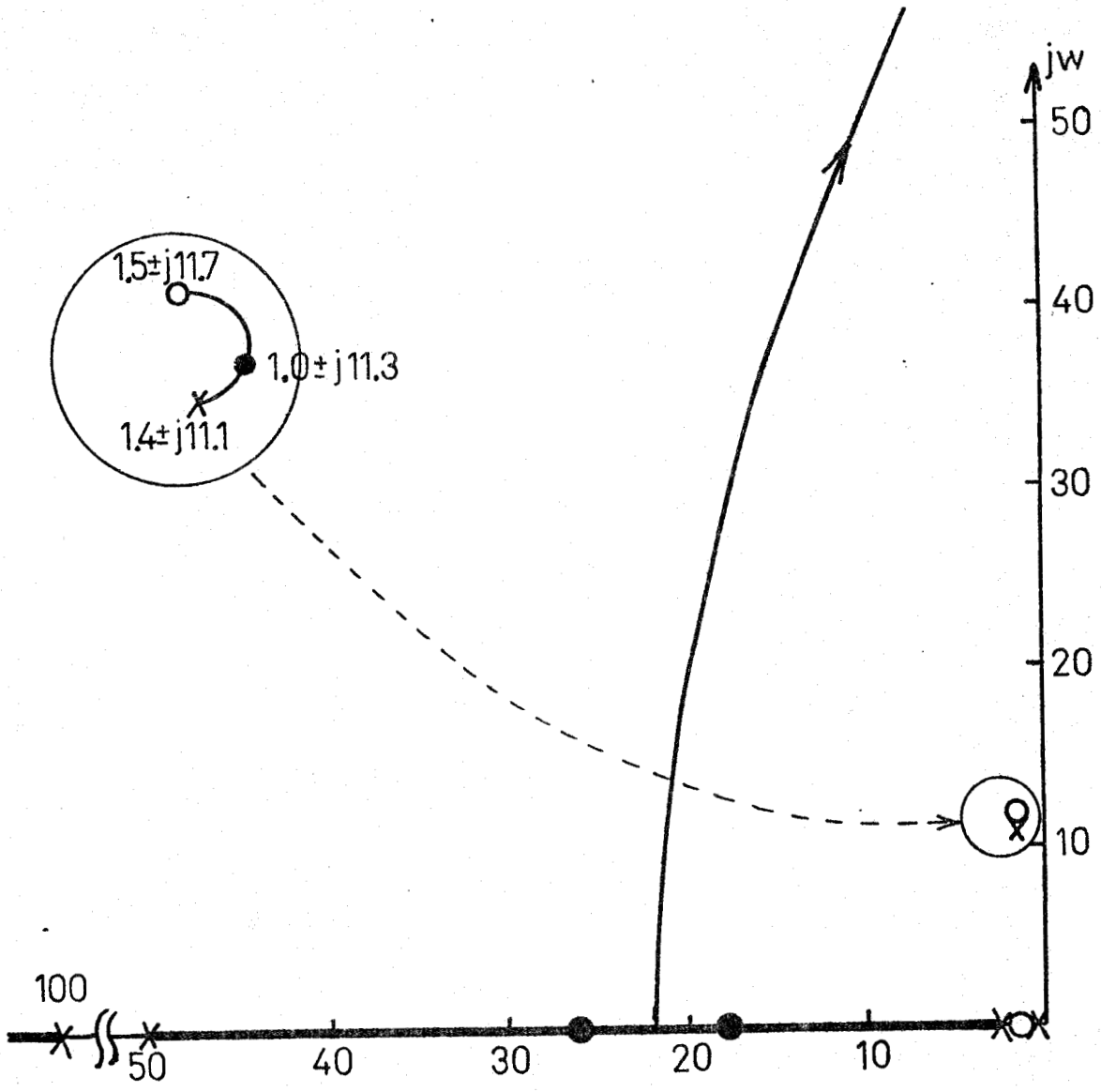

Figure 6.2 Root locus of Sundance system with "standard" AVR and on-line machine model.

• Eigenvalues for AVR gain of 100

reduced by a nearby zero introduced by the current feedback. In the present case, the error involved in locating the complex roots of V_t / E_f during the identification process becomes more critical. Furthermore, it is recalled that the fit of V_t / E_f to the Bode plot found by the identification routines was not exact. A second complex pole-zero pair could have been added to the transfer function.

For these reasons, it was decided to test the accuracy of the generator model when used with the "standard" static AVR. This was done as before by comparing the step response obtained from the reduced order model with that obtained from a USTRAN simulation. The results, shown in figure 6.3 indicated that the machine model is sufficiently accurate for use here without alteration. The dominant oscillatory mode is similar in both cases.

These simulations reveal another interesting fact which becomes apparent when the step response is compared with that obtained for the system with current feedback. This is also shown in figure 6.3. It appears that the use of current feedback in the existing Sundance excitation system considerably increases voltage oscillations.

6.4 Addition of Real Root Series Compensation

Real root series compensation has previously been

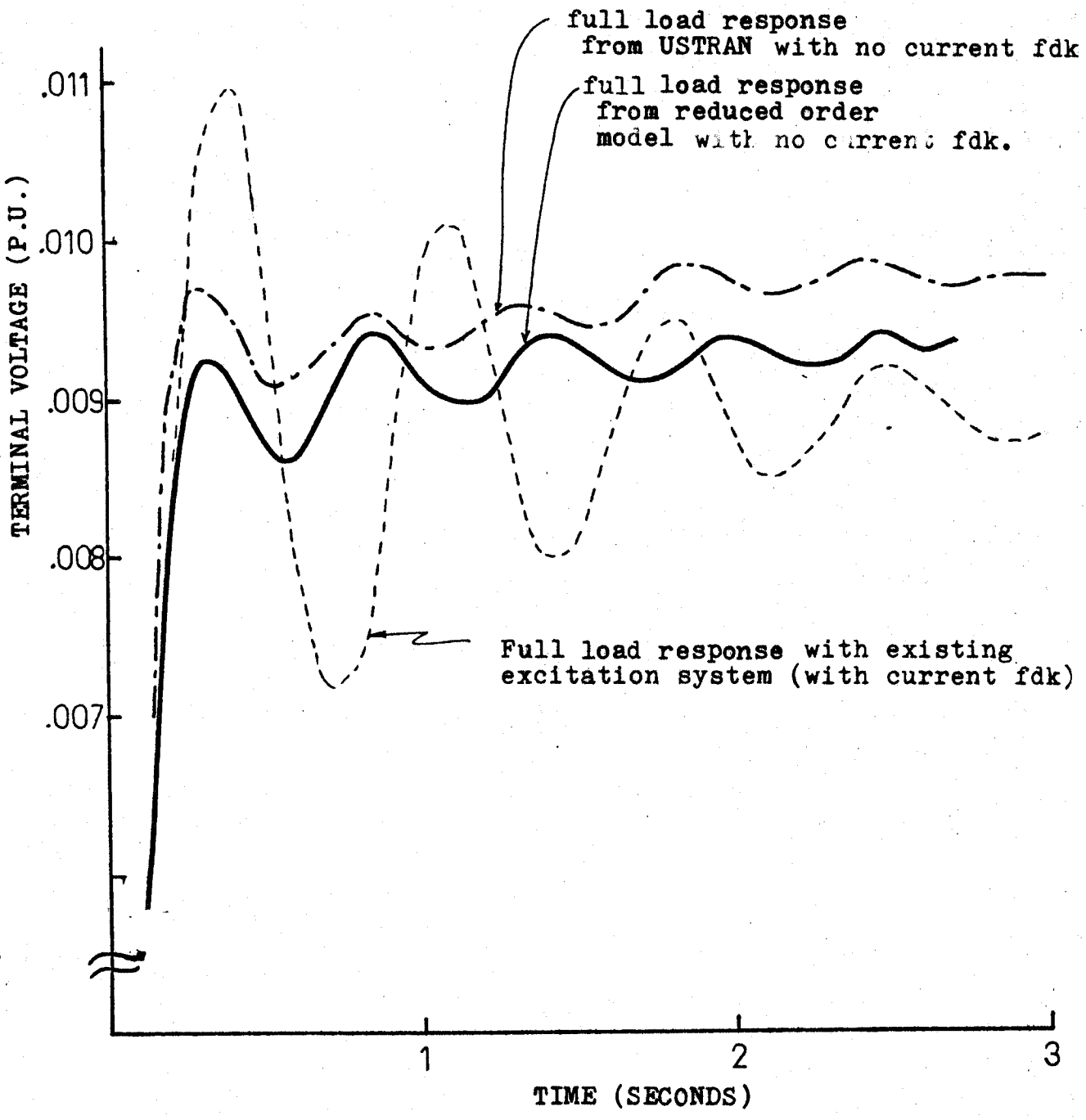

Figure 6.3 Voltage step response of Sundance system with "standard" AVR and machine at full load.

ruled out by others who have done voltage control studies using AVR and generator models similar to those used here [21]. In the reference cited, Raczcowski used series complex compensators to increase the steady state power output of a synchronous generator. The argument used to discount the possible effectiveness of lead-lag compensation was that the pole and zeros introduced by the machine transfer function are too close together to be affected by real root compensators. At first view, this assumption seems correct. Nevertheless an attempt was made to select lead-lag compensator settings that could improve the system response when a "standard" static excitation system is used. The aim was mainly to confirm the above assumption. However the results were surprising.

The ranges of compensator settings used in previous chapters were used here once again. The system eigenvalues were calculated for various combinations of lead and lag settings. The setting selected as the best was maximum lead and no lag compensation:

$$\text{lead:} \quad \frac{1 + T_{A3} S}{1 + T_{A4} S} = \frac{1 + 0.28 S}{1 + 0.039 S}$$

The dominant eigenvalue was moved slightly to the left and closer to the zero as shown in figure 6.4. The movement towards the left was caused by the angle contribution of the lead compensator which increases the depar-

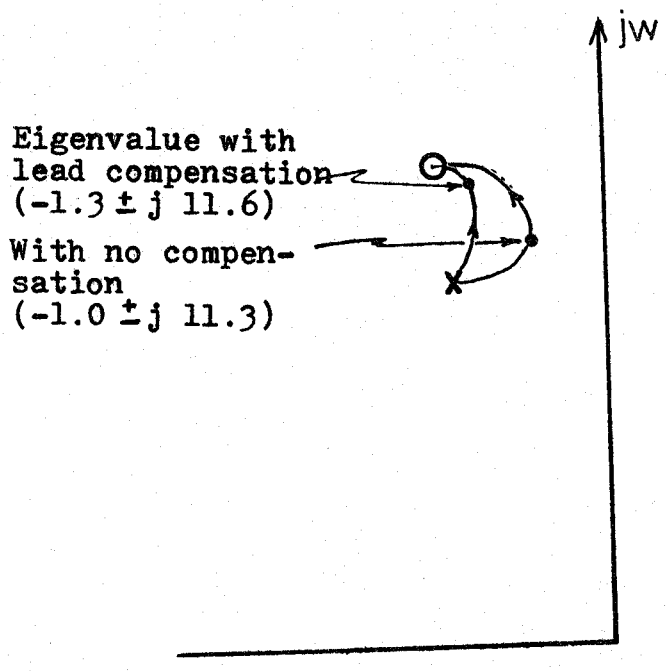

Figure 6.4: Principal branch of the system root locus with and without lead compensation.

ture angle at the complex pole. The movement of the root towards the open loop zero is induced by the increase in "root locus" gain caused by the lead compensator. This

zero is also a closed loop zero because it is introduced by a factor in the V_t / E_f transfer function which is in the forward branch of the system. Any movement of the dominant eigenvalue towards that zero therefore decreases the residue of the root, thus improving the time domain response.

A simulation of the reduced order model of the system confirmed this fact, and a USTRAN simulation of a line outage with the generator at full load was run as a further test. The results of both simulations are illustrated in figure 6.5. These simulations clearly show that real root compensation should certainly not be ruled out as a possible method of improving the on-line performance of static excitation systems. A significant fact is that the improvement in damping was achieved without reducing the rise time of the system response. The step response in figure 6.5 (a) shows that the initial slope of the response is actually increased. The important characteristic of static excitation systems of rapidly increasing field voltage during a system fault is thus not affected.

Another important fact is that this improved setting of the AVR once again had a beneficial effect on the real power oscillations after a disturbance. This is demonstrated in figure 6.6. The responses shown were calculated with the transient stability programs with a

a)

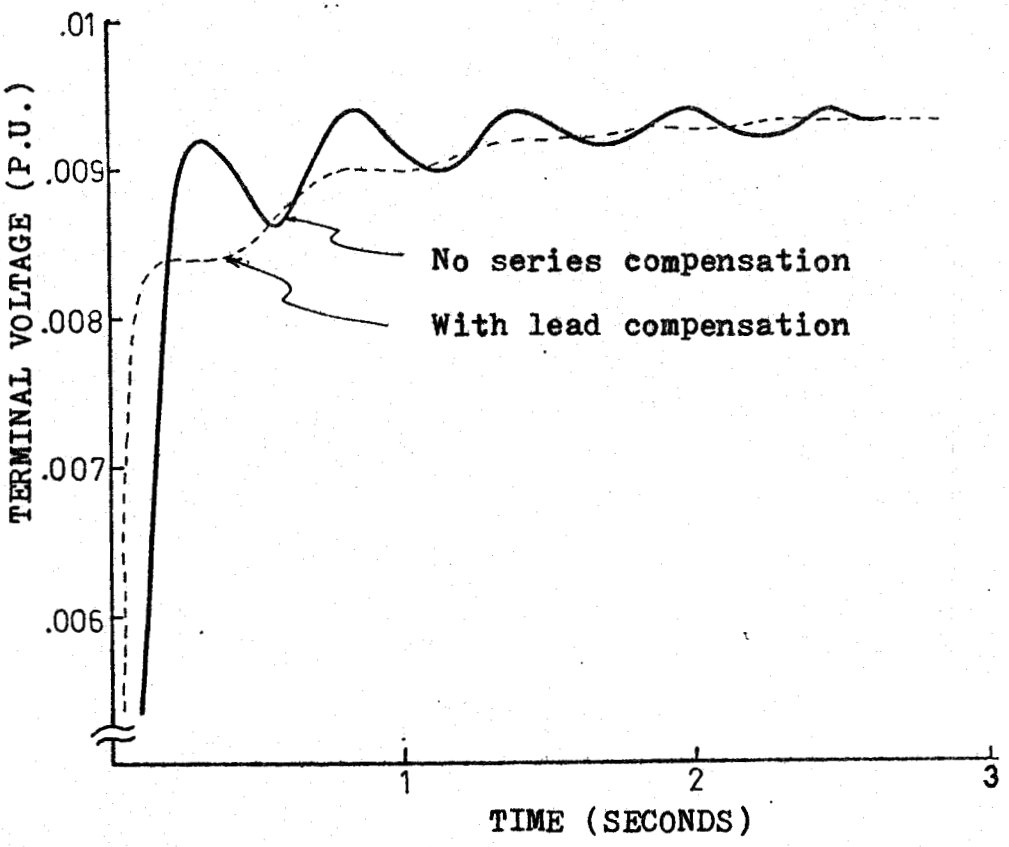

b)

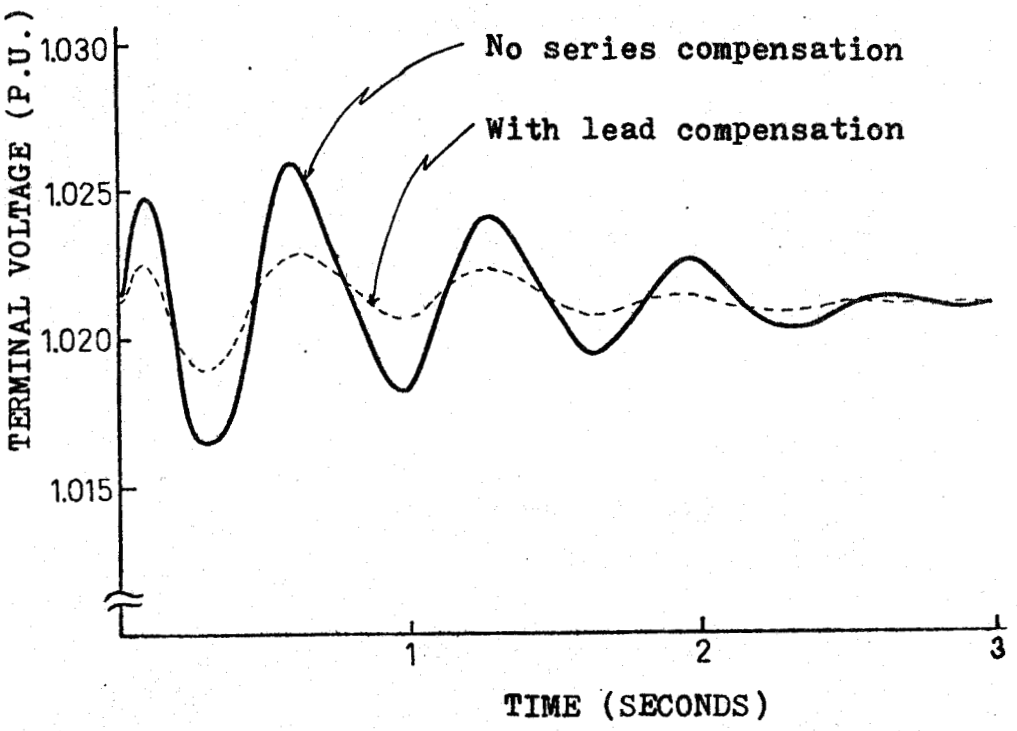

Figure 6.5 Time responses of voltage control system with "standard" static AVR
a) Reduced order model step response
b) USTRAN simulation of line outage

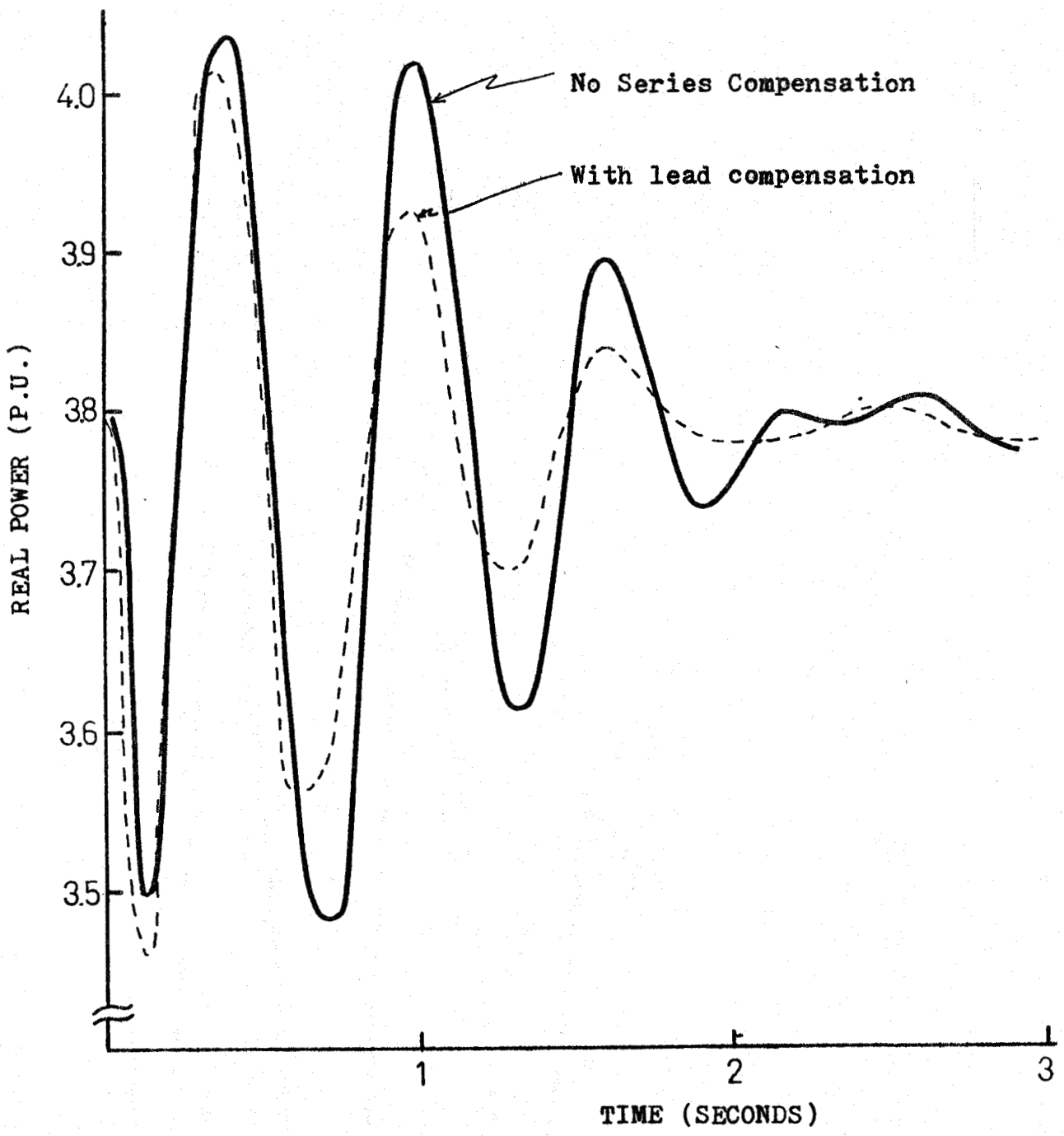

Figure 6.6 Real Power Oscillations with lead compensation

line outage disturbance. The two time responses in the figure correspond to the base case setting of the "standard" AVR where no series compensation is included, and to the lead compensated system with the settings given above.

It has been shown in this section that the addition of real root series compensation to a "standard" static AVR can be very useful in improving the responses of a fully loaded generator. In the following section the effect of complex compensation is examined.

6.5 Addition of Complex Root Compensation

6.5.1 Type 1 Complex Compensator

The two approaches in setting a complex compensator that were described in chapter 5 are applicable to the present case. They are referred to once again as type 1 and type 2 complex compensators.

Although the type 1 complex compensator could be used alone, it was pointed out in its first application with the present Sundance AVR that additional lead-lag compensation could be beneficial. Real root compensators with the same range of adjustment as in the previous studies, were used here once again in conjunction with the type 1 complex compensator. The resulting voltage control system is shown in figure 6.7.

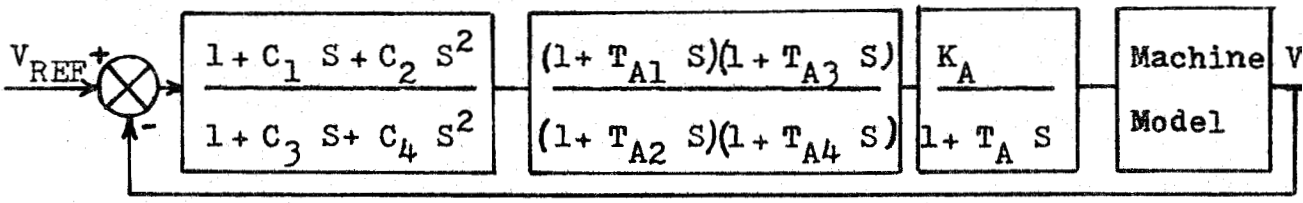

Figure 6.7 "Standard" static AVR with series compensators.

It is recalled that the procedure applied in the case of the type 1 compensator is to cancel the dominant system roots with compensator zeros. The complex compensator poles are then placed further to the left so that the roots introduced by the compensator are well damped.

In this case the compensator zeros were placed at $-1.4 \pm j\ 11.1$. Various locations for the poles were then tested. These locations are shown in figure 6.8.

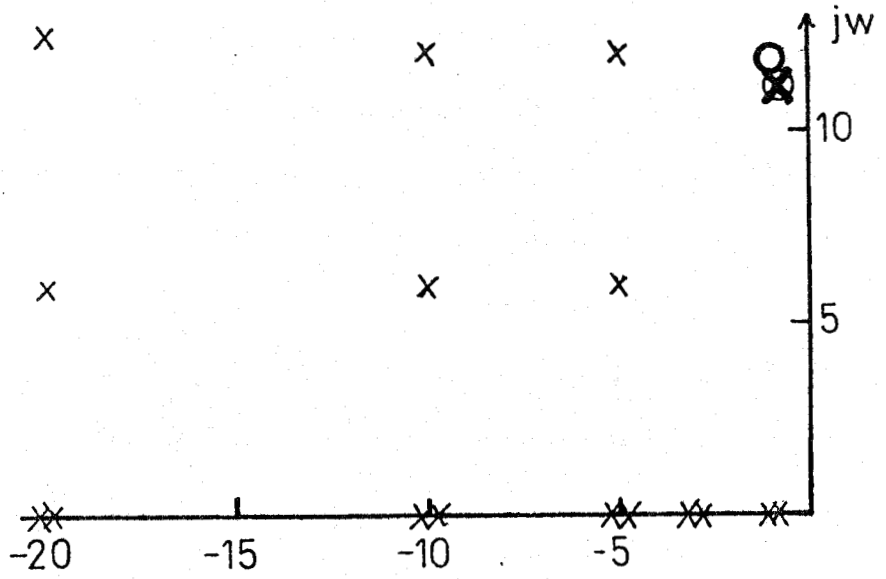

Figure 6.8 Trial locations of type 1 complex compensator poles

The eigenvalue search was begun with compensator poles located relatively close to the system roots. As the study progressed, it became apparent that better results could be achieved by moving the poles more to the left. The limit to which this was done was determined from the increase in high frequency gain caused by the compensator. The compensator transfer function with the poles set at the selected extreme location ($-20 \pm j\ 12$) and with the zeros at $-1.4 \pm j\ 11.1$ is:

$$\frac{Y}{X} = \frac{1 + \frac{2(.125)\,S}{11.2} + \left(\frac{S}{11.2}\right)^2}{1 + \frac{2(.86)\,S}{23.3} + \left(\frac{S}{23.3}\right)^2}$$

The asymptotic approximation of the Bode plot of this transfer function is shown in figure 6.9. The high frequency gain of the compensator is 12 dB. This compares with a high frequency gain of 14 dB for the maximum setting of the lead compensator that is being intalled at the Sundance plant.

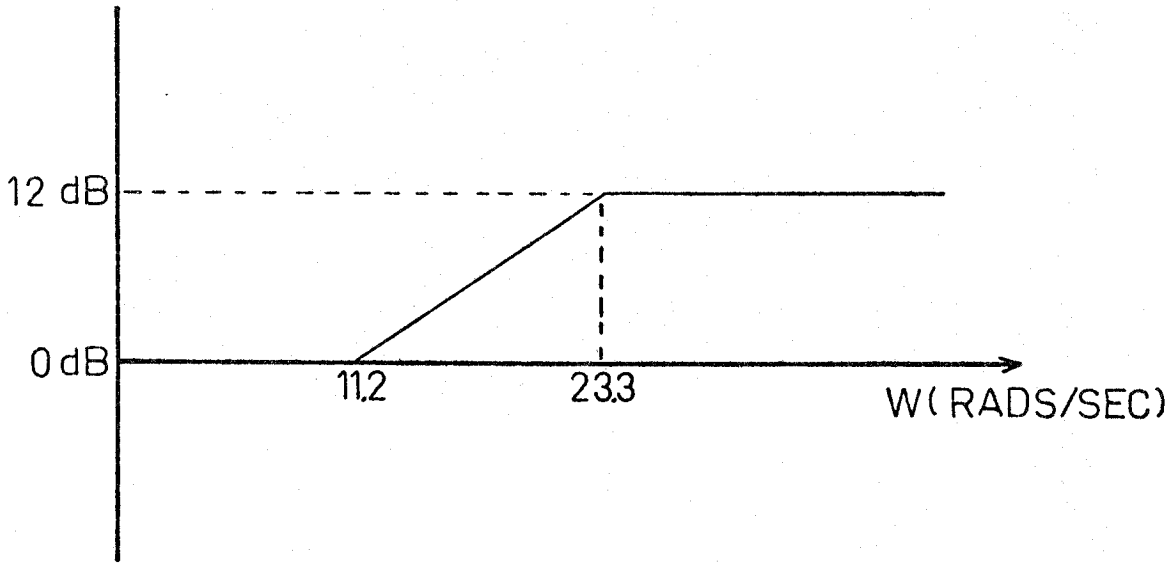

Figure 6.9 Asymptotic Bode Plot of Type 1 Complex Compensator with poles at $-20 \pm j\,12$

For each of the complex compensator settings shown in Fig.6.8, the system eigenvalues were calculated with various combinations of lead and lag settings. The steady-state gain of the AVR was kept constant at 100. The eigenvalues were examined and the most promising root configurations were singled out for further study. The addition of the compensators resulted in the creation of either one or two new pairs of complex closed loop poles depending on the particular settings. Figure 6.10 shows the best dominant root configurations found for these two cases along with the corresponding time responses. The compensator settings that resulted in these responses are given below.

Setting "A"

Complex Compensator:

Zeros at $-1.4 \pm j\ 11.1$

Poles at $-10. \pm j\ 6$

Lead: $\dfrac{1 + .28\ S}{1 + .039\ S} = \dfrac{7.1\ (S + 3.6)}{(S + 25.6)}$

Lag: $\dfrac{1 + .2\ S}{1 + 1.1\ S} = \dfrac{0.17(S + 5)}{(S + .9)}$

Setting "B"

Complex Compensator:

Zeros at $-1.4 \pm j\ 11.1$

Poles at $-10. \pm j\ 6.0$

Lead: $\dfrac{1 + .067\ S}{1 + .039\ S} = 1.7\ \dfrac{(S + 14.9)}{(S + 25.6)}$

No lag compensation

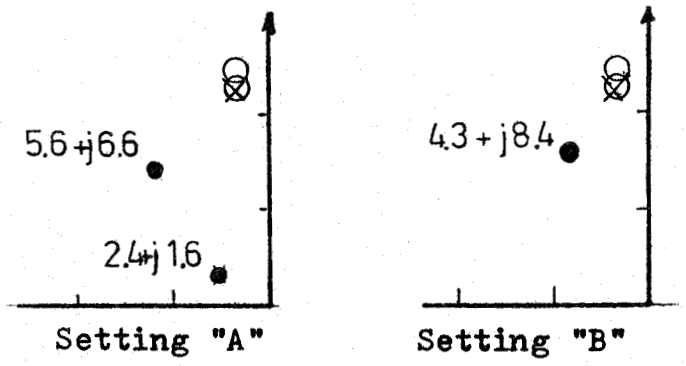

(a)

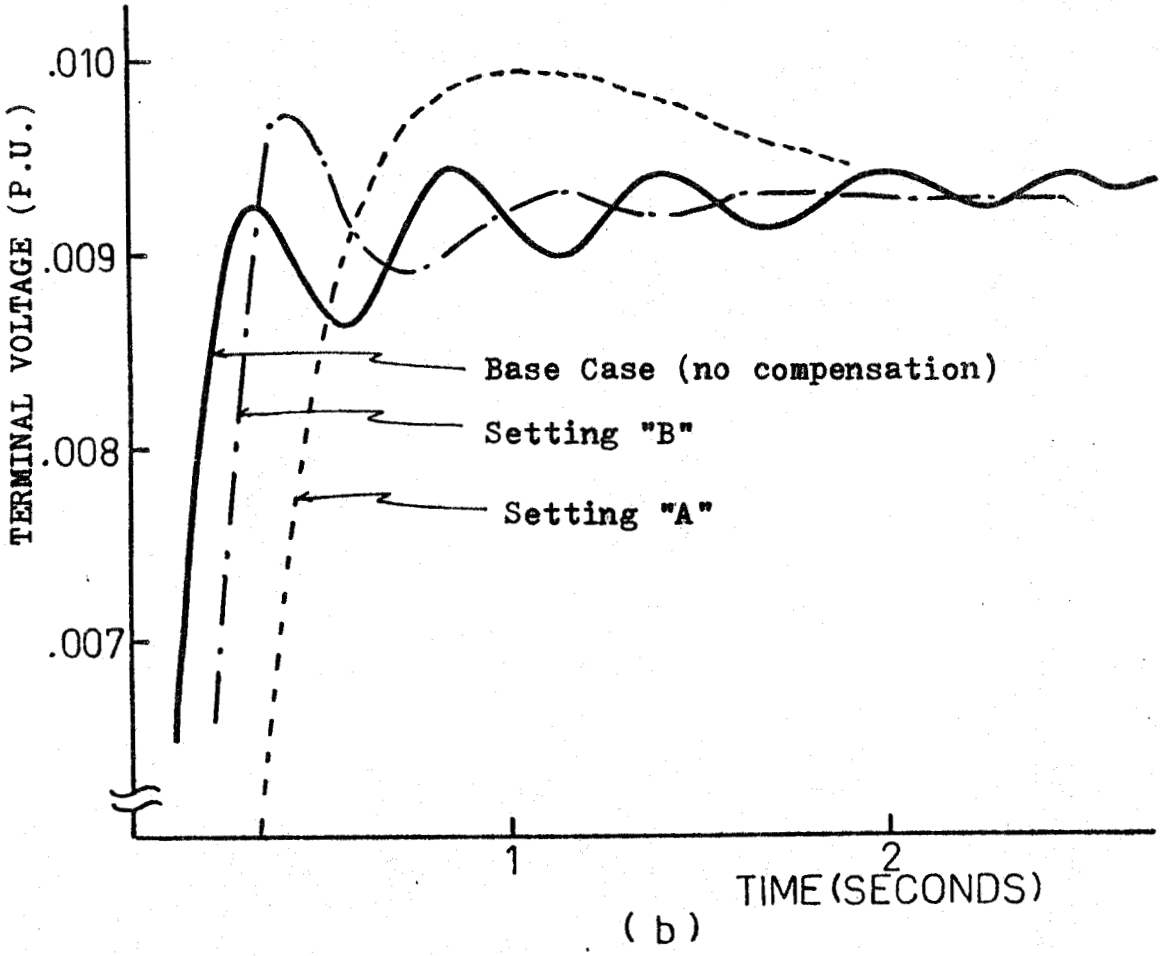

(b)

Figure 6.10 Effects of Type 1 complex compensator for the best 2 settings

a) System dominant eigenvalues
b) Reduced order model step responses

With setting "B", some increase in damping was obtained compared to the base case setting, (no series compensation), although the improvement was not as great as was previously obtained with lead compensation. A USTRAN simulation revealed that the addition of a type 1 complex compensator with the above settings does not improve the voltage response at all compared to the base case. This is shown in figure 6.11.

It appears that the type 1 complex compensator cannot be made useful with this particular system and with the range of compensator settings selected. This occurs essentially because of the fairly good response of the original uncompensated system. The dominant roots of that system have only a small residue because of the proximity of the closed loop zeros. The type 1 complex compensator further reduces the residue at those roots and introduces one or more new pairs of better damped roots. However, these new roots have higher residues than the cancelled roots and they must be moved quite far to the left in order to achieve an overall improvement in response. This does not appear possible if the compensator settings are limited within the ranges used in this study.

6.5.2 Type 2 Complex Compensator

In the case studied in previous chapters, that is, the case of an excitation system with field current feed-

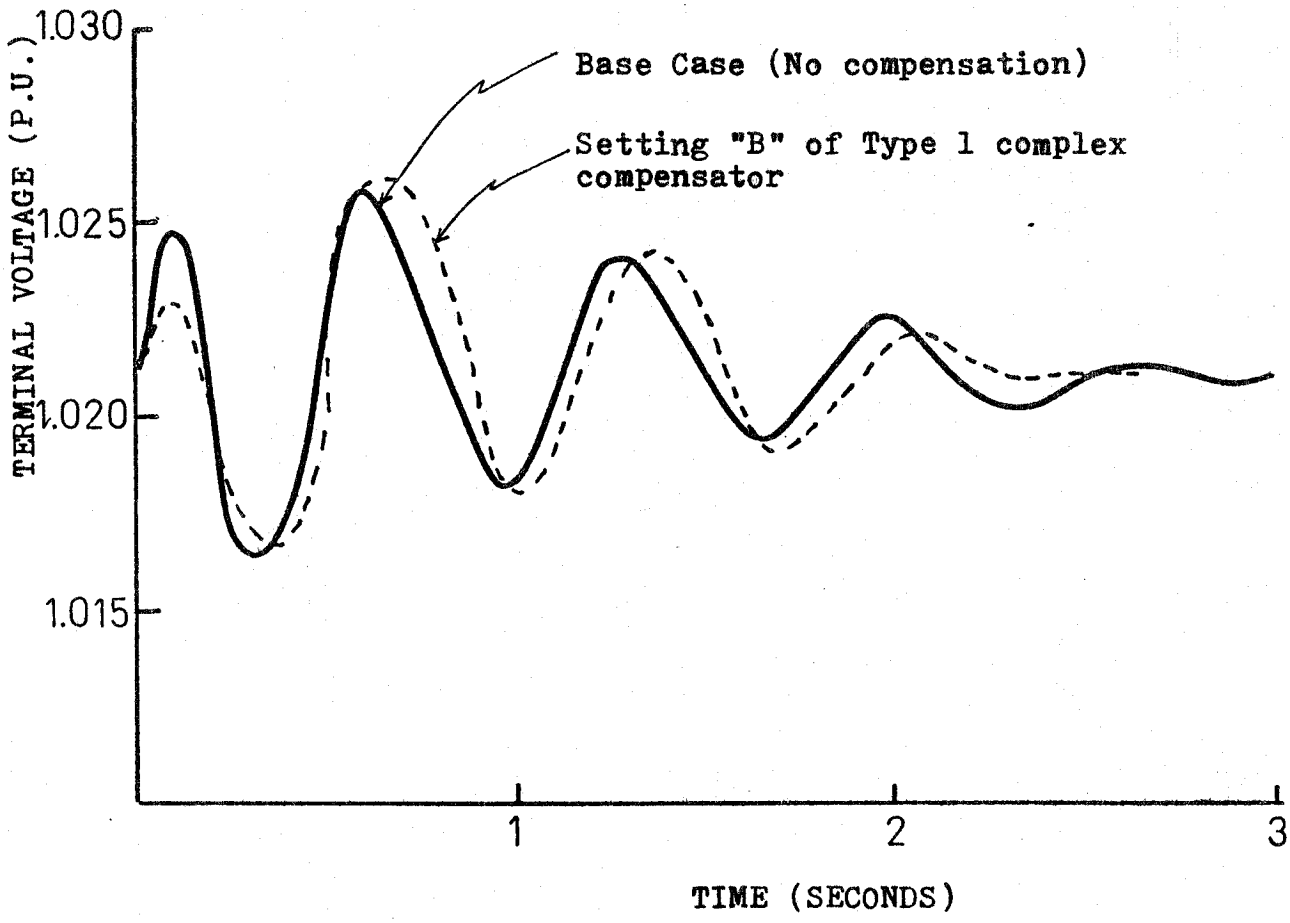

Figure 6.11 USTRAN simulation with Setting B of Type 1 complex compensator

back, the addition of a type 2 complex compensator produced excellent improvement in response. In the case of the "standard" AVR being studied here, the addition of the type 2 complex compensator produced poor results.

As was discussed in chapter 4, the tuning procedure for this compensator is to place the compensator zeros over the system poles and the compensator poles over the system zeros. The selected settings thus were:

Compensator poles at $-1.5 \pm j\ 11.7$

Compensator zeros at $-1.4 \pm j\ 11.1$

No additional real root compensation was required.

The reduced order model simulation of this case, shown in figure 6.12 (a) naturally shows greatly increased damping of oscillations. This is because the compensator essentially has the effect of removing the complex roots of the reduced order generator model. A USTRAN simulation provided a more realistic test. As can be seen in figure 6.12 (b), the compensator has almost no effect whatsoever on the response.

The immediate conclusion from this is that the complex poles and zeros of the machine on-line model are not accurately placed. This is due to errors in the identification routines and in the fitting of transfer functions to the Bode plots. It was noted in chapter 2 that the damping factors of the lightly damped complex roots of the machine model could be measured to only $\pm 25\%$ accuracy.

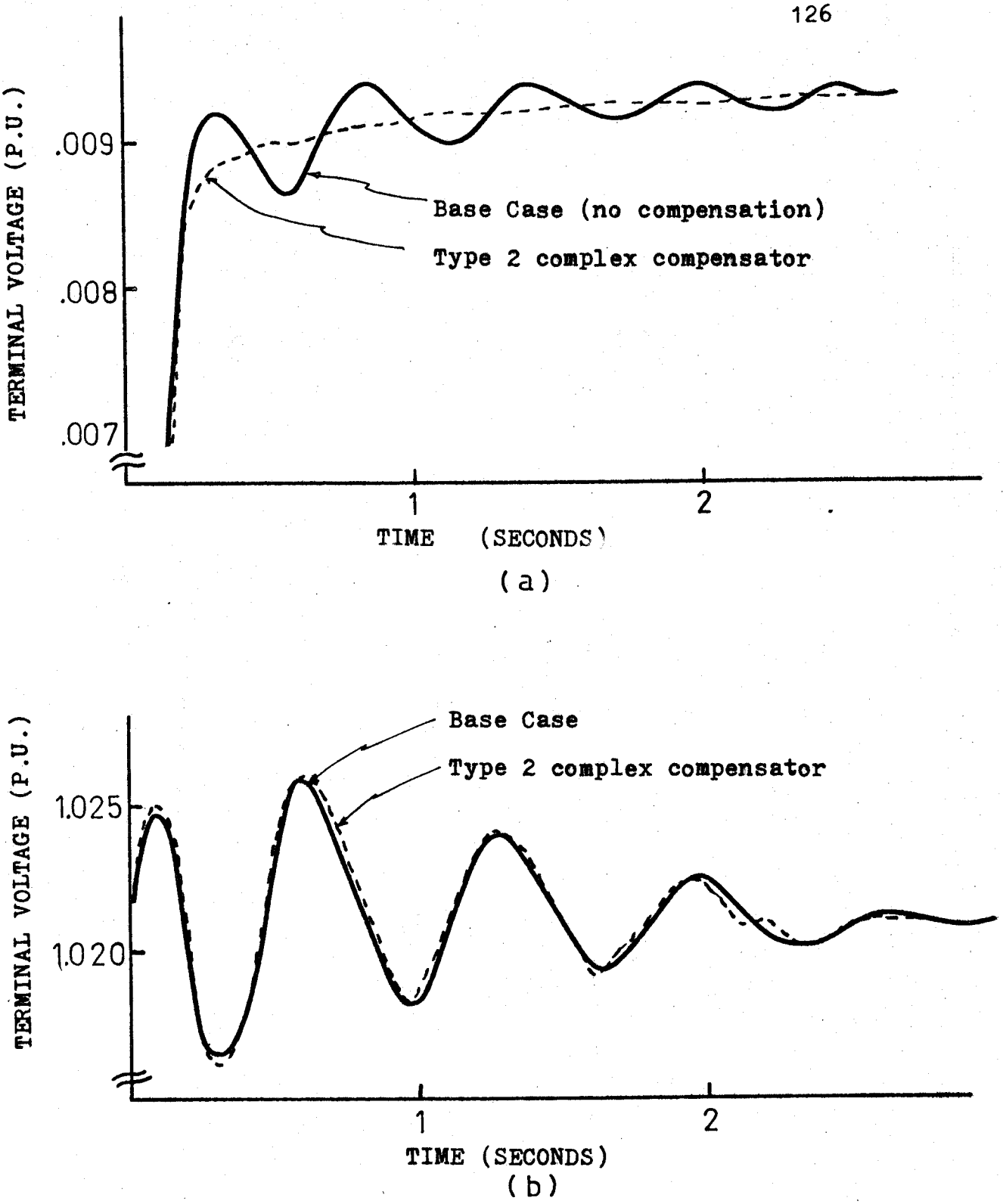

Figure 6.12 Full load voltage response of system with "standard" AVR and type 2 complex compensator
a) Reduced order model simulation
b) USTRAN simulation

Because of the proximity of the system poles and zeros, the settings of the compensator must be much more accurate in this case than with the system discussed in previous chapters. In the previous case the open circuit poles and zeros related to the system dominant roots were much more separated.

For the system at hand (with no current feedback), there is a possibility of determining more accurate settings for the type 2 complex compensator. This could be done by varying the compensator pole and zero locations around the present settings and simulating the system with the transient stability program for each case. A performance criterion such as settling time or integral square-error could then be used to establish a good setting. This process would however rely too heavily on the accuracy of the models and parameters used in the USTRAN program. Results obtained from such a fine tuning process would be meaningless. In the event of the implementation of this type of compensator, the calculated settings would not provide more than a starting point for tests at the plant itself.

7. CONCLUSION

The study reported in this thesis has investigated the feasibility of tuning automatic voltage regulators for on-line generator conditions. In order to permit the use of classical control theory, a reduced order model in the form of transfer functions was used for the on-line generator. This model permitted tuning of static AVR's to considerably improve the dynamic voltage response of the Sundance voltage control system compared to the response obtained when the AVR is tuned for open circuit conditions. The AVR which is being installed at Sundance 3 has features not normally included with static AVR's, notably, field current feedback and series lead lag compensation. It was demonstrated that, with no hardware modifications at all, this system can be retuned to significantly improve performance when the generator is loaded. Further improvement was achieved by adding complex compensators. An investigation of the effects of load variations revealed that lead lag compensators can be tuned for full load conditions with no ill-effects occurring at other loading levels. In the case of complex compensators however, a more thorough investigation of the performance at various loading le-

vels is required. Finally, the performance of the Sundance 3 plant was investigated with the excitation system replaced with one where no current feedback is included. This revealed that, contrary to previous assumptions, lead lag compensation can be useful with such a system. However, there was some difficulty in tuning complex compensators for this particular system.

The main conclusion to be drawn from this project is that it is feasible to set AVR's for on-line rather than for open circuit conditions and that such a process is certainly worthwhile. The basic ingredient for this process, the reduced order on-line generator model is available from many sources. It was obtained in this case by using an identification process on a detailed model of the power system. Others [21] have obtained a similar model by using a 3rd order differential equation developed by Reggiani [27]. Alternate techniques for reducing high order system matrices while maintaining the dominant system eigenvalues are available [28]. These methods offer a completely computerized approach for obtaining reduced order on-line generator models but they require a state space model of the power system and more complex algorithms.

With most static excitation systems presently being installed, the gain is the only adjustable feature. Manufacturers and utilities have been satisfied with the benefit to the system transient stability due

to the high speed and high gain of these AVR's. Little consideration has been given until now to the addition of series compensators to these excitation systems with the aim of improving dynamic stability. This project has shown that such an addition should be seriously considered.

An important result of these studies was that, in all cases examined, any improvement achieved in the terminal voltage response of the generator was accompanied by a notable increase in the damping of system real power oscillations. This indicates that in cases where the addition of a power stabilizer is being considered, preliminary studies should include re-tuning of the AVR.

In the study reported here, the tuning of an AVR where a power stabilizer is included was not investigated. Such a study would be useful. There is every indication that additional series compensation in the AVR could be of benefit in that case also.

8. REFERENCES

1. Bollinger, K. E., Laha, A. K., "Multi-machine Controller Studies Using Optimal and Approximate Controllers", IEEE Summer Power Meeting, July 1972, paper C72 471-1-Abstract PAS Vol. 91, Nov./Dec. 1972, pp.2259.

2. Yu, Y., Vongsuriya, Wedmann, L., "Application of Optimal Control Theory to a Power System", IEEE Trans. on PAS, Vol. 89, pp. 55-62, January 1970.

3. Schleif, F.R., Hunkins, H.D., Martin, G.E., and Hatton, E.E., "Excitation Control to Improve Power System Stability", IEEE Transactions on PAS, Vol. 98, pp.1426-1434, June, 1968.

4. Keay, F.W., and South, W.H., "Design of a Power System Stabilizer Sensing Frequency Deviation," IEEE Trans. on PAS, Vol. 90, pp. 705-713, March/April, 1971

5. Bollinger K., Laha A., Hamilton R. and Harras T., "Power Stabilizer Design Using Root-Locus Methods" IEEE Trans. on PAS., Vol 94 pp. 1484-1488, Sept./Oct., 1975.

6. Bollinger K.E., Laha A.K., Winsor R.A., "System Models From Transient Stability Program", Proceedings IEEE PICA Conf., TPx11-6, pp. 330-334, June 1975.

7. Park, R.H., "Two Reaction Theory of Synchronous Machines" AIEE Transactions, pp. 716-730, July 1929.

8. Bollinger, K.E., "Power System Damping Using Speed Signals", M.Sc. Thesis in Elect. Eng., University of Saskatchewan, 1968.

9. Bollinger, K.E., Winsor, R.A., Laha,A.K., Gilchrist,R., "On Line Identification of Power System Transfer Functions" Paper presented at the 1975 Spring Meeting of the C.E.A., Vancouver, B.C.

10. Snowden, H.K., "Frequency Response of Large Power Systems Using Computer Simulations", B.A.Sc. Report in Elect. Eng., University of Saskatchewan, 1975

11. Fitzgerald, A.E.,and Kingsley, C. "Electric Machinery", McGraw Hill,1961.

12. Heffron, W.G., and Phillips, R.A., "Effects of a Modern Amplidyne Voltage Regulator on the Under Excited Operation of Large Turbine Generators", AIEE Trans., Vol. 71 pp. 692-697, August, 1952.

13. deMello, F.P. and Concordia, C.,"Concepts of Synchronous Stability as Affected by Excitation Control", IEEE Trans. on PAS, Vol. 88, pp.316-329, April,1969.

14. Podmore, R., "Power System Dynamic Simulation Program Users' Manual". A report sponsored by N.R.C. and supervised by Dr. R.J. Fleming of the Power Systems Research Group, University of Saskatchewan.

15. Bollinger, K.E., "Power Stabilizer Design", a report to Calgary Power Ltd., Sept., 1974.

16. Ewart D.N. and deMello,F.P., "FACE-A Digital Dynamic Analysis Program", Proc. 1967 PICA Conf., pp. 83-94.

17. Ewart, D.N., Schultz, R.P., "FACE Multi-Machine Power System Simulator Program", Proc. 1969 PICA Conf. pp.133-153.

18. IEEE Committee Report, "Guide for Excitation Control System Dynamic Performance Criteria and Evaluation Test Procedures", Preliminary Report, Sept., 1975.

19. Manchur, G. and Watson, W., "Experience with Supplementary Damping Signals for Generator Static Excitation Systems, "IEEE Trans. on PAS, Vol. 92, pp.199-203, Jan./Feb., 1973.

20. IMSL Manual, Vol. 1 and 2, Published by International Mathematical and Statistical Libraries Inc.

21. Raczkowski, C., "Complex Root Compensator - A New Concept for Dynamic Stability Improvement", IEEE Trans. on PAS., Vol 93 pp.1842-1848, Nov./Dec., 1974.

22. Keay, F.W., Raczkowski, C., and South, W.H., "Excitation System Complex Compensation", IEEE Trans. on PAS., Vol. 93, pp. 1444-1448, Sept./Oct., 1974.

23. Bingen, P., Landgren, G.L., Keay, F.W., and Raczkowski, C., "Dynamic Stability Tests on a 733 MVA Generator at Kincaid Station", IEEE Trans. on PAS, Vol. 93, pp. 1328-1334, Sept./Oct., 1974.

24. Ogata, K., "Modern Control Engineering", Prentice - Hall Publ. Co., 1970.

25. IEEE Committee Report, "Computer Representation of Excitation Systems", IEEE Trans. on PAS., Vol. 87, pp. 1460-1463, June, 1968.

26. Fleming, R.J., "Electric Power System Modelling and Control", Class Notes, Dept. of Elect. Eng., University of Saskatchewan.

27. Regianni, F., and Saccomanno F., "Consideration Upon Stability Margins with Special Regard to the Effects of Generator Excitation System and Voltage Regulator Characteristics", CIGRE 1966, Paper 330.

28. Altalib, H.Y., and Krause, P.C., "Dynamic Equivalents by combinations of Reduced Order Models of System Components", Paper No F 76 211-3. Presented at the 1976 IEEE Winter Power Meeting.

APPENDIX I

The following is an extract from the installation instructions for a Magnestat voltage regulator, type VM21, form C3, manufactured by Associated Electrical Industries Ltd.

The main components of the AVR are two magnetic amplifiers and an amplidyne. Three internal loops of derivative feedback are provided for stabilization. Sections (f) and (h) describe the procedure for adjusting these.

SECTION 3

3.3 Initial Adjustments

When the voltage regulator is operated for the first time, the following sequence of operations is recommended:

(a) Set switch SW2 to "Hand", SW71 to "Off".

(b) Operate the generator on open circuit, start the motor amplidyne set by means of the start button, check its direction of rotation, then set the excitation by means of RV131 to give normal generator voltage.

(c) Check the polarity of the amplidyne exciter at voltage regulator terminals 518, 519. Terminal 519 should be positive with respect to 518. If incorrect, check amplidyne field connections.

(d) Check the polarity of the main exciter at voltage regulator terminals 516, 517. Terminal 516 should be positive with respect to 517. If incorrect, check exciter field and armature connections.

(e) With meter switch SW1 at position "Output", adjust voltage control RV7 and observe that meter M1 reading varies and set to a low reading of about 5mA. (Meter K = 2).

(f) Set anti-hunt controls to the nominal values given in Supplement 1 at the end of this book.

(g) Adjust voltage control RV7 to bring meter M2 pointer zero, then turn SW2 to "Auto". Observe that the voltage regulator takes over control without appreciable change in generator.

(h) Trim settings of anti-hunt controls as follows:

(i) If the regulator is fitted with a kVA limit panel first check that control RV95 is set at zero.

(ii) Turn RV2 in a counter-clockwise direction until hunting of excitation or generator voltage just commences, then turn clockwise 1 or 2 divisions and lock.

(iii) Repeat (i) using RV3.

(iv) Repeat (i) using RV4.

In the case of (ii) and (iii) hunting will take the form of rapid oscillation of the pointer of meter M1 in SW1 position 'Output' and may not be very marked.

Capacitor switches SW4 and SW5 may be adjusted if RV2 and RV3 appear to have insufficient range to give adequate stability.

(v) Rotate RV7 rapidly by a small amount: if appreciable oscillation of AC voltage and of meter M1 in position 'Output' of SW1 is observed, readjust RV2 and RV3.

APPENDIX II

The constants of the Heffron-Phillips model shown in figure 2.1, for a generator supplying power to an infinite bus are given below. These are taken from reference 26.

$K_1 = \left.\frac{\partial T_e}{\partial \delta}\right|_{V_q'}$ is the change in electrical torque for a change in rotor angle with constant flux linkages in the d-axis.

$$K_1 = \frac{V_{qo}V_{bo}}{A}\left[R_e \sin\delta_{1bo} + (X_e + X_d^1)\cos\delta_{1bo}\right]$$

$$+ \frac{I_{qo}V_{bo}}{A}\left[(X_q-X_d^1)(X_e + X_q)\sin\delta_{1bo} - R_e(X_q-X_d^1)\cos\delta_{1bo}\right]$$

$K_2 = \left.\frac{\partial T_e}{\partial v_q^1}\right|_{\delta}$ is the change in electrical torque for a change in d-axis flux linkage with constant rotor angle.

$$K_2 = \left[\frac{R_e V_{qo}}{A} + I_{qo}\left(1 + \frac{(X_e+X_q)(X_q-X_d^1)}{A}\right)\right]$$

K_3 is an impedance factor

$$K_3 = \left[1 + \frac{(X_e+X_q)(X_d-X_d^1)}{A}\right]^{-1}$$

$K_4 = \frac{1}{K_3}\frac{\partial v_q^1}{\partial \delta}$ is the demagnetizing effect of a change in rotor angle

$$K_4 = \frac{V_{bo}(X_d-X_d^1)}{A}\left[(X_e+X_q)\sin\delta_{1bo} - R_e\cos\delta_{1bo}\right]$$

$K_5 = \left.\frac{\partial V_t}{\partial \delta}\right|_{V_q^1}$ is the change in terminal voltage with a change in rotor angle for constant V_q^1

$$K_5 = \frac{V_{do}}{V_{to}} X_q \left[\frac{R_e E_o \sin \delta_{1bo} + (X_e+X_d^1) V_{bo} \cos \delta_{1bo}}{A}\right] + \frac{V_{qo}}{V_{to}} X_d^1 \left[\frac{R_e V_{bo} \cos \delta_{1bo} - (X_e+X_q) V_{bo} \sin \delta_{1bo}}{A}\right]$$

$K_6 = \left.\frac{\partial V_t}{\partial V_q^1}\right|_{\delta}$ is the change in terminal voltage with a change in V_q^1 for constant rotor angle

$$K_6 = \frac{V_{qo}}{V_{to}} \left[1 - \frac{X_d^1(X_e+X_q)}{A}\right] + \frac{V_{do}}{V_{to}} X_q \frac{R_e}{A}$$

$$A = \left[R_e^2 + (X_e+X_d^1)(X_e+X_q)\right]$$

The symbols used above are:

I_{qo}, i_q = quadrature axis stator current

R_e = tie line resistance

V_{bo}, v_b = bus voltage

V_{do}, v_d = direct axis component of terminal voltage

V_{qo}, v_q = quadrature axis component of terminal voltage

X_e = equivalent system reactance

X_d = direct axis synchronous reactance

X_d^1 = direct axis transient reactance

X_q = quadrature axis synchronous reactance

δ_{1bo} = steady state torque angle between rotor quadrature axis and bus voltage axis

APPENDIX III

The subroutine listed below produces a filtered noise signal with a specified lead-in length. The routine differs from SEQG [15] in that the random sequence of binary numbers is filtered only after the lead-in section has been added. Also, the filter cutoff frequency, the filter integration step size and the lead-in length can be specified. The parameters in the calling sequence of the subroutine are listed below.

A - The output vector containing the filtered PRBS of order IDIM

CLPER - Clock period in seconds. This determines the minimum pulse width contained in the PRBS

NOTE: $1 / CLPER = f_c$

NINT - The number of pulses in one period, T, of the PRBS

IDIM - The number of output points required from the filtered PRBS.

FFILT - Fourth order filter corner frequency

NFILT - Number of filter integration steps in one period of the PRBS

ALDN - Lead-in length specified as a multiple of one period

```
                      C
                      C
C001                        SUBROUTINE SEQSI(A,CLPER,NINT,IDIM,FFILT,NFILT,ALDN)
0002                        REAL XDOT(4),XST(4),A1(4,4),B1(4)
C003                        REAL A(1),B(12000)
C004                        T=NINT*CLPER
C005                        IX=154237
C006                        IS=NFILT
                      C
                      C GENERATE ONE PERIOD OF BINARY SEQUENCE
                      C
C007                        DO 5 I=1,NINT
C008                        X=-1.
C009                        CALL GAUSS(IX,1.,0.,V)
C01C                        IF(V.GE.C.) X=1.
0011                  5     A(I)=X
                      C
                      C ADD LEAD IN TO FRONT OF SEQUENCE
                      C
C012                        N3=(1.-ALDN)*NINT
C013                        N4=IFIX(ALDN*NINT)
C014                        DO 10 I=1,N4
C015                  10    B(I)=A(I+N3)
C016                        DO 15 I=1,NINT
0017                  15    B(I+IFIX(NINT*ALDN))=A(I)
                      C
                      C FILTER THE SEQUENCE
                      C     DEFINE CONSTANTS AND INITIALIZE VARIABLES
                      C
C018                        DO 20 I=1,4
C019                        XST(I)=C.
C02C                        XDOT(I)=C.
0021                        B1(I)=C.
C022                        DO 20 J=1,4
C023                  20    A1(I,J)=C.
C024                        AA=2.*3.1416*FFILT
C025                        DO 25 I=1,4
C026                        A1(I,I)=-AA
C027                        IF(I.EC.4) GO TO 25
0028                        A1(I+1,I)=AA
C029                  25    CONTINUE
C03C                        B1(1)=AA
                      C
                      C DEFINE DERIVATIVES OF FILTER MODEL AND INTEGRATE
                      C STORE (1+ALDN)*IDIM SAMPLES IN OUTPUT VECTOR
                      C
C031                        I=0
0032                        J=C
C033                  26    I=I+1
C034                        X=B(I)
C035                  27    J=J+1
C036                        DO 30 L=1,4
C037                        XDOT(L)=B1(L)*X
C038                        DO 30 K=1,4
C039                  30    XDOT(L)=XDOT(L)+A1(L,K)*XST(K)
C04C                        DO 35 K=1,4
```

```
      55    XST(K)=XST(K)+XOUT(K)*T/FLOAT(IS)
            Y=XST(4)
      C
      C END OF SEQUENCE TEST
      C
            IF(J.GT.IFIX((ALDN+1.)*IS)) GO TO 50
      C
      C RECORD OUTPUT IF RECORD TIME IS REACHED
      C
            IF((J-1)*IDIM/IS*(IS/IDIM)+1.EQ.J) A((J-1)*IDIM/IS+1)=Y
      C
      C IF ONE COMPLETE CLOCK PERIOD IS NOT COMPLETED CONTINUE FILTERIN
      C
            IF(T/FLOAT(IS)*FLOAT(J).LT.T/FLOAT(NINT)*FLOAT(I)) GO TO 27
      C
      C CHECK IF ALL OF SEQUENCE HAS BEEN FILTERED
      C
            IF(I.LT.IFIX((ALDN+1.)*NINT)) GO TO 26
      50    CONTINUE
            RETURN
            END
```